

Ral G-Proteins and the Exocyst Complex are Mediators of the Cellular Response to Nutrients

APPROVED BY SUPERVISORY COMMITTEE

Ral G-Proteins and the Exocyst Complex are Mediators of the Cellular Response to Nutrients

by

BRIAN OLIVER BODEMANN

DISSERTATION / THESIS

Presented to the Faculty of the Graduate School of Biomedical Sciences

The University of Texas Southwestern Medical Center at Dallas

In Partial Fulfillment of the Requirements

For the Degree of

DOCTOR OF PHILOSOPHY

The University of Texas Southwestern Medical Center at Dallas

Dallas, Texas

December, 2011

Ral G-Proteins and the Exocyst Complex are Mediators of the Cellular Response to Nutrients

Brian Bodemann

The University of Texas Southwestern Medical Center at Dallas, 2011

Michael A. White, Ph.D.

The small G-proteins, RalA and RalB, are important mediators of cellular responses to viral infection and nutrient availability. Prior work has demonstrated that the exocyst complex is an important effector of Ral G-protein signaling. The eight member exocyst contains two Ral effector proteins, Exo84 and Sec5, which contribute to distinct cellular responses. During viral infection, RalB promotes the activation of the innate immunity signaling kinase, TBK1, through direct assembly on a Sec5-containing subcomplex of the exocyst. Macroautophagy is an important cellular process which facilitates cellular adaptation to nutrient deprivation as well as the clearance of intracellular pathogens. The study of macroautophagy in mammalian cells has described induction, vesicle nucleation, and membrane elongation complexes as key signaling intermediates driving autophagosome biogenesis. How these components are recruited to nascent autophagosomes is poorly understood, and although much is known about signaling mechanisms that restrain autophagy, the nature of positive inductive signals that can promote autophagy remain cryptic. I report that RalB is localized to nascent autophagosomes. RalB and its effector Exo84 are required for nutrient starvation-induced autophagocytosis, and RalB activation is sufficient to promote autophagosome formation. Through direct binding to Exo84, RalB induces the assembly of ULK1 and Beclin1-VPS34 complexes on the exocyst, which are required for isolation membrane formation and maturation. Thus, RalB-Exo84 signaling is a primary adaptive response to nutrient limitation that directly engages autophagocytosis through mobilization of the core vesicle nucleation machinery. Conversely, I find that Sec5 associates with mTORC1, a key inhibitor of autophagy. Intriguingly, I find that the Ral-Sec5 activated kinase, TBK1, is necessary for amino acid stimulation of mTORC1 activity. Thus, distinct Ral-dependent subcomplexes of the exocyst mediate the cellular response to nutrient availability.

TABLE OF CONTENTS

i.	PRIOR PUBLICATIONS	v
ii.	LIST OF FIGURES & TABLES	vi
iii.	LIST OF ABBREVIATIONS	vii
iv.	CHAPTER ONE:	
	Nature Reviews Cancer Paper: Ral GTPases and Cancer: linchpin support of the tumorigenic platform	p. 1–20
v.	CHAPTER TWO:	
	a. Part One: the Exocyst Complex	p. 19–21
	b. Part Two: Ral-dependent exocyst signaling events	p. 21–26
vi.	CHAPTER THREE:	
	a. Cell Paper: RalB and the Exocyst Mediate the Cellular Starvation Response by Direct Activation of Autophagosome Assembly	p. 27–69
	b. Unpublished observations in support of Ral–exocyst regulation of autophagy	p. 70–72
vii.	CHAPTER FOUR:	
	a. Part One: RalA is a positive regulator of cell growth signaling pathways	p. 73–77
	b. Part Two: The exocyst is a proximal integrator of both growth and renewal signaling pathways	p. 77–82
viii.	CONCLUDING REMARKS	p. 83
ix.	BIBLIOGRAPHY	p. 84–98

PRIOR PUBLICATIONS

Trever G Bivona, Steven E Quatela, **Brian O Bodemann**, Ian M Ahearn, Michael J Soskis, Adam Mor, John Miura, Heidi H Wiener, Latasha Wright, Shahryar G Saba, Duke Yim, Adam Fein, Ignacio Pérez de Castro, Chi Li, Craig B Thompson, Adrienne D Cox, Mark R Philips. PKC regulates a farnesyl-electrostatic switch on K-Ras that promotes its association with Bcl-XL on mitochondria and induces apoptosis. *Molecular Cell* (2006) vol. 21 (4) pp. 481-93

Angelique W Whitehurst, **Brian O Bodemann**, Jessica Cardenas, Deborah Ferguson, Luc Girard, Michael Peyton, John D Minna, Carolyn Michnoff, Weihua Hao, Michael G Roth, Xian-Jin Xie, Michael A White. Synthetic lethal screen identification of chemosensitizer loci in cancer cells. *Nature* (2007) vol. 446 (7137) pp. 815-9

Brian O Bodemann and Michael A White. Ral GTPases and cancer: linchpin support of the tumorigenic platform. *Nature reviews Cancer* (2008) vol. 8 (2) pp. 133-40

James P Madigan, **Brian O Bodemann**, Donita C Brady, Brian J Dewar, Patricia J Keller, Michael Leitges, Mark R Philips, Anne J Ridley, Channing J Der, Adrienne D Cox. Regulation of Rnd3 localization and function by protein kinase C alpha-mediated phosphorylation. *The Biochemical journal* (2009) vol. 424 (1) pp. 153-61

Brian O Bodemann, Anthony Orvedahl, Tzuling Cheng, Rosalyn R Ram, Yi-Hung Ou, Etienne Formstecher, Mekhala Maiti, C Clayton Hazelett, Eric M Wauson, Maria Balakireva, Jacques H Camonis, Charles Yeaman, Beth Levine, Michael A White. RalB and the Exocyst Mediate the Cellular Starvation Response by Direct Activation of Autophagosome Assembly. *Cell* (2011) vol. 144 (2) pp. 253-67.

LIST OF FIGURES AND TABLES

CHAPTER ONE:

Box 1	p. 11
Box 2	p. 12
Figure 1	p. 15
Figure 2	p. 16
Figure 3	p. 17
Table 1	p. 18

CHAPTER TWO:

Figure 4	p. 20
Table 2	p. 20

CHAPTER THREE:

Figure 5	p. 40
Figure 6	p. 43
Figure 7	p. 45
Figure 8	p. 47
Figure 9	p. 49
Figure 10	p. 51
Figure 11	p. 53
Figure 12	p. 55
Figure 13	p. 57
Figure 14	p. 59
Table 3	p. 61
Figure 15	p. 70
Figure 16	p. 72

CHAPTER FOUR:

Figure 17	p. 77
Figure 18	p. 78
Figure 19	p. 79
Figure 20	p. 80
Figure 21	p. 81

LIST OF ABBREVIATIONS

Akt	RAC-alpha serine/threonine-protein kinase	RalGAP	Ral-specific GTPase activating protein
AMPK	AMP-activated protein kinase	RalGDS	Ral Guanine nucleotide Dissociation stimulator
aPKC	atypical protein kinase C		
Atg14	Autophagy gene 14		
Beclin1	Coiled-coil myosin-like BCL2-interacting protein	RalGPS1	Ral GEF with PH domain and SH3 binding motif 1
[Ca ²⁺] _i	intracellular Calcium concentration	RalGPS2	Ral GEF with PH domain and SH3 binding motif 2
CaM	Calcium Calmodulin	RalGEF	Ral-specific Guanyl nucleotide exchange factor
FIP200	200 kDa FAK family kinase-interacting protein	RBD	Ral binding domain
FKBP38	FK506 binding protein 8, 38kDa	RGL1	Ral Guanine nucleotide Dissociation stimulator like 1
Glut4	glucose transporter type 4	RGL2	Ral Guanine nucleotide Dissociation stimulator like 2
IKK _ε	IKK-related kinase epsilon	RGL3	Ral Guanine nucleotide Dissociation stimulator like 3
mTOR	mammalian target of rapamycin	Rheb	ras homolog enriched in brain
mTORC1	mTOR complex 1	S6K1	Ribosomal S6 kinase 1
mTORC2	mTOR complex 2	Sec	Secretory mutant
Myo1c	Myosin 1C	SLC7A5	solute carrier family 7 (cationic amino acid transporter, y ⁺ system), member 5
PAR-3	protease-activated receptor 3	SLC3A2	solute carrier family 3 (cationic amino acid transporter, y ⁺ system), member 2
PAT1	proton-assisted amino acid transporter 1	TAS1R1	Taste receptor, type 1, member 1
PAT4	proton-assisted amino acid transporter 4	TAS1R3	Taste receptor, type 1, member 3
PI-(3)-P	Phosphatidyl inositol 3 phosphate	TBK1	Tank binding kinase 1
PI(3)K	Phosphatidyl inositol 3 kinase	TSC1	tuberous sclerosis tumor suppressor complex 1
PLD1	Phospholipase D1	TSC2	tuberous sclerosis tumor suppressor complex 2
RNAi	small RNA-mediated gene interference	ULK1	unc-51-like kinase 1
RA	Ras Association domain	v-SNARE	Vesicular soluble NSF attachment protein receptor
RagA	Ras-related GTP-binding A	VPS34	Vacuolar protein sorting 34
RagB	Ras-related GTP-binding B		
RagC	Ras-related GTP-binding C		
RagD	Ras-related GTP-binding D		
Ral	Ras-like GTPase		

CHAPTER ONE:

Ral GTPases and Cancer: linchpin support of the tumorigenic platform, *Nature Reviews Cancer*, 2008.

The Ras-like (Ral) guanyl nucleotide-binding proteins, RALA and RALB, first surfaced over 20 years ago when Pierre Chardin isolated their cognate genes from a hybridization screen of B-lymphocyte cDNAs using degenerate probes that contained highly conserved Ras sequences (1). With 82% identity to each other at the amino-acid level, we now know that RALA and RALB represent the inclusive roster for the Ral branch of the over 170-strong Ras family G-protein tree (2). Following their initial discovery, the functional relevance of Ral proteins remained enigmatic for some time; however, they gained notoriety after recognition that a class of guanyl nucleotide exchange factors with biochemical specificity for Ral proteins (see BOX 1 for a review of the G-protein cycle) were direct effectors of oncogenic Ras. Importantly, both gain-of-function and loss-of-function studies identified Ral activation as a proximal consequence of Ras expression that could contribute to Ras-induced oncogenic transformation in cell culture model systems (3-8). As effectively summarized in recent reviews, numerous studies have subsequently explored the participation of Ral proteins in cell regulatory networks, implicating these G-proteins in the seemingly diverse but potentially related processes of cell proliferation, motility, protein sorting and maintenance of cellular architecture (3, 4). Here, we will focus on recent developments that are defining causal relationships between Ral activation and cancer and providing mechanistic accounts of the molecular framework engaged by Ral proteins to support tumorigenic transformation.

Ral and tumorigenicity

Measurements of the relative accumulation of Ral-GTP versus Ral-GDP in cells and tissues have revealed chronic RALA and RALB activation in tumour-derived cell lines versus non-tumorigenic counterparts, and, perhaps more significantly, in tumour samples versus normal tissues (9-11). Studies employing transient (12) or stable (10) RNA inhibition (RNAi) of *RALA* or *RALB* expression in human cell culture models

had no overt consequences on the proliferation or survival of normal or tumorigenic cells under adherent conditions, but severely impaired the anchorage-independent proliferation of cancer cell lines (10, 12). This suggested that chronic RALA activation was an obligate component of the pathological regulatory framework that promotes the bypass of normal proliferative restraints. By contrast, RALB was found to be essential for the survival of a variety of tumour-derived cell lines, but was not limiting for the survival of non-cancerous proliferating epithelial cells (10). Importantly, sensitivity to RALB depletion was conferred on both telomerase-immortalized human mammary and bronchial epithelial cultures upon expression of oncogenic Ras. Thus, RALA and RALB appear to collaborate to promote the bypass of normal restraints on both cell proliferation and survival, at least in a tissue culture setting (12).

This relationship was also revealed by Said Sebt and colleagues through studies of geranylgeranyltransferase 1 inhibitors (GGTI), which are currently undergoing advanced preclinical evaluation as therapeutic agents targeting cancer cell proliferation and survival (13). Both RALA and RALB are peripheral membrane proteins as a consequence of carboxy-terminal geranylgeranylation, and both require membrane association for biological activity (4). GGTI exposure therefore abrogates Ral function together with that of all other proteins that require this modification for activity (13). Remarkably, expression of a GGTI-resistant RALB variant, which was modified by replacement of C-terminal geranylgeranylated sequences with those that specify farnesylation, conferred resistance to GGTI-induced pancreatic cancer cell apoptosis, but not to GGTI-dependent inhibition of anchorage-independent proliferation. However, a GGTI-resistant farnesylated RALA variant failed to deflect GGTI-induced apoptosis of adherent cell cultures, but rescued anchorage-independent cell proliferation. Thus, the RALA–RALB proliferation and survival axis appears to be a key target of GGTIs that accounts at least in part for the biological consequences of GGTI exposure on cancer cell behavior (13).

Further indications of a crucial role for Ral G-protein signaling in human cancers comes from the discovery, by Bill Hahn and colleagues, that RALA is a functionally relevant target of the protein phosphatase 2A (PP2A) A β (also known as PPP2R2B) tumour suppressor (14). PP2A A β is a structural subunit of the serine–threonine protein

phosphatase 2A, and somatic mutations and gene deletions of PP2A A β have been found in a significant percentage of human lung, breast and colon cancers (15-19). RALA is phosphorylated on serines 183 and 194 in cells, potentially by Aurora kinase A together with other, yet to be identified kinases (14, 20). These phosphorylation sites are bona fide PP2A substrates and are associated with a fivefold increase in the GTP-bound active pool of RALA (14). Remarkably, complementation of RNAi-mediated depletion of endogenous *RALA* with wild-type RALA, but not with RALA variants with alanine substitutions at positions 183 or 194, restored the anchorage-independent growth and tumour-formation properties of human embryonic kidney cells that had been transformed by PP2A A β suppression. This strongly suggests that dephosphorylation of RALA is a major mechanism by which PP2A A β normally restricts tumour progression (14). An analogous phosphorylation on serine 181 of KRAS disturbs the association of a stretch of lysine residues within the C terminus of KRAS with the negatively charged inner surface of the plasma membrane, thereby disrupting plasma membrane association and resulting in redistribution of KRAS to endomembrane domains and altered signalling properties (21). Given that serines 183 and 194 of RALA flank a region of positively charged residues within the sequences that specify membrane targeting, a similar mechanism might also govern the subcellular localization of RALA. Perhaps phosphorylation has a role in regulating the shuttling of RALA between internal membranes and the plasma membrane, which might be crucial for its association with upstream regulators and/or downstream effectors.

The effects of Ral *in vivo*

A key hallmark of tumorigenic progression is the release from dependence on matrix association for cell-cycle progression and survival. Competency for anchorage-independent proliferation is probably a prerequisite for both primary tumour growth and development of metastatic lesions (22). Although observations made using traditional monolayer-adherent cultures do not always predict the behaviour of cells within a three-dimensional extracellular matrix, and cannot predict the consequences of epithelial cell-stromal cell communication (23), the studies described above predict that Ral proteins could make obligate contributions to primary tumour formation. This prediction has been

explored using both xenograft models and genetic ablation of the Ral-activating protein and Ras effector RALGDS (BOX 2) in mice.

Chris Counter's group found that chronic depletion of RALA in a large panel of human pancreatic cancer cell lines, through stable integration of shRNA expression constructs, impaired or eliminated the capacity of these cells to form tumours following subcutaneous inoculation of nude mice (10, 11). A similar study from Kathleen Kelly, in the setting of human prostate cancer, found that chronic RALA depletion inhibited bone metastasis in the absence of overt consequences on subcutaneous tumour formation (24). Neither study implicated RALB in the generation of primary tumours; however, the Counter group found that chronic RALB depletion severely impaired or eliminated the capacity of several pancreatic cancer lines to generate lymph-node metastases following tail vein injection (11). Interestingly, Ral-dependent gene-expression patterns that might contribute to metastatic behaviour have recently been uncovered by genomic expression profiling (25, 26).

Although these studies clearly convict Ral proteins as key offenders in the maintenance of tumorigenicity, further work is needed to determine whether the biological consequences observed reflect distinct contributions of Ral signalling to tumorigenicity in diverse cell types, and/ or distinct sensitivities to the tissue microenvironment, and/or differences in phenotypic penetrance as a consequence of residual RALA or RALB protein expression. Additional genetic evidence for a cancer cell-selective dependency on Ral signalling for survival comes from the generation of mice with a homozygous deletion of *Ralgds* by Chris Marshall's group (27). *Ralgds*-null mice are viable and overtly normal. However, using a model of topical carcinogen-induced skin papillomas, these investigators found deletion of *Ralgds* resulted in delayed onset and decreased incidence of papillomas that failed to progress to metastatic disease. Histological evaluation of carcinogen-induced lesions indicated that proliferation rates were similar but apoptosis rates were higher in papillomas from *Ralgds*-null mice relative to their heterozygous or wild-type litter mates (27). These observations suggest that RALGDS activity is required to deflect induction of programmed cell death that would otherwise occur in response to aberrant mitogenic signals.

Ral Effectors

Despite high sequence similarity to HRAS, KRAS and NRAS, Ral G-proteins engage a distinct cadre of proximal effector proteins compared with the other 35 members of the Ras subclass of small G-proteins. This is probably the consequence of divergence of key residues in the 'effector loop' of Ral proteins, which biochemically specifies G-protein–effector interactions (2). The most fully characterized effector relationships are outlined in FIG. 1, and include the CDC42 and Rac-family GTPase-activating protein RLIP (also known as RLIP76 and ralA binding protein 1 (RALBP1)) (28, 29), the Y-box transcription factor ZO-1-associated nucleic acid-binding protein (ZONAB, also known as cold shock domain protein A (CSDA)) (30), and two subunits of the exocyst complex, SEC5 (also known as exocyst complex component 2 (EXOC2)) (31, 32) and EXO84 (also known as EXOC8) (33). The mechanistic contributions of this functionally diverse group of proteins to RALA- and/or RALB-dependent support of tumorigenic transformation is mostly unknown; however, a number of relationships are coming to light that might begin to account for Ral-dependent modulation of cell proliferation and survival.

RLIP

RLIP is the founding member of the Ral effector family, and has been strongly implicated in the regulation of coated-pit endocytosis through association with clathrin adaptor proteins (34, 35). Short interfering RNAs that target *RLIP* can impair the survival of some human cancer cell lines in culture and can impair xenograft tumour growth (36, 37). Although it is tempting to speculate that aberrant regulation of receptor-mediated endocytosis in the context of chronic Ral activation could have profound consequences on mitogenic signal durations and pathway-specific response coupling, no evidence for this has been reported.

By contrast, Russell Peiper's group has recently generated mechanistic evidence that the RALA–RLIP effector pathway functions as a latent tumour-suppressor mechanism that can be engaged by tumour necrosis factor-related apoptosis-inducing ligand (TRAIL, also known as TNFSF10) to suppress translation of the anti-apoptotic protein FLIP (also known as CASP8 and FADD-like apoptosis regulator (CFLAR)) (38).

As a consequence, chronic RALA activation can sensitize cells to apoptosis by weakening the brakes that restrain activation of the apoptosome. Intriguingly, two additional proteins engaged on activation of Ral — Jun N-terminal kinase (JNK, also known as mitogen-activated protein kinase 8 (MAPK8)) (39) and nuclear factor κ B (NFKB) (40) — can modulate FLIP protein accumulation through induction of protein turnover (41) or activation of gene expression, respectively (42) (FIG. 2). This raises the possibility that FLIP is a convergence point for combinatorial signals that couple Ral regulatory network activity to cell-death response thresholds.

ZONAB

The Y-box transcription factor ZONAB is a tight junction-associated protein (43) that was isolated in a RALA–GTP-interaction trap assay³⁰. In low-density epithelial cultures ZONAB localizes to the nucleus and participates in the activation of genes that promote cell-cycle progression, including *CCND1* (encoding cyclin D1) and *PCNA* (encoding proliferating cell nuclear antigen) (FIG. 1). The formation of tight junctions between neighbouring epithelial cells allows ZO-1 (also known as tight junction protein 1 (TJP1)) to recruit ZONAB to the plasma membrane, thereby restricting its capacity to engage gene targets in the nucleus (44). This relationship presents ZONAB as a key component of the molecular framework that couples cell density to proliferation control. Indeed, ZONAB depletion is sufficient to impair proliferation of non-tumorigenic human mammary epithelial cultures, whereas overexpression can deflect cell contact-mediated inhibition of cell-cycle progression (45, 46). Given that the latter is a hallmark of tumorigenic transformation, mobilization of ZONAB upon Ral activation becomes a compelling scenario that may partially account for the capacity of Ral protein activation to relieve proliferative restraints.

Ral and the exocyst

Regulation of the SEC6–8 complex, also known as the exocyst, is a major occupation of Ral proteins in cells, and might represent an overarching context for many of the cell biological systems that are responsive to Ral G-protein activation (3). The exocyst is a large multiprotein complex responsible for the appropriate targeting and

tethering of a subset of secretory vesicles to specific dynamic plasma membrane domains (FIG. 1), including the basolateral surface of epithelial cells, the growth cones of differentiating neuronal cells, sites of synapse formation, the mitotic abscission plane and the leading edge of migrating epithelial cells (47-49). This has direct consequences on the establishment of appropriate cellular architecture, and the generation and maintenance of functionally specialized plasma-membrane domains. Ral proteins engage the exocyst by direct interaction with two distinct subunits, EXO84 and SEC5, to promote assembly and function of the full heterooctomeric complex (33). Beyond physical association, the mechanistic basis for Ral-dependent exocyst assembly and mobilization has yet to be established. However, it is clear that the Ral–exocyst regulatory node is directly employed for the maintenance of epithelial cell polarity (31), cell motility (50) and cytokinesis (51). Deregulation of these activities would be expected to have acute consequences on tumour cell proliferation and metastasis, but direct functional relationships of the exocyst to tumour initiation or progression remain to be uncovered.

Subverting host defence signaling

Another important factor that might explain the occurrence of Ral activation in tumorigenesis is the RALB-specific contribution to cancer cell survival through activation of TANK-binding kinase 1 (TBK1) (9). This kinase is a central node in the regulatory network required to trigger host defence gene expression in the face of a virally compromised environment (52-61). Through a process that is tethered to the exocyst, but perhaps independent of canonical exocyst function, the RALB–SEC5 effector complex directly recruits and activates TBK1 in response to viral exposure. Although dispensable for survival of normal cells in culture, constitutive engagement of this pathway in a variety of cancer cells, through chronic RALB activation, restricts initiation of apoptotic programmes that are normally activated in the context of oncogenic stress (9). The functional relationship of the RALB–SEC5–TBK1 activation complex with tumour cell survival indicates that oncogenic transformation can commandeer cell-autonomous host defence signalling to deflect cell-death checkpoint activation. This relationship exposes a novel aspect of the aberrant cell regulatory programmes supporting tumorigenicity, and offers the possibility that proteins like TBK1 might be conceptually

ideal candidate targets for the development of drugs with a large therapeutic window (FIG. 3).

TBK1 occupies the non-canonical branch of the I κ B kinase family together with IKK ϵ (also known as IKBKE). These kinases are 48% identical at the aminoacid sequence level and share the job of directly mobilizing the interferon regulatory factor 3 (IRF3) and IRF7 transcription factors to drive the interferon response. Whereas TBK1 is constitutively expressed, IKK ϵ is engaged as an immediate early gene product of innate immune signaling (62).

A convergent observation with the study described above was the isolation of IKK ϵ in a screen by Hahn and colleagues for artificially myristoylated kinases that could cooperate with extracellular signal-regulated kinase activation to transform telomerase-immortalized human embryonic kidney cells (63). Importantly, these investigators found that the genomic locus encoding IKK ϵ is frequently amplified in breast cancers, and IKK ϵ expression is required for breast cancer cell survival. A pressing question is the identity of the TBK1 and IKK ϵ substrates that support cancer cell survival and represent the heart of a potential tumour-specific vulnerability. Chronic activation of TBK1 and IKK ϵ in cancer cell lines is correlated with increased transcriptional activity of IRF3, a canonical TBK1 substrate (54), and induction of interferon-response gene (IRG) expression (9, 63). Given the contribution of inflammatory signals in general and TBK1 in particular to a productive tumour microenvironment (64, 65), together with the observation that poor patient outcome is associated with increased IRG expression in tumours (66), IRF3 stands out as a logical TBK1 and IKK ϵ effector in cancer. However, at the cell-autonomous level, IRF3 depletion did not mimic the consequences of TBK1 or IKK ϵ depletion on survival, suggesting that distinct substrates are responsible for this phenotype (9, 63). Although possible redundancy with IRF7 has not been explored, the caspase inhibitor X-linked inhibitor of apoptosis protein (XIAP, also known as BIRC4) has been reported as a candidate TBK1 substrate (66), and IKK ϵ can drive chronic NF κ B activation in tumour cells to deflect cell death (63, 67). The *Drosophila melanogaster* TBK1 and IKK ϵ orthologue, ik2, drives *D. melanogaster* IAP protein turnover by promoting phosphorylation-dependent polyubiquitylation and degradation. This relationship apparently relieves restraints on non-apoptotic caspase activity rather than

driving cell death (68). The biological relevance of a conserved TBK1–XIAP relationship in mammalian cells is unknown, however it is intriguing to note that loss-of-function XIAP mutations cause X-linked lymphoproliferative syndrome.

Mutations in human cancer

The most compelling indications of the relevance of regulatory systems to the initiation or progression of cancer invariably come from human genetics. For example, numerous somatic mutations associated with disease have been identified in every regulatory node surrounding the core Ras family members, including loss-of-function mutations in GTPase-activating proteins (for example neurofibromin 1 (NF1)), and gain-of-function mutations in Ras guanyl nucleotide exchange factors (such as SOS1), Ras effectors (such as Raf proteins kinases and phosphatidylinositol 3-kinases) and the Ras proteins themselves (69). Such evidence for the Ral regulatory network, if it exists, remains to be uncovered (70). Corollaries to the canonical oncogenic Ras mutations that obliterate GTPase activity and therefore freeze Ras proteins in the ‘on’ conformation might never be forthcoming for Ral proteins owing simply to the biology of Ral effector engagement. For example, multiple observations indicate that Ral proteins must cycle between GDP and GTP conformations for productive mobilization of the exocyst. However recent large-scale cancer genome sequencing efforts have identified a cadre of mutations in genes encoding proteins proximal to Ral function, including Ral guanyl nucleotide exchange factor proteins, components of the exocyst machine and TBK1 (TABLE 1). Whether these somatic cell mutations represent a rich source of functional relevance or are simply passenger mutations that randomly accumulate during tumour evolution remains to be explored.

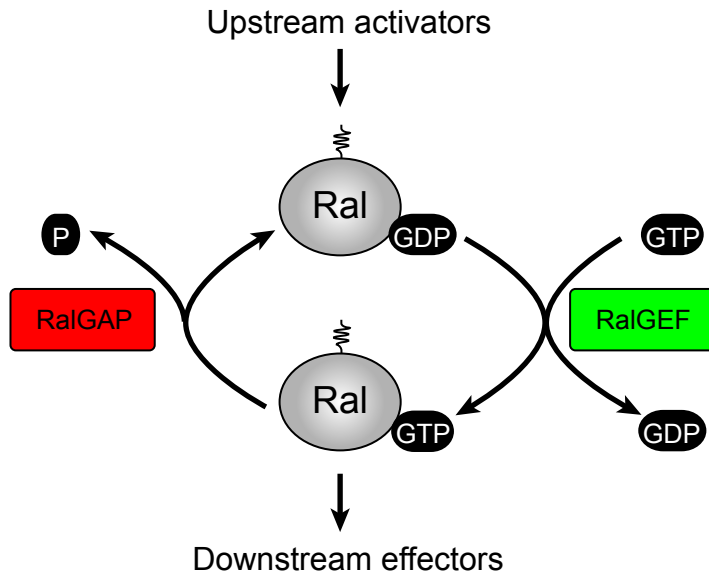
Future prospects

Although numerous compounds have been identified that kill cancer cells, the difficulty in identifying drugs that are efficacious at concentrations that avoid damage to normal cells and tissues remains an obvious bottleneck in the successful translation of new therapies into the clinic. This circumstance has spurred intense efforts to identify key molecular aberrations that drive tumour initiation and progression as an initial step

towards deriving agents with a high therapeutic index together with low toxicity. However, the cell-autonomous events that drive the genesis of human cancers are multifarious and complex. This context makes identification of broadly applicable targeted intervention strategies a seemingly daunting task. However, widespread evidence suggests that a unifying principle governing formation of a 'minimal oncogenic platform' is the co-dependent aberrant regulation of core machinery driving proliferation and suppressing apoptosis. Conditional dependencies on linchpin proteins engaged to drive these pathways during tumorigenesis might represent optimal intervention targets. Recent observations have indicted Ral G-proteins as key offenders in the corruption of the core cell-autonomous machinery driving oncogenic transformation. Further elaboration of the molecular systems engaged by RALA and RALB and their mechanistic relationships is required to help define the utility of targeting this network for cancer therapy.

BOX 1: The G-protein cycle

BOX 1

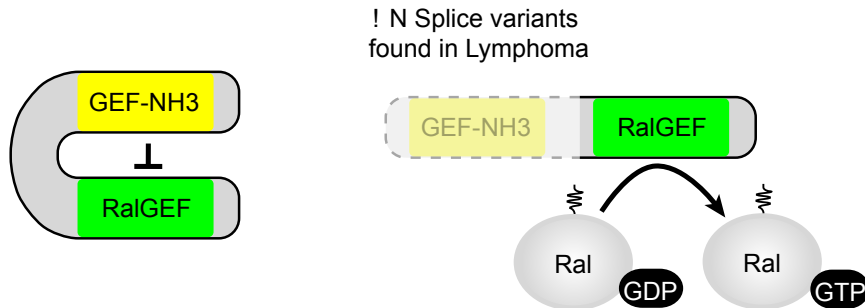


Akin to the vast majority of Ras family members, Ral proteins are coupled to the regulation of dynamic cell biological processes by cycling through guanyl nucleotide-dependent conformational transitions. GTP loading, at a 1:1 molar ratio, is required for effector binding and is driven by association with Ral-specific guanyl nucleotide exchange factors (GEFs). Diverse signalling inputs can engage these exchange factors; including growth factors, hormones, membrane depolarization and even pathogen surveillance machinery (4, 9). The transition to the ‘off-state’ requires hydrolysis of bound GTP through complementation of Ral’s weak intrinsic catalytic activity (71) by GTPase activating proteins (GAPs) (72).

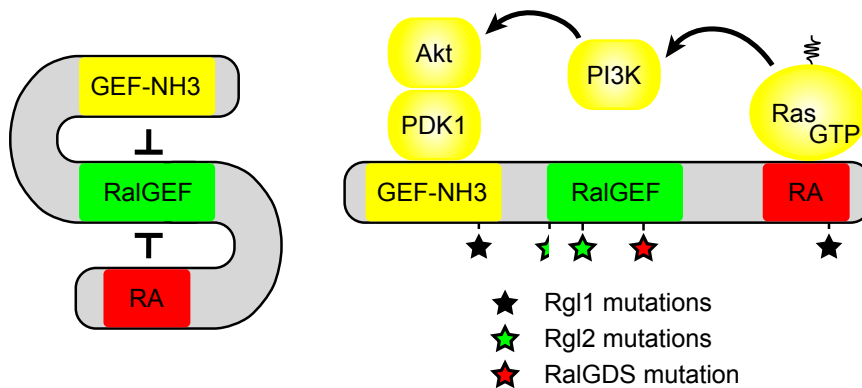
BOX 2 : The RalGEF family and their regulatory cues

BOX 2

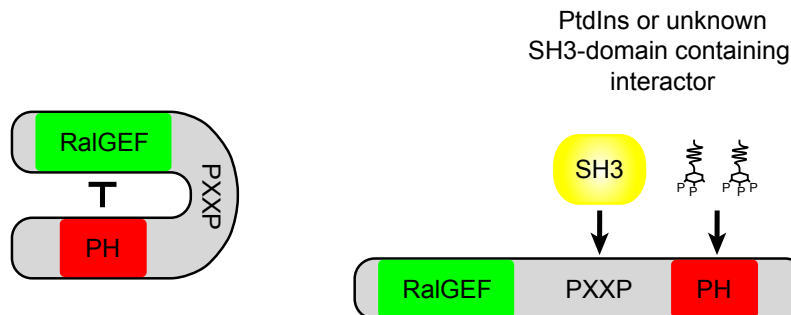
A



B



C



Ral GTPases are engaged in response to a broad variety of mitogenic, trophic and hormonal signals by a diverse group of guanyl nucleotide exchange factors (GEFs) that fall into two major groups: those that can be directly Ras-responsive through a carboxy-terminal Ras-binding domain (RALGDS, RGL1, RGL2), and those that are apparently mobilized by phosphatidylinositol second messengers through a C-terminal pleckstrin homology (PH) domain (RALGPS1, RALGPS2)⁴. Virtual expression profiling, based on

UniGene annotation of expressed sequence tags, suggests that all five members are broadly expressed in both normal tissues and tumours. In addition, human retinal G-protein coupled receptor (RGR) has promiscuous exchange factor activity towards Ras G-protein family members, including Ral (73). The mechanistic basis of RalGEF activation is poorly understood; however, a series of observations suggest that one important aspect involves relief of autoinhibitory interactions of amino-terminal and/or C-terminal regulatory motifs (indicated in the figure in yellow and red, respectively) with the catalytic domain (indicated in green). In the case of RGR (**A**), N-terminal truncation mutants found in lymphoma exhibit cell transformation activity in cell culture (73) and transgenic expression in thymocytes of p15INK4b (also known as Cdkn2b)-defective mice induce a high incidence of thymic lymphomas (74). Consistently with this regulatory motif, 3-phosphoinositide-dependent protein kinase 1 (PDPK1) associates with the N terminus of RALGDS to relieve autoinhibition of catalytic activity in response to epidermal growth factor receptor activation (75, 76). RALGDS is also a direct effector of Ras–GTP through the C-terminal Ras association (RA) domain (**B**). Ras-dependent derepression of intramolecular autoinhibitory interactions is an emerging theme among Ras–effector relationships (2). Finally, the RALGPS2 PXXP–PH domains have dominant inhibitory activity (**C**), decreasing Ral–GTP accumulation by 50% when expressed in HEK 293 cells. The sensitivity of RalGPS2 activity to wortmannin suggests that this domain is responsive to phosphatidyl inositol kinase activity (77). Intriguingly, a collection of RalGEF mutations have been identified in human tumours that are distributed among sequences encoding both catalytic and regulatory regions (TABLE 1). Activating mutations in the Ras exchange factor SOS1 cause a distinctive form of Noonan Syndrome, a developmental disorder characterized by facial dysmorphism, short stature, congenital heart defects and skeletal anomalies (78). These mutations cluster in or near the N-terminal GEF domain which is important in maintaining the protein in its autoinhibited form. The functional consequences of the identified RalGEF mutations, if any exist, remain to be determined. PtdIns, phosphatidyl inositol; SH3, SRC homology 3.

FIGURE 1: Cell biological systems modulated by direct Ral–effector relationships

Ral proteins engage multiple effectors to direct distinct but perhaps interlocking dynamic biological processes. RALA has a major role in secretory vesicle trafficking through the exocyst, but can also participate in the regulation of gene expression and protein translation through ZO-1-associated nucleic acid-binding protein (ZONAB) and RLIP (also known as ralA binding protein 1), respectively. RALB can directly engage the SEC5 subunit of the exocyst to facilitate host defence responses. Chronic activation of RALA and RALB in cancer probably uncouples the indicated machinery from normal regulatory cues to promote pathological cell proliferation. CDC42, cell division cycle 42; ER, endoplasmic reticulum; IRF3, interferon regulatory factor 3; NFκB, nuclear factor κB; TBK1, TANK-binding kinase 1.

Figure 1

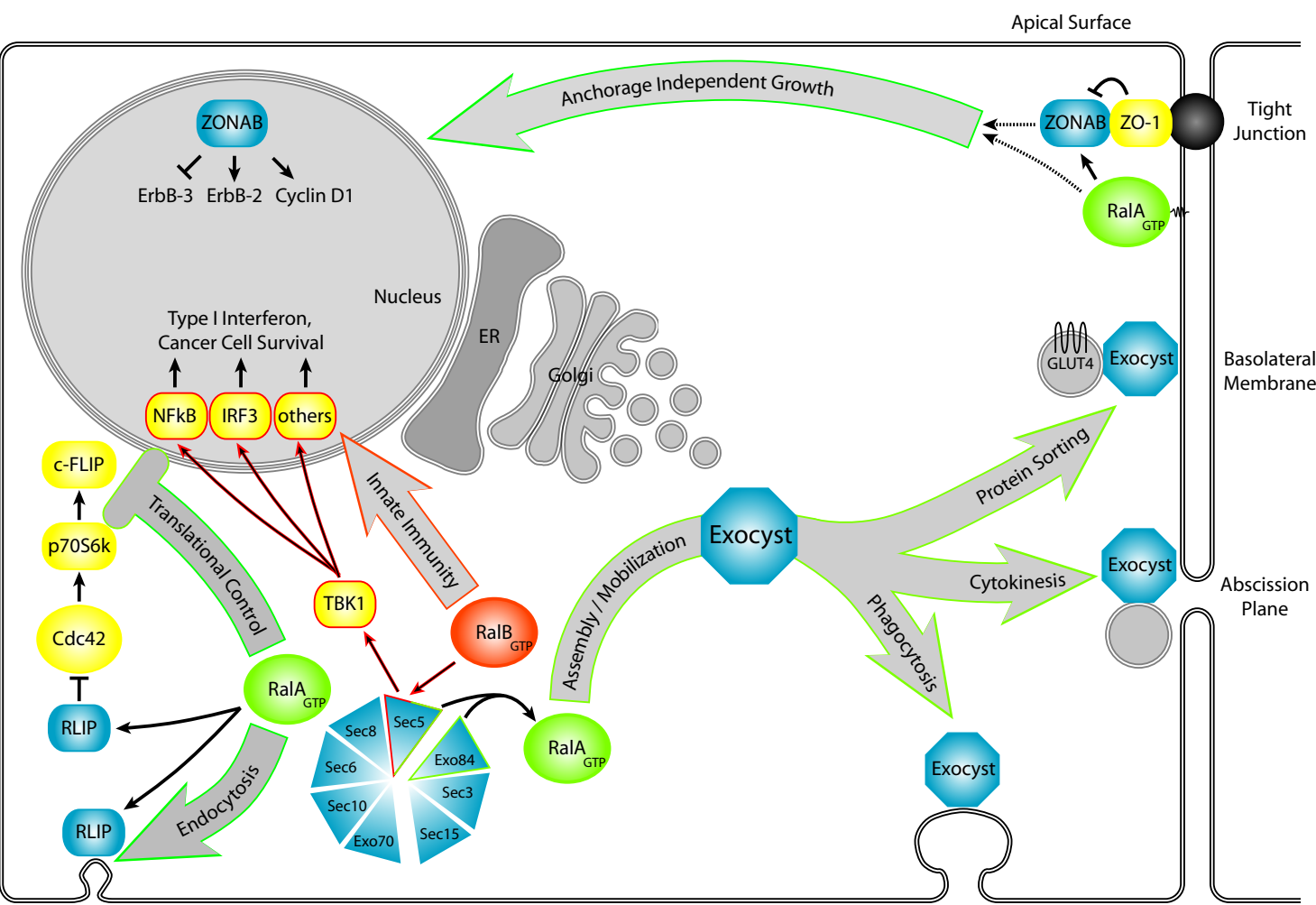
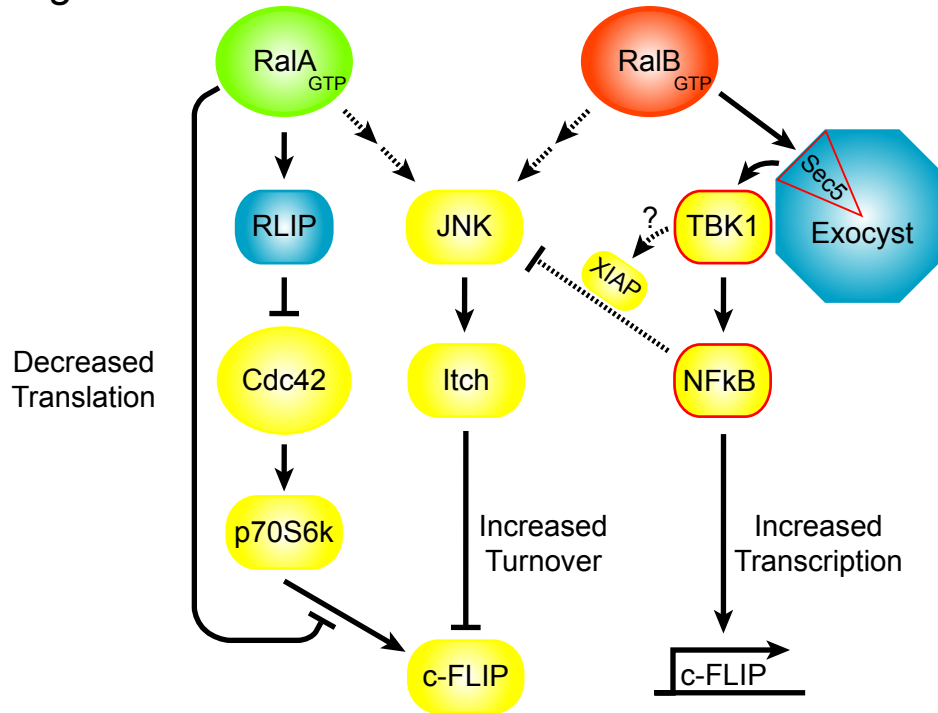


Figure 2: Combinatorial integration of Ral activity by FLIP

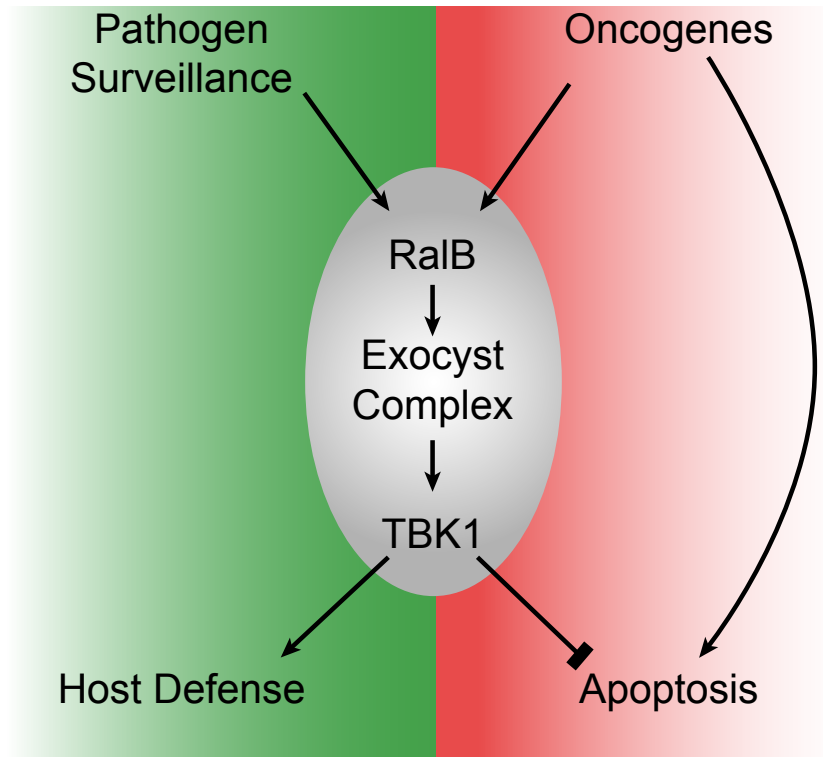
Figure 2



Distinct effector use by RALA and RALB may have opposing consequences on the accumulation of the pro-survival factor FLIP. RALA can inhibit FLIP through both increased protein turnover, following activation of the Jun N kinase (JNK)–ITCH pathway, and reduced translation following inhibition of CDC42. By contrast, activation of nuclear factor κ B (NF κ B) by RALB would be expected to increase FLIP mRNA expression. TBK1, TANK-binding kinase 1; XIAP, X-linked inhibitor of apoptosis protein.

Figure 3: Oncogenic subversion of host defence signaling

Figure 3



In non-tumorigenic epithelia, RALB participates in antiviral surveillance and response signaling by facilitating activation of TANK-binding kinase 1 (TBK1; green). Chronic activation of RALB as a consequence of oncogene expression can engage TBK1 to support cell survival in the face of oncogenic stress (red). The latter represents a conditional dependency on TBK1, loss of which can be synthetically lethal with upstream oncogenic gain-of-function mutations.

Table 1: Mutations in genes encoding proteins proximal to Ral function

Gene	Mutations in cancer
RalGDS	colon (R496L) (79)
Rgl1	breast (Y209S, V734M) (79)
Rgl2	skin (W272*, G314R) (80)
RgR	lymphoma (Δ N splice variants) (73)
Sec6	breast (Y59N, A514D) (79)
Sec8	colon (S220F, A599T, frameshift) (79)
TBK1	breast (D296H), colon (G410R) (81)

CHAPTER TWO

Part One: The Exocyst Complex

The exocyst was identified through the isolation of temperature-sensitive secretory (*sec*) mutants of the yeast *Saccharomyces cerevisiae*. Ten of the *sec* genes were implicated in transport from the Golgi to the cell surface, and six *sec* genes encode subunits of the octomeric exocyst complex: Sec3p, Sec5p, Sec6p, Sec8p, Sec10p, and Sec15p (82). The two remaining exocyst components, Exo70p and Exo84p, were biochemically identified from the purified yeast complex or the homologous mammalian complex, respectively (82, 83). The metazoan exocyst complex has a similar role in membrane trafficking to its yeast counterpart, and each of the eight subunits shares sequence similarity with the equivalent yeast subunit. The canonical function of the fully formed hetero-octomeric exocyst complex is to tether vesicles at the site of membrane fusion; however, a number of subunit and subcomplex specific activities have been described which contribute to the tethering process or to altogether unrelated processes. Specifically, Sec3 and Exo70 have been described to demarcate exocytic sites (84, 85). In addition, Sec15 is necessary for proper localization of a subset of exocyst subunits (Sec5 and Sec8, but not Sec6) to neuron terminals (86).

The structures of larger domains of four exocyst subunits have been solved: residues 382–699 of Sec15 (87), residues 67–623 of yeast Exo70p (88, 89), residues 523–753 of yeast Exo84p (88), and residues 411–805 of yeast Sec6p (90). The structures of each have a tandem repeat of helical-bundle units, which has no detectable architectural similarity to structures in the Dali database (91). The bundles pack together to create elongated rod-like structures. Secondary structure predictions of the other four exocyst subunits suggest that their structures may also be composed of similar helical bundles (91). Mapping of the binding sites for Sec8p and Sec10p on the Exo70p structure indicates that interactions are distributed along the length of the rod structure, which supports a model where the subunits pack together in an elongated side-to-side fashion (88). Quick-freeze/deep-etch electron micrographs of exocyst complexes also lend support to a model of side-to-side interactions of rod-shaped subunits (91). As illustrated in Figure 4, the rod-shaped architecture of individual exocyst subunits provides the

exocyst with a dynamic interaction interface for loading different effector molecules onto the surface of the exocyst. The exposed surface of one exocyst subcomplex may have many unique binding sites in comparison to subcomplexes of different composition or the fully assembled exocyst holocomplex.

Figure 4

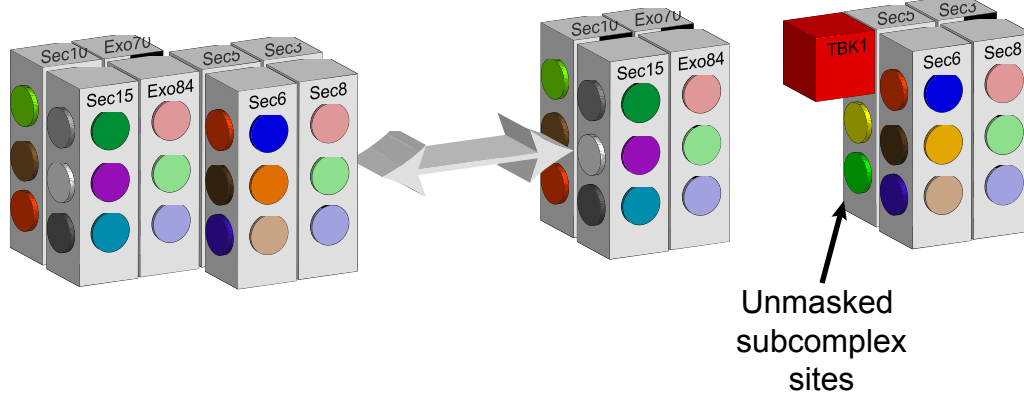


Figure 4: Rod-like exocyst complex assembly

Using yeast two hybrid and *in vitro* transcription and translation assays, many intracomplex interactions between exocyst subunits have been described. These results are summarized in Table 2.

TABLE 2 (adapted from (91))	
Subunit	Exocyst subunit interactions
Sec3	Sec5 (92), Sec8 (92)
Sec5	Sec3 (92), Sec6 (92), Exo84 (33)
Sec6	Sec5 (92), Sec8 (92, 93), Sec10 (93), Exo70 (92)
Sec8	Sec3 (92), Sec6 (92, 93), Sec10 (92, 93), Exo70 (92)
Sec10	Sec6 (92), Sec8 (92, 93), Sec15 (92), Exo70 (92)
Sec15	Sec10 (92), Exo70 (92), Exo84 (92)
Exo70	Sec6 (92), Sec8 (93), Sec10 (93), Sec15 (92), Exo84 (92)
Exo84	Sec5 (33), Sec15 (92), Exo70 (92)

Because each subunit can form multiple interactions, there are a very large number of

different subcomplexes which can be formed. The selective contribution of a given subunit to a specific cell process can be investigated using RNAi; however, it is difficult to definitively describe the composition of a subcomplex which is utilized by the cell during a specific process. In addition, the dynamic re-assembly of exocyst subunits during a process may be critical to exocyst function. To gain understanding of the function of exocyst subcomplexes towards a given cell process, I hypothesize that one must use multiple approaches:

- (1) The composition of exocyst subcomplexes must be monitored during the cell process. If focused on a particular subunit, one could immunoprecipitate that subunit. Then, separate the immunoprecipitated subcomplexes using a size exchange column.
- (2) Using RNAi, the contribution of each subunit can be investigated.
- (3) Using complementation assays, RNAi phenotypes for each subunit could be complemented with point mutants for a specific subunit which are selectively uncoupled from binding to individual exocyst binding partners.

At the time of writing this document, only approach #2 is fully utilized. For approach #1, we lack antibodies for each subunit which are capable of immunoprecipitating the larger exocyst holocomplex. For approach #3, we have not identified point mutants of the individual exocyst subunits which selectively uncouple specific subunit interactions. Future endeavors generating these tools will greatly assist in unraveling the composition and contribution of exocyst subcomplexes to distinct biological phenotypes.

Part Two: Ral-dependent exocyst signaling events

As mentioned in chapter one, a distinct feature of the mammalian exocyst complex in contrast to the yeast exocyst complex is the association of members Sec5 and Exo84 with Ral GTPases. There is no homologue for the Ral GTPases in yeast, and the Ral binding domains of mammalian Sec5 and Exo84 are absent in their yeast homologues. Thus, the co-evolution of the Ral and Ral–exocyst interactions in metazoans may represent an adaptation to the unique phenotypes of individual cells within a multicellular organism. Consistent with this hypothesis, Ral–exocyst complex has been implicated in a number of cell biological phenotypes which are unique to multicellular

organisms. The most commonly described function of the Ral–exocyst complex is the delivery and tethering of vesicles at specific subcellular locales. In polarized epithelial cells, Ral–exocyst function is required for appropriate sorting of membrane proteins to the basolateral membrane but not the apical membrane (31, 33). The activation of both RalA and RalB contribute to neurite branching but not neurite extension in cortical and sympathetic neurons (94). RalA and an Exo84-containing subcomplex of the exocyst were recently described to be necessary to establish neuronal polarity (95). Specifically, RalA was shown to regulate the association of the exocyst with two key mediators of neuronal polarity, aPKC and PAR-3, during the early stages of neuronal polarization (95). Thus, the function of Ral–exocyst complexes in adaptive cell processes can be arbitrarily broken into two classes:

- (1) Passive: Processes where delivery of membrane and proteins to discrete subcellular locales in which the enrichment of certain proteins defines that distinct phenotype (Example: basolateral membrane sorting).
- (2) Active: Processes where the exocyst orchestrates not only delivery to discrete subcellular locales but also assembly and activation of the signal transduction cascades which contribute to the adaptive cell process (Example: neuronal polarity).

Although it is convenient to define these two classes, it is possible that the Ral–exocyst complex may participate actively in each adaptive cell process and only the absence of our knowledge of this contribution may lead us to consider that the Ral–exocyst complex may be a passive contributor to a given cell process.

Phenotype Study: RalA mediates insulin-stimulated delivery of GLUT4

Insulin stimulates glucose uptake in adipose and muscle tissues by stimulating the translocation of the glucose transporter Glut4 to the plasma membrane. The exocyst plays a critical role in insulin-mediated glucose uptake by facilitating the docking of Glut4 vesicles to the plasma membrane (49, 96). The growing literature on this phenotype provides us with many insights into the intricacies of how Ral–exocyst complex functions during an adaptive cell process. As outlined in chapter one, Ral proteins are regulated by RalGEFs (positive, increase Ral·GTP) and RalGAPs (negative, decrease Ral·GTP). There

have been two RalGAP protein complexes identified, RalGAP1 and RalGAP2. Each complex contains a unique alpha subunit, RalGAP α_1 or RalGAP α_2 , and a common beta subunit, RalGAP β . These complexes are structurally and catalytically similar to the tuberous sclerosis tumor suppressor complex, which acts a GAP protein for the small G-protein, Rheb (72). During insulin stimulation, activation of the protein kinase Akt by PI-(3)-kinase is critical for Glut4 trafficking to the plasma membrane (97). Upon insulin stimulation of adipocytes, Akt phosphorylates the alpha subunit of RalGAP1 and relieves the inhibition of RalGAP1 on RalA (98). RalA then associates with Sec5 and stimulates exocyst assembly, which facilitates the delivery and tethering of Glut4 at the plasma membrane (99). Although one or several RalGEFs likely contribute to this process, none have been implicated to date.

Upon docking at the plasma membrane, it is hypothesized that RalA and Sec5 must dissociate to allow exocyst interaction with v-SNARE complexes, which facilitate the fusion of tethered vesicles with the plasma membrane. Because a constitutively 'active' mutant RalA(G23V), which cannot hydrolyze GTP, can increase glucose uptake independent of insulin administration, it is unlikely that RalA-Sec5 interactions are dissociated by stimulation of RalA-GTP hydrolysis by RalGAP proteins (99). Intriguingly, the interaction of RalA and Sec5 is reported to be dissociated by phosphorylation of Sec5 in the Ral Binding Domain (RBD) at Ser-89 by PKC (99). Although within the RBD of Sec5, Ser-89 is not part of the RalA-Sec5 interaction interface; therefore, it follows that Ser-89 phosphorylation may allosterically alter the Ral-GTP binding interface of Sec5. A phospho-mimetic S89D mutation had reduced affinity for RalA-GTP, which adds support to this conclusion (99). In addition to the GTP-regulated association of RalA with Sec5, RalA exhibits GTP-independent association with the atypical myosin protein, Myo1c (100). Myo1c acts as a motor protein for trafficking RalA-exocyst associated Glut4 containing vesicles along actin cables for plasma membrane delivery (100). The association of Myo1c with RalA required the second messenger calcium (100). The Ca²⁺-bound Calmodulin (CaM) served as the light chain for Myo1c within the RalA-Myo1c complex, and Ca²⁺-bound CaM was required for complex formation *in vitro* (100). The contributions of RalA and the exocyst to insulin-stimulated Glut4 delivery reveals several key features of Ral-exocyst function:

- (1) Ral proteins are actively inhibited by RalGAP complexes before stimulation.
- (2) Dissociation of Ral–exocyst complexes may be achieved through phosphorylation of the Ral effector member of the exocyst complex.
- (3) Ral proteins may associate with motor proteins in a regulated (calcium) but GTP-independent manner.

Phenotype Study: Distinct Ral–exocyst complexes contribute to cytokinesis

The ultimate step of cell division is cytokinesis, which is required for high-fidelity chromosomal segregation. In metazoans, cytokinesis consists of actino-myosin ring formation and cleavage furrow ingression, which create a cytoplasmic bridge. The abscission of the cytoplasmic bridge requires mobilization of secretory vesicles and exocytosis (101-105). The exocyst complex is required for late cytokinesis and is recruited to the midbody for the abscission of the intracellular bridge (103). Defects in cytokinesis can manifest as the fusion of nascent ‘daughter cells’ leading to binucleate cells or in lingering daughter cell attachments as an outcome of failed or delayed abscission. The depletion of RalA is reported to significantly increase the percentage of binucleate cells but not intracellular bridges (9, 51, 106). Conversely, RalB depletion does not affect the percentage of binucleate cells but strongly induced the accumulation of cells with intracellular bridges (106). Complementation of RalA and RalB depleted cells with effector-selective point mutants reveals that RalA and RalB share Exo84 and PLD1 as effectors for cytokinesis, and Sec5 is a RalA-specific effector in cytokinesis (106). RalA and Sec5 co-localize at the midbody ring, and both RalA and Sec5 are required for the recruitment of exocyst components to the midbody rings early during cytokinesis (106). Conversely, RalB is not enriched on the midbody until late-stage cytokinesis and is dispensable for the recruitment of exocyst components to the midbody early during cytokinesis (106).

As described in chapter one, there are six RalGEFs in the human genome, which ‘activate’ RalA and RalB to the effector binding Ral·GTP state. Four of the RalGEFs (RalGDS, RGL1, RGL2, RGL3) contain Ras association (RA) domains which allow for their activation by ‘active’ Ras·GTP, and two RalGEFs (RalGPS1 and RalGPS2) are Ras-independent. In cytokinesis, depletion of either RalGDS and RalGPS2 leads to the

accumulation of binucleate cells similar to that seen in RalA depleted cells (106). In contrast, depletion of RGL1 or RalGPS1 causes an accumulation of intracellular bridges which phenocopies RalB depletion (106). RGL2 and RGL3 are reported to be dispensable for cytokinesis. RalA, RalGDS, and RalGPS2 each localize to the early midbody ring and are necessary for the recruitment of core exocyst components. In contrast RalB, RGL1, and RalGPS1 are not enriched on the midbody until late-stage cytokinesis and are dispensable for recruitment of core exocyst components (106). This landmark study reveals several key features of Ral–exocyst function:

- (1) A discrete subset of both Ras-dependent and Ras-independent RalGEFs couple with RalA (RalGDS and RalGPS2) and RalB (RGL1 and RalGPS1).
- (2) RalA and RalB regulate discrete signaling events but may exhibit coordinated function in the same biological process.
- (3) Ral proteins may utilize multiple effector complexes during a single biological process.
- (4) Ral proteins may utilize the exocyst holocomplex, exocyst subcomplexes, or both during a given biological process.

Distinct Ral–exocyst complexes contribute to innate immunity

As covered in chapter one under ‘Subverting host defence signaling’, the hyper ‘activation’ of RalB within cancer cells supports suppression of oncogene-induced cell death by triggering the assembly and activation of the kinase TBK1 on the Ral effector and exocyst subunit, Sec5. Surprisingly, this signaling pathway is utilized in normal cells during viral infection (9). TBK1 is an important node in the regulatory network required to trigger host defense gene expression in response to viral expression. Both RalA and RalB were ‘activated’ to the GTP-bound state during the course of an infection with Sendai virus, but only RalB was necessary for the activation of TBK1 (9). From the seed of this singular observation, grew the fruit that would become this thesis—I hypothesized that both Ral proteins likely regulated some of the many cell processes which occur during the course of a viral infection, such as, cytoskeleton remodeling, gene transcription, vesicle trafficking, apoptosis, and macroautophagy to name a few. There are many cell behaviors which occur in response to viral infection; however, one

observation by Dr. Yu-Chen Chien lead us to focus on macroautophagy. Dr. Chien observed that during the course of Sendai infection, RalB localized to discrete cytosolic punctae of which some but not all were acidic. First, the reader must understand that my main interest in joining Dr. White's lab was to investigate spatially and temporally discrete signal transduction networks regulated by small G-proteins. When Dr. Chien left the lab to further her career, I began to investigate the connection between the Ral proteins and macroautophagy. Macroautophagy, which will be further described in chapter three, is a dynamic membrane-driven process which requires the concerted assembly of signal transduction cascades at dynamically assembled membranes for the construction of a discrete double-membrane structure called the autophagosome. I hypothesized that the Ral-exocyst vesicle trafficking network regulated the formation of autophagosomes during viral infection because, as reviewed in this chapter, the Ral-exocyst network had been described to regulate both discrete membrane trafficking events as well as the activation of signal transduction networks, and these roles are uniquely suited to solve the complex problem of how to coordinate the dynamic assembly of autophagosomes. In retrospect, this hypothesis was overreaching given the information we had at the time; however, we ultimately found that the Ral-exocyst network was an integral regulator of autophagosome biogenesis.

CHAPTER THREE

Part One: RalB and the exocyst mediate the cellular starvation response by direct activation of autophagosome assembly (Cell, 2011)

INTRODUCTION

The critical role of macroautophagy (herein referred to as autophagy) in tissue homeostasis, cellular adaptation to nutrient restriction and in clearance of pathogens and dysfunctional organelles suggests *de novo* generation of the double-membrane autophagosome requires responsiveness to inductive signals that specify location, contents, and duration (107-109). A number of key signaling events have been identified that specify autophagosome biogenesis. Among the earliest is the de-phosphorylation of inhibitory mTOR-dependent sites on the ULK1-Atg13-FIP200 induction complex (110, 111). This presumably releases ULK1 activity to facilitate auto-phosphorylation of the ULK1-ATG13-FIP200 complex and assembly with the vertebrate-specific autophagy protein ATG101 (110-113). Through currently undescribed mechanisms, this leads to the activation of an autophagy specific class III PI(3)K complex, the Beclin1-ATG14L-VPS34-VPS15 complex. This activity coats a cup-shaped isolation membrane with phosphatidylinositol-3-phosphate, PI(3)P, which serves as a recruitment signal for the ATG16-ATG5/ATG12 component of the isolation membrane elongation machinery (114). Two ubiquitin-like molecules, ATG12 and LC3, undergo conjugation to ATG5 and phosphatidylethanolamine respectively to promote autophagosome formation. ATG12 is activated by ATG7 (E1), transferred to ATG10 (E2), followed by covalent linkage to an internal lysine on Atg5 (115, 116). In the second conjugation system, LC3 is first cleaved by the cysteine protease, ATG4, which exposes a C-terminal glycine residue. ATG7 (E1) activates LC3 and transfers it to ATG3 (E2) (117-119). LC3 is then conjugated to phosphatidylethanolamine with assistance of ATG5/12 conjugates (120-122). The lipidated LC3, LC3-II, coats the inner and outer surfaces of the autophagosome, and along with ATG5, serves as a discrete marker of autophagosomes and autophagosome precursors, respectively (122-125). These key signaling events are coordinated with dynamic membrane events to culminate in the formation of a double-membrane autophagosome. The autophagosome ultimately fuses with a lysosome that

facilitates the turnover of engulfed material by lysosomal/vacuolar acid hydrolases. How signaling intermediates are coordinated with the dynamic membrane events during the autophagosome biogenesis is currently unknown.

RalA and RalB are close relatives to the founding members of the Ras GTPase superfamily. They are engaged in response to mitogenic, trophic, and hormonal signals by a diverse group of guanyl nucleotide exchange factors that fall into two major groups: those that are directly Ras-responsive via a carboxyterminal Ras binding domain and those that are apparently mobilized by phosphoinositide second messengers via a carboxyterminal pleckstrin homology domain (4, 126). While a number of Ral-GTP effector proteins have been identified that couple RalA/B activation to dynamic cell biological processes, an overarching occupation of the Ral GTPases is the direct regulation of the Sec6/8, or exocyst, complex (4, 126). Two members of the heterooctameric exocyst complex, Sec5 (*EXOC2*) and Exo84 (*EXOC8*), are bona fide effector molecules that mediate RalA/B regulation of dynamic secretory vesicle targeting and tethering processes (31-33, 126). RalA-dependent mobilization of exocyst holocomplex assembly is critical for maintenance of apical/basolateral membrane identity in polarized epithelial cells (31, 33) and for insulin-stimulated Glut4 delivery to the plasma membrane in adipocytes (100). Distinct from regulation of membrane trafficking, RalB has been demonstrated to mediate signal transduction cascades supporting the host defense response. Upon Toll-like receptor activation, RalB/Sec5 complex assembly directly participates in activation of the innate immune signaling kinase TBK1 to facilitate an interferon response (9). This combination of roles, vesicle trafficking/tethering and signal cascade assembly/activation, suggests that Ral/exocyst effector complexes may coordinate dynamic membrane trafficking events with stimulus-dependent signaling events.

Here we show that the small G-protein, RalB, and an Exo84-dependent subcomplex of the exocyst are critical for nutrient starvation and pathogen-induced autophagosome formation. Native RalB proteins localize to sites of nascent autophagosome formation and accumulate in the “active” GTP-bound state under nutrient limited conditions. RalB,

but not its close homolog RalA, is required for autophagosome biogenesis and is sufficient to activate autophagy in human epithelial cells. The mechanism of action is through direct triggering of vesicle nucleation by assembly of an active ULK1-Beclin1-VPS34 initiation complex on the RalB effector protein Exo84. Thus, the RalB-Exo84 effector complex defines a key proximal regulatory component of the cellular response to nutrient deprivation.

RESULTS

Association of the exocyst with autophagosome assembly machinery.

Accumulating observations indicate direct participation of the heterooctameric exocyst (aka Sec6/8) complex in adaptive responses to pathogen challenge (9, 127-129). Most strikingly, core innate immune signaling through TBK1 and STING is supported by the Sec5 subunit of the exocyst (9, 128, 129). To help generate molecular leads that may account for the participation of exocyst components in host defense signaling, we used high throughput yeast two-hybrid screening to isolate a cohort of proteins that can associate with exocyst subunits (130). Among this cohort, both negative (*RUBICON*) and positive (*FIP200*, *ATG14L*) modulators of autophagy were isolated in the first-degree interaction neighborhood of Sec3 (see methods). Given the functional convergence of Ral/exocyst signaling and autophagy in pathogen recognition and clearance, we examined the association of exocyst components and autophagy proteins in human epithelial cell cultures. The interaction of Sec3 with RUBICON and ATG14L was validated by expression co-IP (Figure 5A,B). In addition Exo84 and Sec5 could interact with RUBICON and ATG14L, as would be expected if autophagosome machinery/exocyst interactions occur in the context of multisubunit exocyst complexes (Figure 5C,D,E,F). Immunoprecipitation of the core exocyst subunit, Sec8, recovers all characterized components of the exocyst complex (131). Therefore, to examine if the exocyst may be associated with the LC3-modification machinery that drives elongation of isolation membranes, we probed Sec8 complexes for the presence of ATG5/ATG12 conjugates. As shown, Sec8-ATG5/ATG12 complexes were recovered from both overexpression co-IPs (Figure 5G) and by co-immunoprecipitation of endogenous proteins (Figure 1H), indicating a physical integration of the exocyst and autophagosome

assembly machinery.

RalB signaling is required and sufficient for induction of autophagosome formation.

Mobilization of exocyst assembly in response to regulatory inputs is a major occupation of the Ras-like GTPases RalA and RalB (9, 31-33, 94, 100, 106, 132-136). To examine the potential participation of Ral GTPase signaling in the regulation of autophagy, we first tested the consequence of blocking Ral-GTP/effector interactions on amino acid starvation-induced autophagosome accumulation and on isolation membrane encapsulation of bacterial pathogens. Expression of the minimal Ral-binding domain of the Ral effector RalBP1/RLIP76 (RLIP(RBD)) is dominant inhibitory to the action of endogenous RalA and RalB proteins through direct competition with Ral effector molecules (9, 31). As previously demonstrated (137, 138), serum and amino-acid starvation of HeLa cells with Earle's Basic Salt Solution (EBSS) induced re-localization of endogenous LC3 protein from a diffuse cytosolic distribution to a condensed punctate pattern, and significantly decreased the total LC3 signal; consistent with starvation-induced autophagosome formation and maturation. RLIP(RBD) expression blocked both LC3 punctae formation and LC3 turnover (Figure 5I). As a surrogate measure for autophagic flux, we quantitated the total endogenous LC3 signal of individual cells following amino acid starvation, and found that RLIP(RBD) expression inhibited LC3 protein turnover in a dose-dependent fashion (Figure 5K). To investigate the contribution of Ral signaling to pathogen-responsive LC3 modification of membranes, mRFP-LC3 expressing HeLa cells were infected with GFP-labeled *Salmonellae typhimurium*. As expected if Ral signaling supports this response, RLIP(RBD) expression blocked recruitment of LC3 to internalized *Salmonellae* (Figure 5J). In addition, we found that ectopic expression of RalB was sufficient to induce the accumulation of LC3 punctae in cervical cancer cells (Figure 5L,M) and in immortalized bronchial epithelial cells (Figure 5N,O) in the absence of amino acid starvation or pathogen exposure. Remarkably, RalB(G23V) expression in nutrient rich conditions was sufficient to induce an accumulation of LC3 punctae that was 4-5 fold higher than that induced by amino acid deprivation (Figure 5O). This accumulation is likely associated with increased autophagic flux as RalB(G23V)-induced LC3 punctae were further increased by

chloroquine-mediated inhibition of autophagosome turnover (Figure 5O; $P=0.011$, student's T-test), and this correlated with accumulation of phosphatidylethanolamine-conjugated LC3 (Figure 5P). Thus Ral signaling appears to be necessary and sufficient to engage autophagy. Evaluation of interactions between Ral signaling and autophagy in animals was carried out in *Drosophila* dRal hypomorphs (Ral^{35d}), which have a weak loss-of-bristle phenotype associated with post-mitotic cell-specific apoptosis (132). Depletion of ATG14L, ATG1 (ULK1), ATG8a (LC3), ATG6 (Beclin) or VPS34, by in vivo expression of corresponding dsRNA, significantly enhanced the Ral^{35d} phenotype (Table 3).

To directly investigate the individual contributions of human Ral GTPases and exocyst proteins to regulated autophagosome biogenesis, we next tested the consequence of siRNA-mediated RalA, RalB, and exocyst subunit depletion on nutrient-starvation induced autophagy. Depletion of RalA, in a stable GFP-LC3 expressing cell line, had no consequence on GFP-LC3 signal accumulation or punctae formation. In contrast, RalB depletion significantly impaired starvation-induced LC3 punctae formation and LC3 turnover (Figure 6A). The extent of autophagosome inhibition observed upon RalB depletion, as monitored by quantitation of GFP-LC3 punctae and total GFP-LC3 signal intensity, was equivalent to that seen upon depletion of the known components of autophagosome formation, ATG5 or Beclin1 (Figure 6B,C). An equivalent analysis of the exocyst subunits Sec8, Sec5 and Exo84 indicated selective contributions of exocyst components to presumed autophagosome formation. Depletion of Sec8, a central exocyst subunit, had equivalent consequences as depletion of RalB, ATG5 or Beclin1. In contrast, among the two Ral effectors in the exocyst, Sec5 and Exo84, only Exo84 depletion impaired starvation-induced LC3 punctae formation and increased LC3 accumulation (Figure 6B,C). Evaluation of each of the 8 exocyst subunits suggested that in addition to Sec8 and Exo84, Sec3 and Exo70 are limiting for support of autophagocytosis (Figure 6D, and Figure 12A). The selective requirement for Exo84 versus Sec5 indicates that RalB regulation of autophagy is likely independent of the previously characterized RalB/Sec5/TBK1 signaling pathway (9). Additional observations supporting RalB-selective support of autophagosome formation were made through examination of

starvation-induced changes in endogenous LC3 localization and LC3 post translational modification (Figure 6E,F,G). These combined observations indicate that RalB and discrete components of the exocyst are required for autophagosome formation in multiple biological contexts. Activation of endogenous Ral GTPases may also be sufficient to induce autophagy, as depletion of endogenous RalGAP in the absence of nutrient limitation was sufficient to activate RalB and induce autophagic flux (Figure 12B,C,D,E).

RalB is recruited to sites of nascent autophagosome formation.

To investigate the physical proximity of RalB to autophagosome formation, we examined the subcellular localization of endogenous RalB and components of the autophagosome initiation and elongation machinery. In telomerase and CDK4-immortalized normal human airway epithelial cells (HBEC30-KT), we noticed conspicuous co-localization of endogenous Beclin1 and endogenous RalB in perinuclear structures. Upon amino acid starvation (EBSS for 30 minutes), we observed re-distribution of both RalB and Beclin1 to vesicular structures throughout the cell body (Figure 7A). The majority of these RalB positive structures co-labeled with a GFP-2X-FYVE reporter that localizes to sites of PI-(3)-P enrichment (139), the product of the Beclin1-associated class III PI3K VPS34 (Figure 7B). In addition, we found marked colocalization of endogenous RalB with GFP-ATG5 after a 90-minute incubation in starvation media (Figure 7C). By 4 hours, GFP-LC3 punctae had accumulated, many of which were RalB positive (Figure 7D).

To investigate the recruitment of RalB to a discrete membrane site undergoing LC3-modification, we utilized GFP-expressing *Salmonellae typhimurium* as a detectable, proximal signal for LC3-modification of the vacuole. Three hours after post-infection antibiotic selection to remove extracellular *Salmonellae*, we found that endogenous ATG5 was present along the surface of internalized GFP-*Salmonellae*, which co-localized with RalB (Figure 7E). Finally, an autophagic response of HBEC cells to Sendai virus exposure induced a re-distribution of RalB but not RalA to cytosolic vesicular structures and promoted accumulation of endogenous RalB-ATG5/ATG12 protein complexes (Figure 7F,G).

Nutrient-starvation and RalB drive assembly of Exo84-Beclin1 complexes.

Given that Beclin1, a central regulatory node engaged to initiate autophagic responses to diverse stimuli, colocalized with RalB, we examined the relationship between Beclin1 and exocyst subunits. We found that nutrient starvation induced a dramatic assembly of Exo84/Beclin1 complexes in HEK293 cells (Figure 8A). In stark contrast, abundant Sec5/Beclin1 complexes present under nutrient-rich growth conditions were disassembled within 90 minutes of nutrient deprivation (Figure 8B), which could be reversed by addition of nonessential amino acids (Figure 8C). Sec8/Beclin1 complexes, on the other hand, were present under both nutrient-rich and nutrient-poor growth conditions (Figure 8D). Analysis of Beclin1 deletion constructs indicated that both Exo84 and Sec5 required the amino-terminal BCL2-interacting domain for interaction with Beclin1 (88-150), while the evolutionarily conserved domain (244-337) was dispensable (Figure 13A). However, Exo84 and Sec5 likely have distinct binding determinants within the BCL2-interacting domain, as Beclin1(F123A), which fails to bind BCL2, interferes with Sec5 but not Exo84 association (Figure 8E,F). Importantly, we found that immunoprecipitation of endogenous Beclin1 from nutrient-deprived versus nutrient replete cells resulted in selective coprecipitation of endogenous Exo84 under starvation conditions (Figure 8G). These observations suggest that Beclin1 is recruited to distinct exocyst subcomplexes in response to nutrient availability. Previous observations from our group indicated that discrete macromolecular Exo84 and Sec5 complexes can be detected by density gradient centrifugation in pheochromocytoma cells (33). Accordingly we found that endogenous Exo84 and Sec5 display very distinct localization patterns in epithelial cells (Figure 8H). Likewise, ectopic expression of Exo84 or Sec5 was sufficient to differentially recruit Beclin1 to these distinct subcellular compartments (Figure 8 I,J). The Exo84 compartment and the Sec5 compartment were reminiscent of the staining patterns observed with endogenous Beclin1 in the nutrient starved versus fed states respectively (Figure 7A). Size exclusion chromatography of cleared lysates, from proliferating cells, indicated the bulk of endogenous Exo84 and Sec5 eluted in separate fractions of ~500 kDa and > 700 kDa respectively, both of which partially cofractionated with Beclin1. Intriguingly, the ATG1 ortholog, ULK1, displayed a bimodal distribution presumably representative of distinct high and low molecular weight complexes (Figure

13B).

Consistent with a sentinel role in the cellular response to nutrient deprivation, RalB was activated by nutrient deprivation as indicated by accumulation of the GTP-bound conformation. RalA, on the other hand, was unaffected (Figure 9A). Accordingly, expression of a constitutively active RalB variant (RalB(23V)) was sufficient to induce Beclin1/Exo84 complex formation in the absence of nutrient deprivation (Figure 9B). To examine whether a direct RalB-Exo84 effector interaction was necessary for RalB to drive Exo84-Beclin1 association, we employed partial loss of function RalB variants selectively uncoupled from Exo84 versus Sec5 (106, 135). RalB(G23V,A48W) has a 43-fold higher affinity for Sec5 versus Exo84, and RalB(G23V,E38R) has a 104-fold higher affinity for Exo84 versus Sec5 (135). As shown, RalB(G23V,E38R) was considerably more effective at promoting Exo84/Beclin1 complex formation as compared to its Exo84-binding defective counterpart, RalB(G23V,A48W) (Figure 9C). In contrast to Exo84, Beclin1/Sec5 complexes can be isolated under nutrient rich conditions. Interestingly, inhibition of Ral signaling by RLIP(RBD) expression eliminates the accumulation of Beclin1/Sec5 complexes suggesting that RalA/B signaling under nutrient rich conditions is required for this interaction (Figure 9D). A point mutation of the Ral-binding domain of Sec5(T11A), which abolishes binding to Ral-GTP, also abolished the Sec5-Beclin1 interaction (Figure 9E). No interaction of Beclin1 with RLIP76, an exocyst-independent Ral effector, was observed (Figure 9F); indicating that Ral family modulation of Sec5/Beclin1 and Exo84/Beclin1 complexes is specific. The sufficiency of RalB interactions to drive both Sec5-Beclin1 and Exo84-Beclin1 complexes, coupled with our observations of the selective responsiveness of these complexes to nutrient status, suggested the possibility that nutrient availability results in distinct RalB-effector coupling. Indeed, endogenous RalB preferentially associated with Exo84 in nutrient poor conditions and Sec5 under nutrient rich conditions (Figure 9G,H). Importantly, endogenous ULK1, a key kinase that promotes initiation of autophagy (110, 112, 140), was selectively enriched in RalB immunoprecipitates upon nutrient depletion (Figure 9G). These observations indicate that direct RalB/exocyst effector interactions differentially deliver Beclin1 to Sec5 or Exo84-containing subcomplexes in response to nutrient availability and that RalB/Exo84 complexes may specify activation of

autophagosome formation. Consistent with this, we found that inhibition of Ral signaling by Rlip(RBD), which inhibits autophagy, promoted the association of the autophagy inhibitor protein RUBICON with Exo84 (Figure 9I).

The RalB/Exo84 effector pathway mobilizes VPS34 activity.

To further probe the relationship of Exo84 versus Sec5 complexes to mobilization of autophagosomes, we examined the consequence of nutrient depletion or Ral activation on recruitment of VPS34 to exocyst/Beclin1 complexes. Beclin1 has been heavily implicated as a positive regulatory cofactor of the VPS34 lipid kinase, which is thought to be a biochemical trigger for initiation of autophagosome isolation membrane assembly and elongation (141, 142). Like the Exo84/Beclin1 relationship, we found that nutrient depletion resulted in accumulation of Exo84/VPS34 complexes (Figure 10A). Again, as we had seen with Beclin1, the opposite relationship was observed with Sec5 (Figure 10B). Expression of active RalB in the absence of nutrient depletion mirrored these observations. Namely, RalB(G23V) drove assembly of Exo84/VPS34 complexes (Figure 10C) and drove disassembly of Sec5/VPS34 complexes in a manner dependent upon direct RalB/effector interactions (Figure 10D).

The presence of ATG14L in complex with Beclin1 and VPS34 is thought to specify the participation of this complex in autophagy as opposed to other cell processes where VPS34 activity has been implicated (143-146). We found that dynamic interactions of Exo84 and Sec5 with ATG14L were also remarkably similar to those observed with Beclin1. Specifically, under nutrient rich growth conditions, Exo84 association with ATG14L was induced by RalB(G23V) expression (Figure 10E) while preexisting Sec5/ATG14L complexes were inhibited in the presence of the dominant inhibitory peptide Rlip(RBD) (Figure 10F). Furthermore, RalB(E38R) but not RalB(A48W) expression was sufficient to drive accumulation of PI-(3)-P positive punctae, the product of active VPS34, as visualized by accumulation of the GFP-2X-FYVE probe (Figure 10G,H). Similar results were observed for the accumulation of GFP-LC3 punctae (Figure 10I). These observations suggest that induction of autophagy proceeds through assembly of Beclin1-ATG14L-VPS34 complexes on Exo84, while the interaction of these components with Sec5 may represent organization of inactive components in a

preinitiation complex and/or a signal termination complex. Importantly, the increased accumulation of GFP-LC3 observed upon RalB(G23V) expression was reversed by co-expression of kinase dead mutant ULK1(K46N), suggesting that RalB may act upstream of ULK1 to promote autophagy (Figure 10I).

Active ULK1 assembles on Exo84 upon induction of autophagy.

ULK1 activation is the most apical positive inductive signal, among Atg proteins, yet identified for initiation of autophagy. We have found that RalB is activated upon nutrient starvation and that this correlates with the induction of RalB/ULK1 complexes (Figures 9A and 9G respectively). Remarkably, RalB(G23V) expression was sufficient to promote assembly of ULK1/Beclin1 complexes, which have not been described previously but which may represent a mechanistic link between ULK1 activation and the VPS34 vesicle nucleation complex (Figure 11A). Furthermore, either nutrient depletion or RalB(G23V) expression was sufficient to induce assembly of ULK1/Exo84 complexes (Figure 11B,F). Depletion of Exo84 eliminated the capacity of RalB(G23V) to induce ULK1/Beclin1 complex formation, indicating that Exo84 is required for this assembly event (Figure 11C). In contrast to ULK1/Exo84 interactions, we observed increased Sec5/ULK1 complex assembly when Ral signaling was blocked by expression of Rlip(RBD) (Figure 11D). Analysis of Beclin1 deletion constructs indicated that, unlike Exo84 and Sec5, ULK1 requires the evolutionarily conserved domain (aa 244-337) for Beclin1 association (Figure 14A). Importantly, while ULK1 was present in both Exo84 and Sec5 complexes under nutrient poor conditions (Figure 11E,F), only Exo84-associated ULK1 displayed significant catalytic activity (Figure 11F,G).

ULK1 and mTORC1 have been reported to inhibit each other by reciprocal phosphorylation (110, 147). Consistent with catalytically active Exo84/ULK1 complexes, expression of RalB(G23V) and Exo84 was sufficient to inhibit base-line mTORC1 activity as observed by reduced accumulation of phospho-threonine 389 on p70S6K (Figure 11B). In contrast, expression of RalB(G23V) and Sec5 resulted in increased accumulation of phospho-p70S6K (Figure 11D). Of note, endogenous mTORC1 was present in Sec5 but not Exo84 immunoprecipitates (Figure 14B). The assembly of ULK1 with Exo84 and disassembly of Beclin1 from Sec5 are responsive to mTOR inhibition,

but only upon chronic exposure to rapamycin, suggesting this is a consequence of the indirect effects that mimic nutrient starvation (Figure 14C,D). These combined observations indicate that the RalB/Exo84 effector relationship engages autophagy through direct modulation of a ULK1/Beclin1 initiation complex.

DISCUSSION

Our findings are consistent with a model in which the Ras-like G-protein RalB acts as a regulatory switch to promote autophagosome biogenesis, in response to inductive signaling events, by mobilizing assembly of ULK1/Beclin1/VPS34 autophagy initiation complexes (Figure 11H). RalB is activated during the autophagic response, is localized to sites of incipient autophagosome formation, and is necessary and sufficient for induction of autophagic flux. In response to RalB activation, the direct RalB effector Exo84 is engaged as an essential assembly platform for catalytically active autophagy induction (ULK1/FIP200) and vesicle initiation (Beclin1/ATG14L, VPS34) complexes.

In all cases examined, we found that dynamic assembly of active autophagosome biogenesis machinery on Exo84 was coordinated with disassembly of this same machinery from Sec5. Both Exo84 and Sec5 are Ral family G-protein effectors and subunits of the exocyst, a heterooctameric secretory vesicle trafficking complex (148). Previous work has shown that distinct Exo84 and Sec5 subcomplexes are directly engaged by Ral signaling to mobilize exocyst holocomplex formation in support of the dynamic vesicle targeting and tethering events required for stimulus-dependent exocytosis (31, 33). Remarkably, the Sec5/autophagy protein disassembly event and the Exo84/autophagy protein assembly event, described here, both require direct interaction with active RalB proteins. Thus induction of autophagy through RalB activation triggers dynamic autophagy protein reassembly events centered on two independent exocyst subunits. The tethering of autophagosome biogenesis machinery to distinct exocyst subcomplexes may provide appropriate spatial and temporal resolution of localized autophagic triggers. Consistent with this, we find that Sec5 and Exo84 accumulate in discrete cellular compartments that segregate with localization of Beclin1 pre (Sec5) and post (Exo84) induction of autophagy. It will be of great interest to determine if these locations represent the source location and assembly sites, respectively, of the membrane

proteins required for autophagosome isolation membrane construction. Known exocyst subunit-autonomous mechanisms specifying subcellular localization patterns include interactions with organelle-specific proteins and membrane-selective phosphoinositides (149).

Recent observations indicate that detection of conserved pathogen-associated molecular patterns (PAMPs) by Toll-like receptors will mobilize autophagy together with activation of canonical innate-immune pathway activation (150, 151). Within this context of host defense surveillance and response systems, we have previously shown that RalB can engage Sec5 to activate the innate immunity signaling kinase TBK1 and the subsequent IRF3 transcription factor-dependent interferon response (9). Our observations here indicate that RalB can separately engage Exo84 to facilitate activation of the autophagy kinase ULK1 and induction of autophagosome biogenesis. Together, this suggests that RalB and the exocyst represent a regulatory hub, through bifurcating activation of TBK1 and Beclin1/VPS34, that helps engage concomitant activation of the gene expression and organelle biogenesis responses supporting systemic pathogen recognition and clearance. The required coordination of such time and location-specified responses may account for the adaptation of exocyst function to support of signal transduction cascades in metazoans.

The RalA and RalB G-proteins are signal propagation molecules coupled to mitogenic, trophic and cytokine signaling systems (4, 126). This connectivity potentially provides appropriate functional coupling of autophagic responses to diverse cellular milieus. Ral activation occurs through engagement of one or more of a family of 5 Ral-specific guanyl nucleotide exchange factors that can selectively couple to RalA or RalB through mechanisms that remain to be determined (126). Of note, RalA has recently been shown to promote mTORC1 activation, potentially through PLD1 and phosphatidic acid-dependent mTORC1/2 assembly (152-154). This regulatory relationship could be directly antagonistic to autophagosome biosynthesis given the capacity of mTORC1 to restrain ULK1 activity through direct inhibitory phosphorylation events (110, 112). Whether these are independent or interconnected regulatory arms remains to be determined. However, the RalB GDP/GTP cycle and its effector relationships comprise a regulatory mechanism that can directly control dynamic

transition between metabolic states supporting cell growth versus cell maintenance.

Figure 5

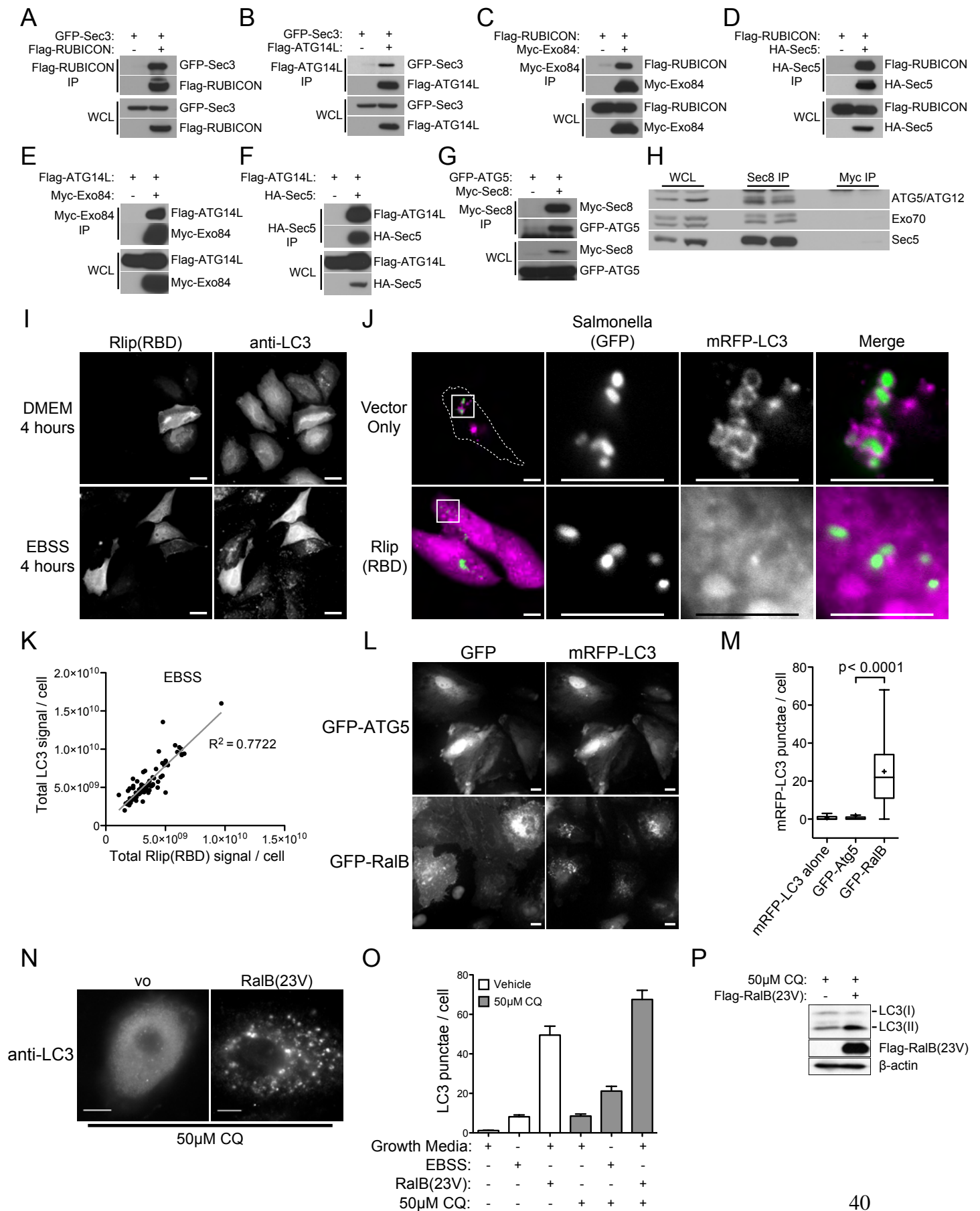


Figure 5: Physical and Functional interaction of the Ral-Exocyst complex with autophagy machinery.

A-G: Exocyst subunits interact with autophagy proteins. The indicated proteins were over-expressed in HEK-293 cells, then immunoprecipitated with an antibody directed to the specified tag. Immunoprecipitates were analyzed for coprecipitation with (A,B) GFP-Sec3; (C,D) Flag-RUBICON; (E,F) Flag-ATG14L; and (G) GFP-ATG5 as indicated. Whole cell lysate (WCL), Immunoprecipitation (IP).

H: Endogenous Sec8 complexes contain ATG5-12 conjugates. The endogenous exocyst complex was immunoprecipitated from HEK-293 cells with anti-Sec8 antibody and analyzed for coprecipitation of ATG5/ATG12 conjugates (Sec8 IP) using anti-ATG5 antibody. Anti-Myc immunoprecipitates served as a negative control (Myc IP). Two independent experiments are shown. Representation of the examined proteins in the input whole cell non denaturing lysates is shown (WCL).

I: Inhibition of Ral signaling blocks the LC3 response to amino-acid starvation. 48 hours post-transfection with Myc-Rlip(RBD) Hela cells were incubated in DMEM or EBSS for an additional 4 hours as indicated. Myc-Rlip(RBD) and LC3 were detected by immunofluorescence using anti-myc and anti-LC3 antibodies, respectively. Vector control cells were similar to untransfected cells. Scale bar 20 μ m.

J: Inhibition of Ral signaling blocks the LC3 response to pathogen infection. Hela cells were transfected with monomeric RFP-LC3 together with Myc-Rlip(RBD) or an empty vector control as indicated. 48 hours post-transfection, cells were infected with *Salmonella typhimurium*-GFP for 1 hour followed by 3 hours of post-infection selection for intracellular Salmonella. Internalized Salmonella and LC3 were visualized using their respective fluorescent fusions. High magnification of the subcellular regions indicated by the boxes are shown in the panels on the right. Dashed lines indicated cell borders as visualized in a saturated exposure. Scale bar 10 μ m.

K: Total fluorescence intensity corresponding to Myc-Rlip(RBD) (anti-myc) and endogenous LC3 (anti-LC3) at single-cell resolution for EBSS-treated cells as shown in (I) (n=82, $R^2=0.7722$).

L: RalB is sufficient to induce accumulation of LC3 punctae. Hela cells expressing monomeric RFP-LC3 together with GFP-ATG5 or GFP-RalB are shown as indicated.

Scale bar 10 μ m.

M: mRFP-LC3 punctae in cells treated as in (L) were quantitated. The distribution of mRFP-LC3 punctae/cell is displayed as box-and-whisker plots. The three bands of the box illustrate the 25th (lower), 50th (middle), and 75th (upper) quartiles. The whiskers go 1.5 times the interquartile distance or to the highest or lowest point, whichever is shorter. The + designates the mean. P-values were calculated using the student's t-test.

N: HBEC3-KT cells expressing RalB(23V) or transfected with vector control were incubated in growth medium containing 50 μ M Chloroquine (CQ), to prevent LC3 turnover by autophagolysosomes, for 4 hours followed by detection of endogenous LC3 with anti-LC3 antibody.

O: RalB is sufficient to induce autophagic flux. HBEC3-KT cells treated as in (N) were incubated in growth media or amino-acid free EBSS (Earle's balanced salt solution) for 4 hours with or without 50 μ M Chloroquine (CQ), to prevent LC3 turnover in autophagolysosomes, as indicated. Immunofluorescence was performed with anti-LC3 antibody and LC3 punctae were quantitated. Data are represented as mean \pm SEM.

P: Whole cell lysates from HBEC3-KT cells transfected with Flag-RalB(G23V) or vector control were analyzed for the relative accumulation of LC3(I) and LC3(II) when incubated in growth medium containing 50 μ M Chloroquine (CQ) for 4 hours. β -actin is shown as a loading control.

See also Table 3.

Figure 6

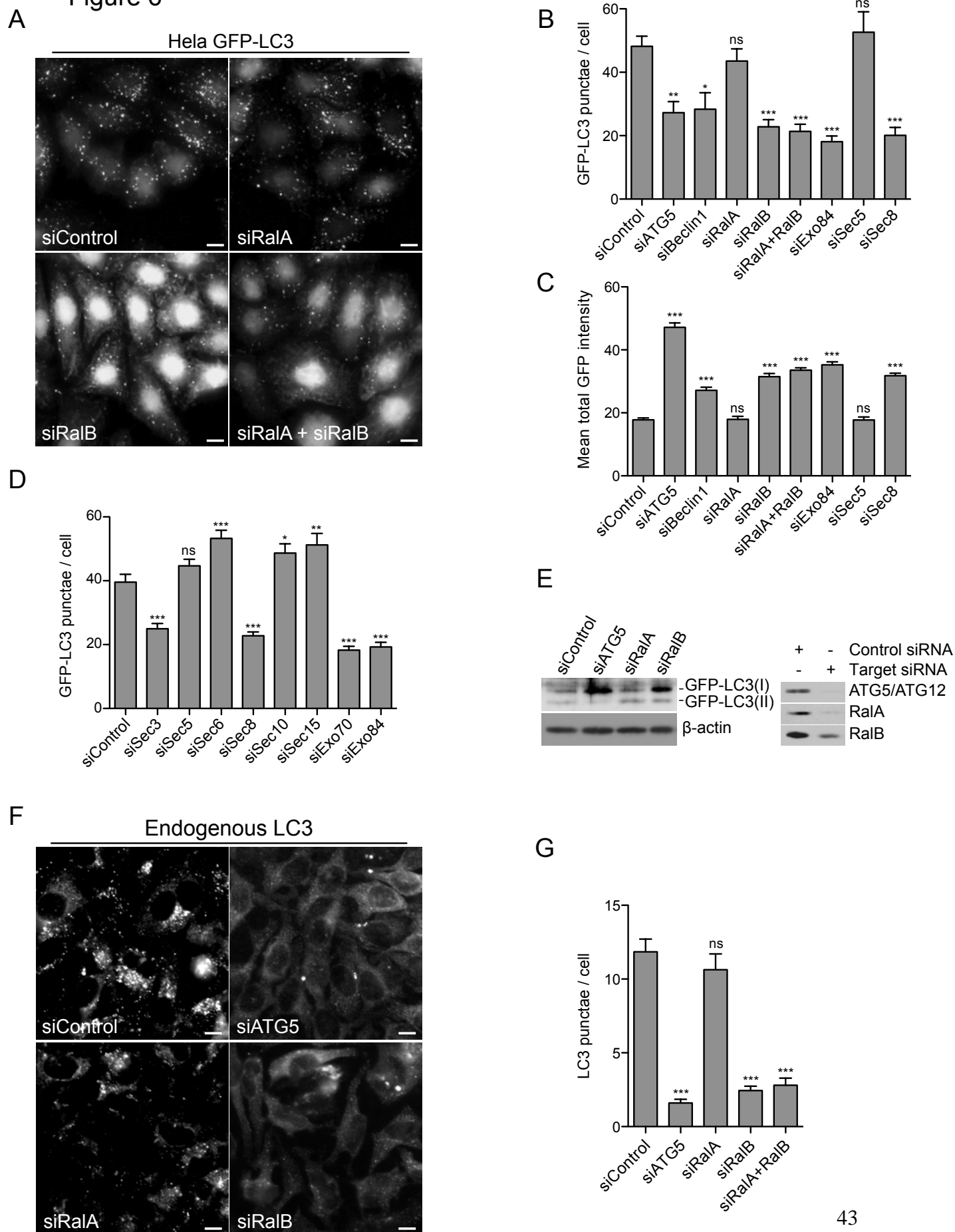


Figure 6: RalB and an Exo84-containing subcomplex of the exocyst are necessary for amino acid starvation induced autophagy.

A: RalB depletion inhibits accumulation of GFP-LC3 punctae. HeLa cells stably expressing GFP-LC3 were depleted of the indicated proteins by siRNA transfection. Cells were imaged by GFP fluorescence 96 hours after transfection. Scale bar 10 μ m.

B: Sec5 and Exo84 selectively participate in accumulation of GFP-LC3 punctae. GFP-LC3 punctae in cells treated as in (A) were quantitated. The mean distribution of GFP-LC3 punctae/cell is displayed as a bar graph, data are represented as mean \pm SEM. P-values were calculated by one-way ANOVA followed by Dunnett's Multiple Comparison Test.

C: Inhibition of GFP-LC3 punctae correlates with accumulation of LC3 protein. The mean total intensity of GFP-LC3 in cells treated as in (A) was quantitated. The distribution of the mean total GFP intensity is displayed as a bar graph, data are represented as mean \pm SEM. P-values were calculated by one-way ANOVA followed by Dunnett's Multiple Comparison Test.

D: A subset of exocyst subunits are limiting for accumulation of GFP-LC3 punctae. The indicated siRNAs were evaluated as in (B).

E: RalB depletion inhibits accumulation of LC3-lipid conjugates. Whole cell lysates from HBEC3-KT cells stably expressing GFP-LC3 transfected with the indicated siRNAs were assayed for the relative accumulation of GFP-LC3(I) and GFP-LC3(II). β -actin is shown as a loading control. siRNA-mediated target depletion is shown 96 hours post transfection (right panels).

F: RalB participates in accumulation of endogenous LC3 punctae. HeLa cells were depleted of the indicated proteins by siRNA transfection. 96 hours after transfection, cells were incubated in amino acid free EBSS for 4 hours. Endogenous LC3 was imaged by anti-LC3 immunofluorescence. Scale bar 10 μ m.

G: Endogenous LC3 punctae in cells treated as in (E) were quantitated. The mean distribution of LC3 punctae/cell is displayed as a bar graph, data are represented as mean \pm SEM. P-values were calculated by one-way ANOVA followed by Dunnett's Multiple Comparison Test.

See also Figure 12.

Figure 7

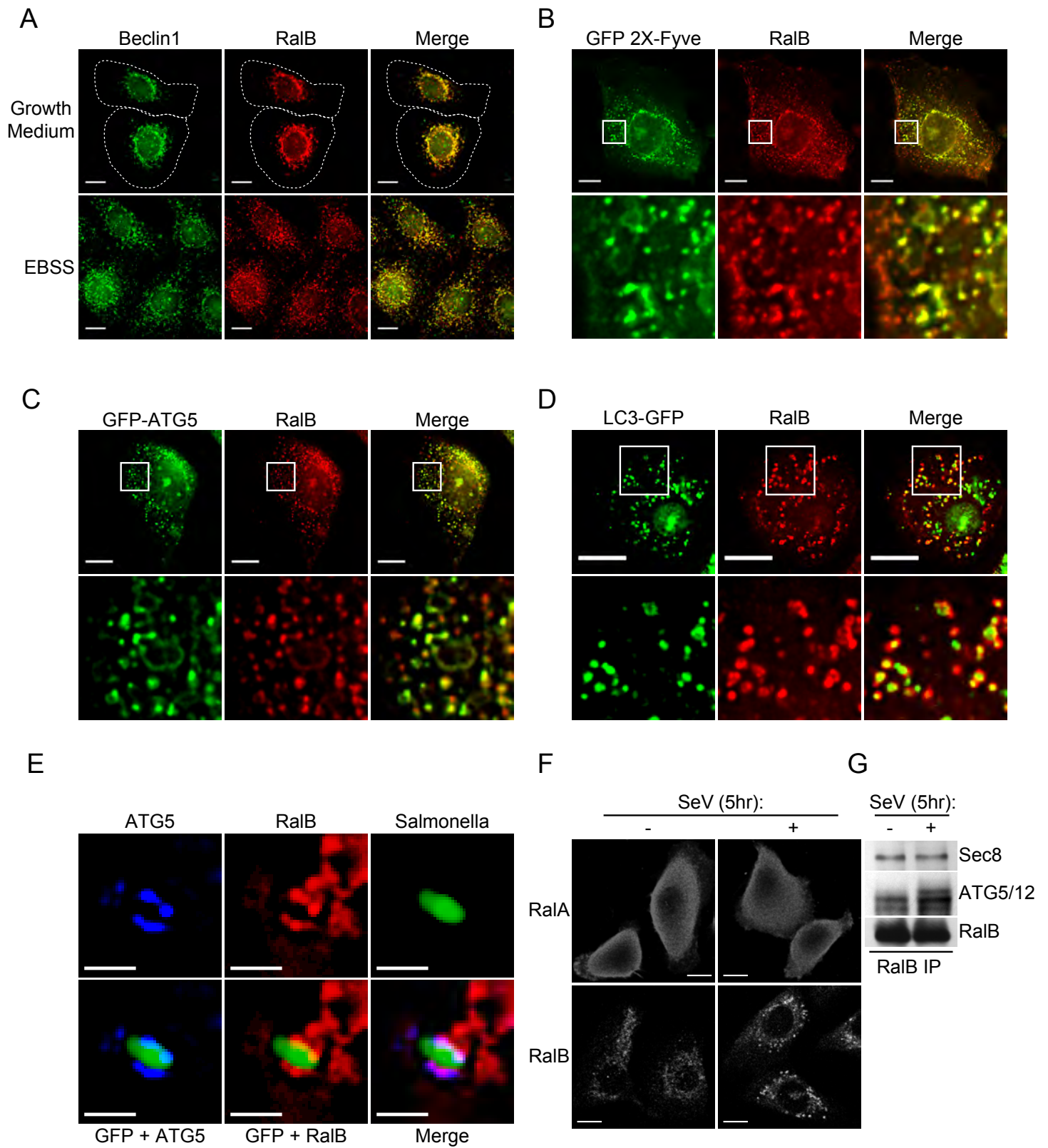


Figure 7: Native RalB colocalizes with autophagy machinery.

A: Beclin1 and RalB colocalize in cells pre and post induction of autophagy. Endogenous immunofluorescence of Beclin1 (anti-Beclin1) and RalB (anti-RalB) in HBEC30-KT cells incubated for 90 minutes in fresh growth medium or EBSS as indicated. Dashed line indicates cell outline. Scale bar 10µm.

B-D: RalB colocalizes with early and late markers of autophagosome biogenesis. HBEC30-KT cells were transfected with (B) GFP-2X-Fyve; (C) GFP-ATG5; and (D) GFP-LC3. Cells were incubated in EBSS for (B) 30 minutes; (C) 90 minutes; or (D) 3 hours. GFP fluorescence and endogenous RalB (anti-RalB) immunofluorescence is shown. High magnification of 10µm X 10µm regions indicated by the boxes are shown in the bottom panels. Scale bar 10µm.

E: ATG5 and RalB are recruited to sites of incipient isolation membrane formation. Endogenous immunofluorescence of ATG5 (anti-ATG5) and RalB (anti-RalB) in HBEC30-KT cells infected with *Salmonella typhimurium*-GFP. Cells were exposed to *Salmonella typhimurium*-GFP for 1 hour followed by 3 hours of post-infection antibiotic selection against extracellular *Salmonella*. Scale bar 2µm.

F: SenV infection selectively alters the subcellular distribution of RalB versus RalA. Endogenous immunofluorescence of RalA (anti-RalA) and RalB (anti-RalB) in HBEC3-KT cells mock infected or infected with Sendai virus for 5 hours. Scale bar 10µm.

G: SenV infection induces accumulation of endogenous RalB/ATG5-12 complexes. Endogenous RalB complexes were immunoprecipitated from mock infected or Sendai virus infected HBEC3-KT cells with anti-RalB antibodies and analyzed for coprecipitation of ATG5/ATG12 conjugates.

Figure 8

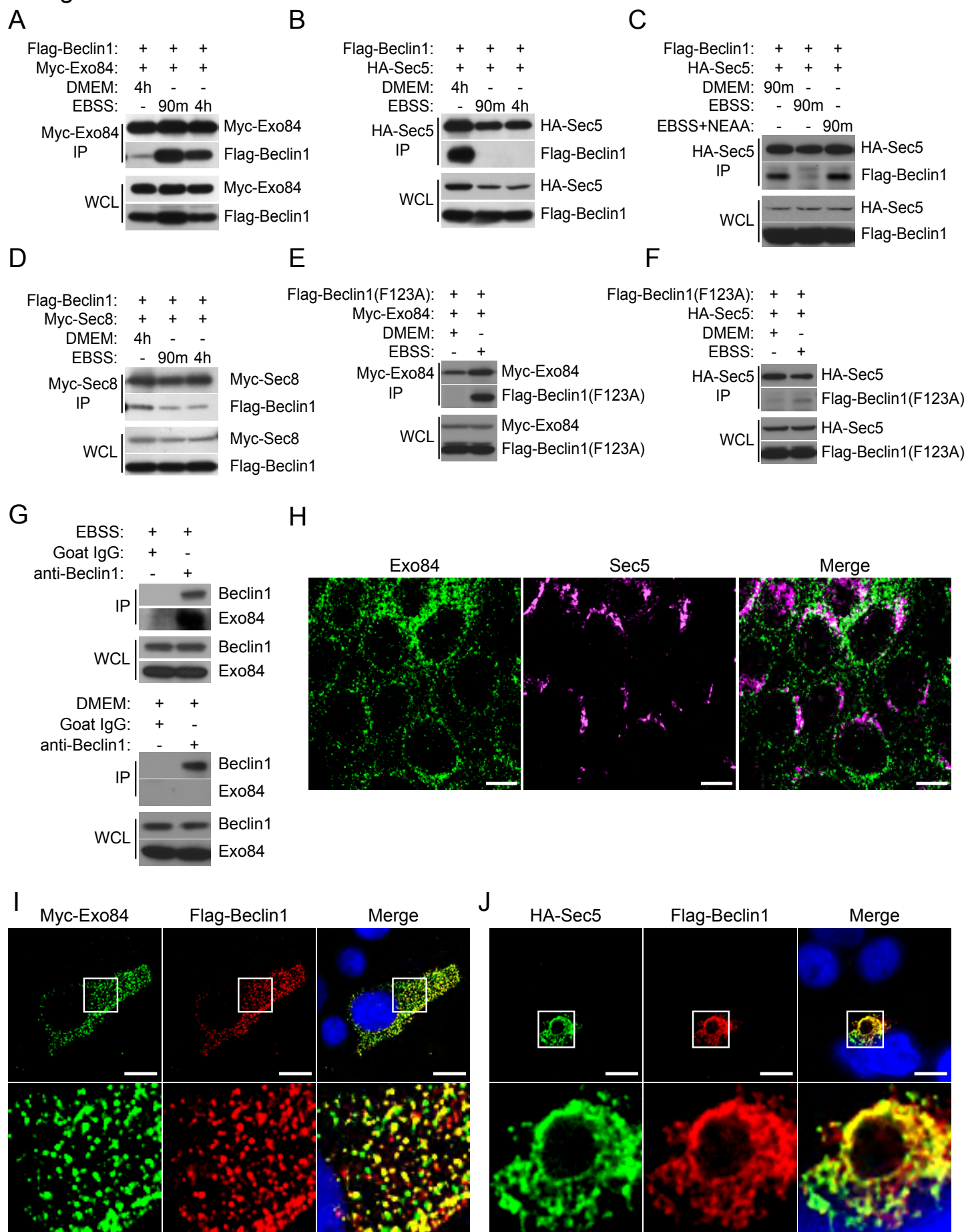


Figure 8: Nutrient deprivation drives assembly of Exo84/Beclin1 complexes.

A-D: Nutrient limitation induces Beclin1/Exo84 interactions and inhibits Beclin1/Sec5 interactions. 48 hours post-transfection with tagged Beclin1 and exocyst expression constructs, HEK-293 cells were incubated in DMEM, EBSS, or EBSS with 1X Non-Essential amino acids for 90 minutes or 4 hours as shown. The indicated proteins were then immunoprecipitated with antibodies directed to the specified tag.

Immunoprecipitates were analyzed for coprecipitation with Flag-Beclin1. Whole cell lysate (WCL), Immunoprecipitates (IP).

E,F: Beclin1(F123A) mutant interacts with Exo84 but not Sec5. Co-expression, co-IPs with the indicated proteins were performed as in (A-D).

G: Endogenous Beclin1/Exo84 complexes accumulate in response to nutrient deprivation. Endogenous Beclin1 was immunoprecipitated from HEK-293 cells incubated in EBSS (top panels) or DMEM (bottom panels) for 90 minutes and analyzed for coprecipitation of Exo84 (IP). Host species-matched non-specific IgG immunoprecipitates served as negative controls. Representation of the examined proteins in the input whole cell non-denaturing lysates is shown (WCL).

H: Exo84 and Sec5 are enriched in distinct subcellular compartments. Endogenous immunofluorescence of Sec5 (anti-Sec5) and Exo84 (anti-Exo84) in MDCK cells. Scale bar 10µm.

I,J: Exo84 and Sec5 can recruit Beclin1 to distinct subcellular compartments. HEK-293 cells were transfected with (F) Flag-Beclin1 and Myc-Exo84; (G) Flag-Beclin1 and HA-Sec5. Immunofluorescence of the indicated fusion tags was performed. High magnification of 10µm X 10µm regions indicated by the boxes are shown in the bottom panels. Scale bar 10µm.

See also Figure 13.

Figure 9

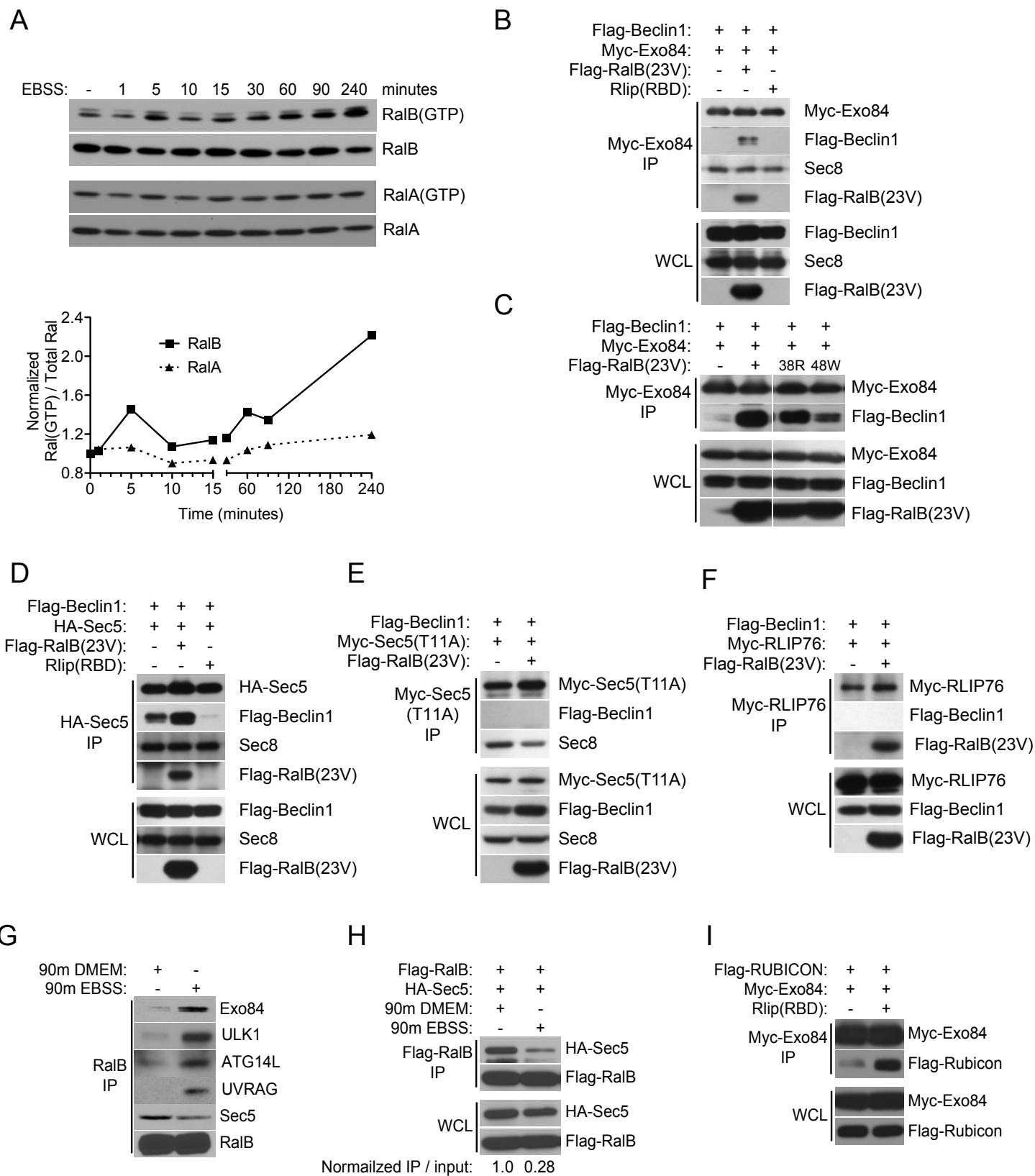


Figure 9: RalB drives assembly of Exo84/Beclin1 complexes through direct RalB-Exo84 effector binding.

A: Amino-acid depletion activates RalB. Endogenous GTP-bound RalA and RalB were collected by GST-Sec5-RBD mediated affinity purification from HEK-293 cells incubated in EBSS for the indicated times and visualized with specific anti-RalA and anti-RalB antibodies. The normalized GTP-loaded index for RalA and RalB was calculated as $\frac{\text{Ral(GTP)}}{\text{Total Ral}}$ to generate the scatterplot.

B-F: RalB regulates Beclin1/exocyst subcomplex interactions. The indicated proteins were expressed in HEK-293 cells and immunoprecipitated with antibodies directed to the appropriate tag. Immunoprecipitates were analyzed for coprecipitation with Flag-Beclin1, Flag RalB(23V), and endogenous Sec8 as shown. Whole cell lysate (WCL), Immunoprecipitation (IP).

G: Nutrient status specifies distinct endogenous RalB/effector interactions. Endogenous RalB was immunoprecipitated with anti-RalB antibody from HEK-293 cells incubated in DMEM or EBSS for 90 minutes as indicated and analyzed for coprecipitation of Exo84, Sec5, ATG14L, UVRAG, and ULK1.

H: 48 hours post-transfection, HEK-293 cells were incubated in DMEM or EBSS for 90 minutes as indicated. Flag-RalB immunoprecipitates were examined for coprecipitation of HA-Sec5. The indicated normalized IP / input ratio was calculated by dividing immunoprecipitated Sec5 by total expressed Sec5, then normalizing the calculated values to DMEM condition.

I: Ral-inhibition induces accumulation of Exo84/Rubicon interactions. Co-expression, co-IPs with the indicated proteins were performed as in (B-F).

Figure 10

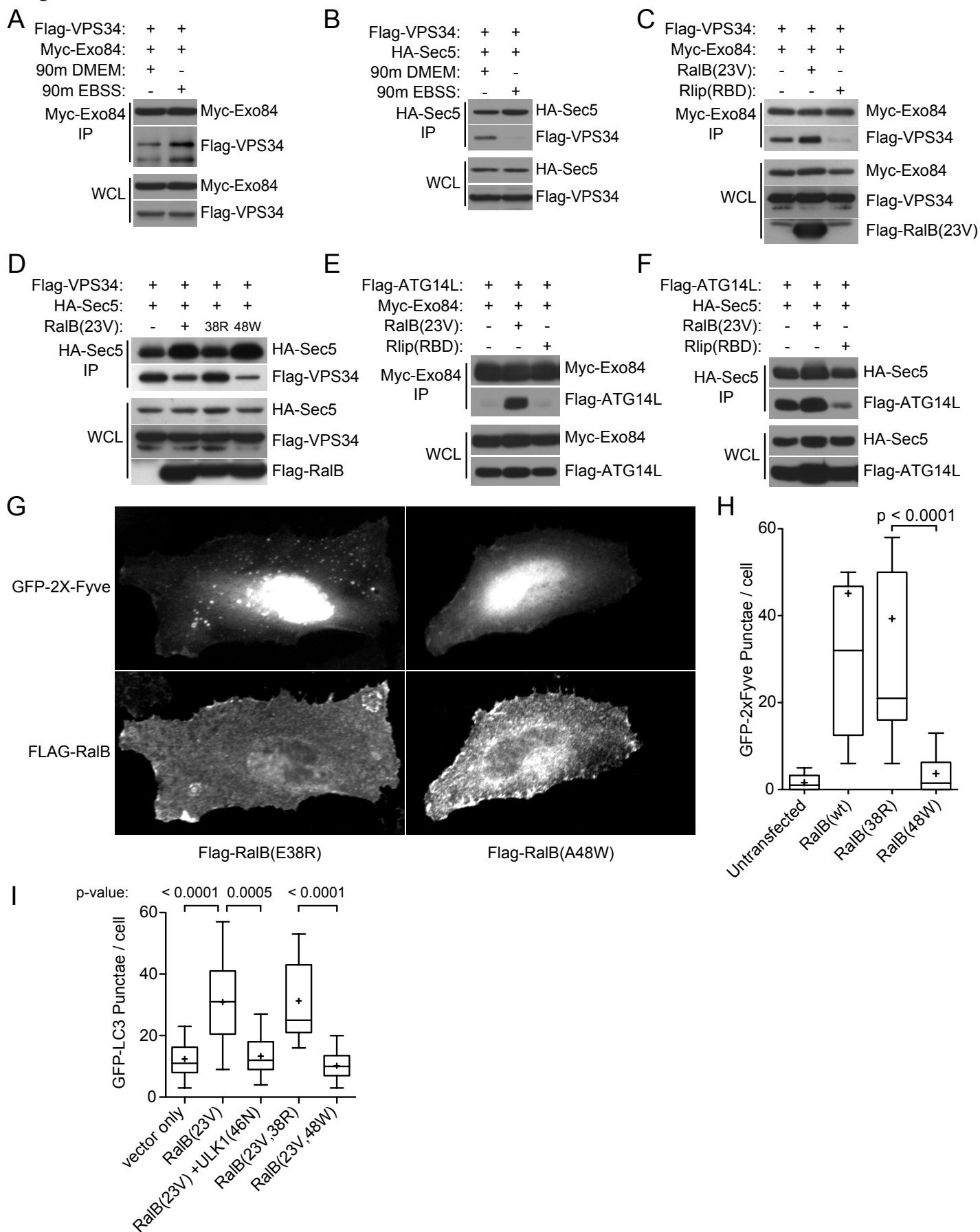


Figure 10: RalB expression drives assembly of Exo84/Vps34 and Exo84/ATG14L complexes.

A-F: VPS34 and ATG14L/exocyst subcomplexes are regulated by nutrient limitation and RalB activation. HEK-293 cells expressing the indicated proteins were incubated in DMEM or EBSS for 90 minutes as indicated. Tagged exocyst subunits were immunoprecipitated and analyzed for coprecipitation with Flag-VPS34 and Flag-ATG14L where indicated.

G: RalB/Exo84 effector interactions mobilize VPS34 activity. Hela cells expressing GFP-2X-Fyve together with RalB partial loss of function mutants Flag-RalB(E38R) or Flag-RalB(A48W) are shown as indicated.

H: GFP-2X-Fyve punctae in cells treated as in (G) were quantitated. The distribution of GFP-2X-Fyve punctae/cell is displayed as box-and-whisker plots. P-values were calculated using the student's t-test.

I: RalB(G23V) and RalB(G23V,E38R) are sufficient to induce accumulation of GFP-LC3 punctae and kinase dead ULK1(K46N) blocks the increase observed with RalB(G23V) expression. Hela cells stably expressing GFP-LC3 were transfected with the indicated constructs then visualized by immunofluorescence of the indicated tags. The distribution of GFP-LC3 punctae/cell is displayed as box-and-whisker plots. P-values were calculated using the student's t-test.

Figure 11

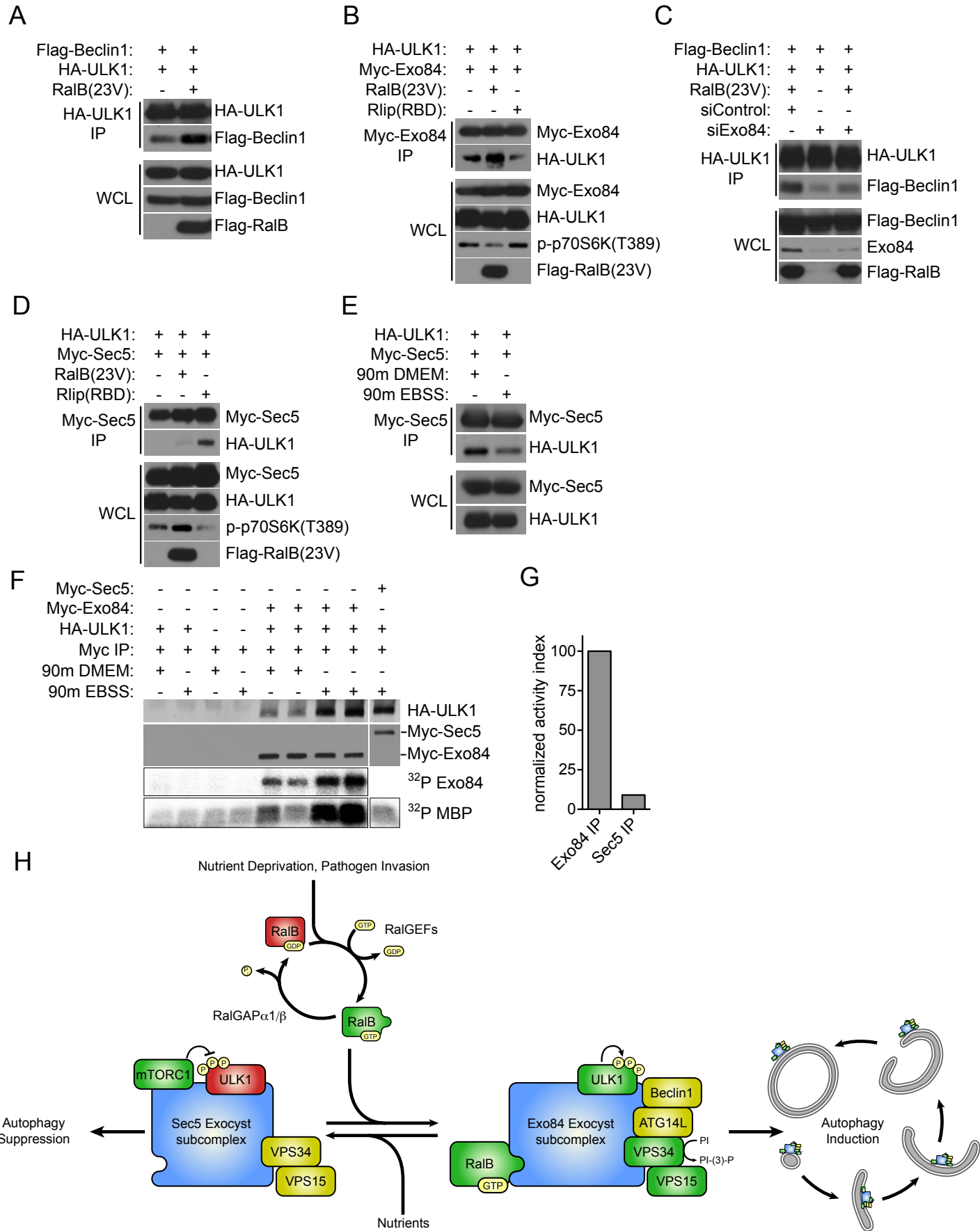


Figure 11: Active ULK1 associates with Exo84.

A: RalB induces ULK1/Beclin1 Complex formation. ULK1 immunoprecipitates were analyzed for coprecipitation with Flag-Beclin1 upon RalB(23V) expression as indicated.

B: ULK1/Exo84 complexes are regulated by RalB. The indicated proteins were expressed in HEK-293 cells. Myc-tagged Exo84 was immunoprecipitated and analyzed for coprecipitation with HA-ULK1.

C: RalB induced ULK1/Beclin1 complexes require Exo84. HEK-293 cells were first transfected with siControl or siExo84 siRNAs before the indicated proteins were expressed 24 hours later. ULK1 immunoprecipitates were analyzed for coprecipitation with Flag-Beclin1 upon RalB(23V) expression as indicated.

D: ULK1/Sec5 complexes accumulate upon Ral inhibition. Co-expression, co-IPs with the indicated proteins were performed as in (B).

E: ULK1/Sec5 complexes dissociate upon nutrient deprivation. Co-expression, co-IPs with the indicated proteins were performed as in (B) with the addition of 90 minute incubation in DMEM or EBSS as indicated.

F: Amino-acid starvation induces association of Exo84 with catalytically active ULK1. Exo84 and Sec5 complexes were assayed for coprecipitation with ULK1 and for associated protein kinase activity as indicated.

G: The normalized activity ratio for EBSS stimulated Exo84 and Sec5 precipitates was calculated by the division of MBP ³²P incorporation by the HA-ULK1 signal coprecipitated from (F).

H: Working model of RalB/exocyst dependent mobilization of autophagy.

See also Figure 14.

Figure 12

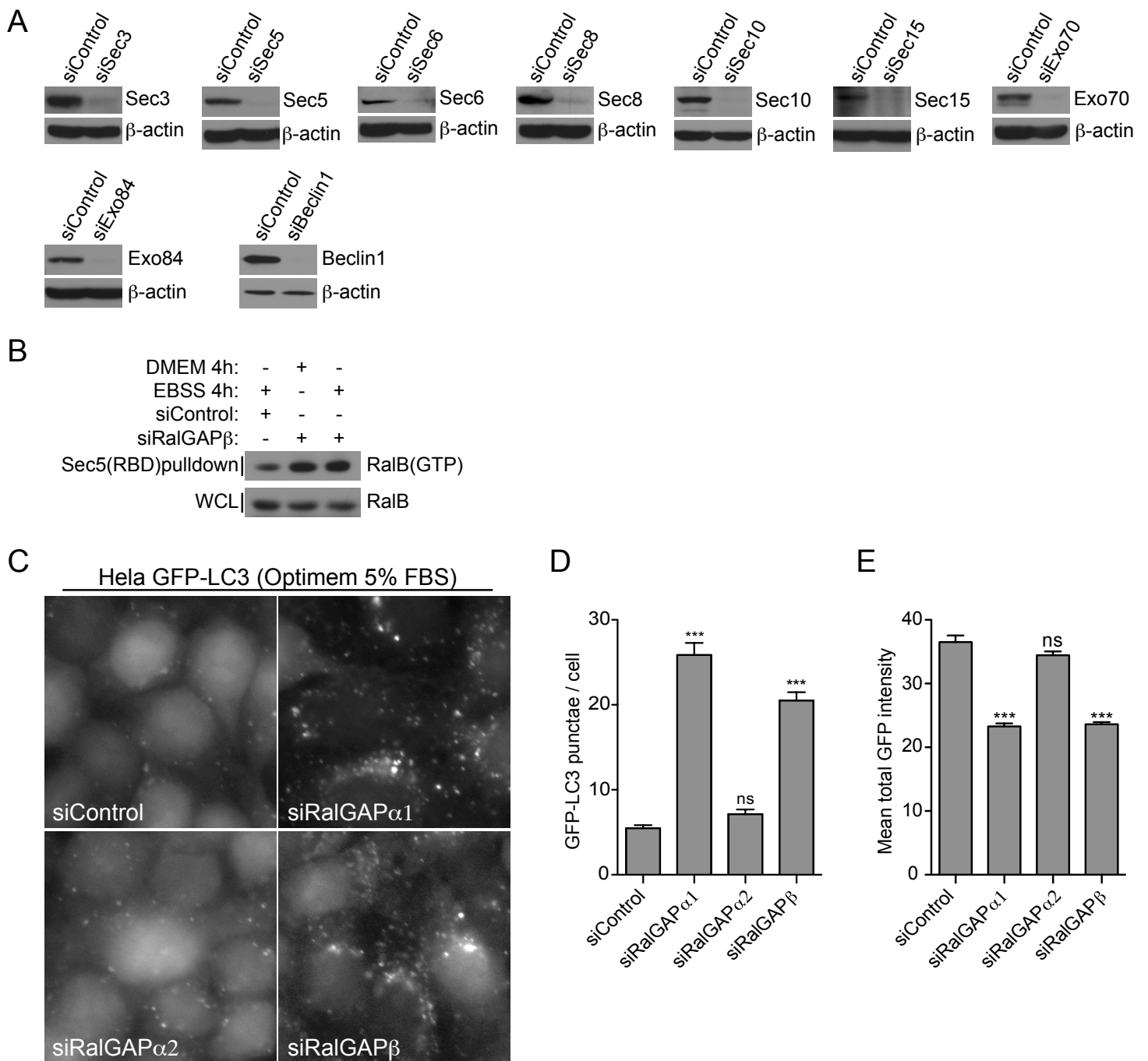


Figure 12: RalB and an Exo84-containing subcomplex of the exocyst are necessary for amino acid starvation induced autophagy, Related to Figure 6.

A: Validation of siRNA mediated protein depletion. HeLa cells stably expressing GFP-LC3 were depleted of the indicated proteins by siRNA transfection. Western blots were performed to confirm protein knockdown.

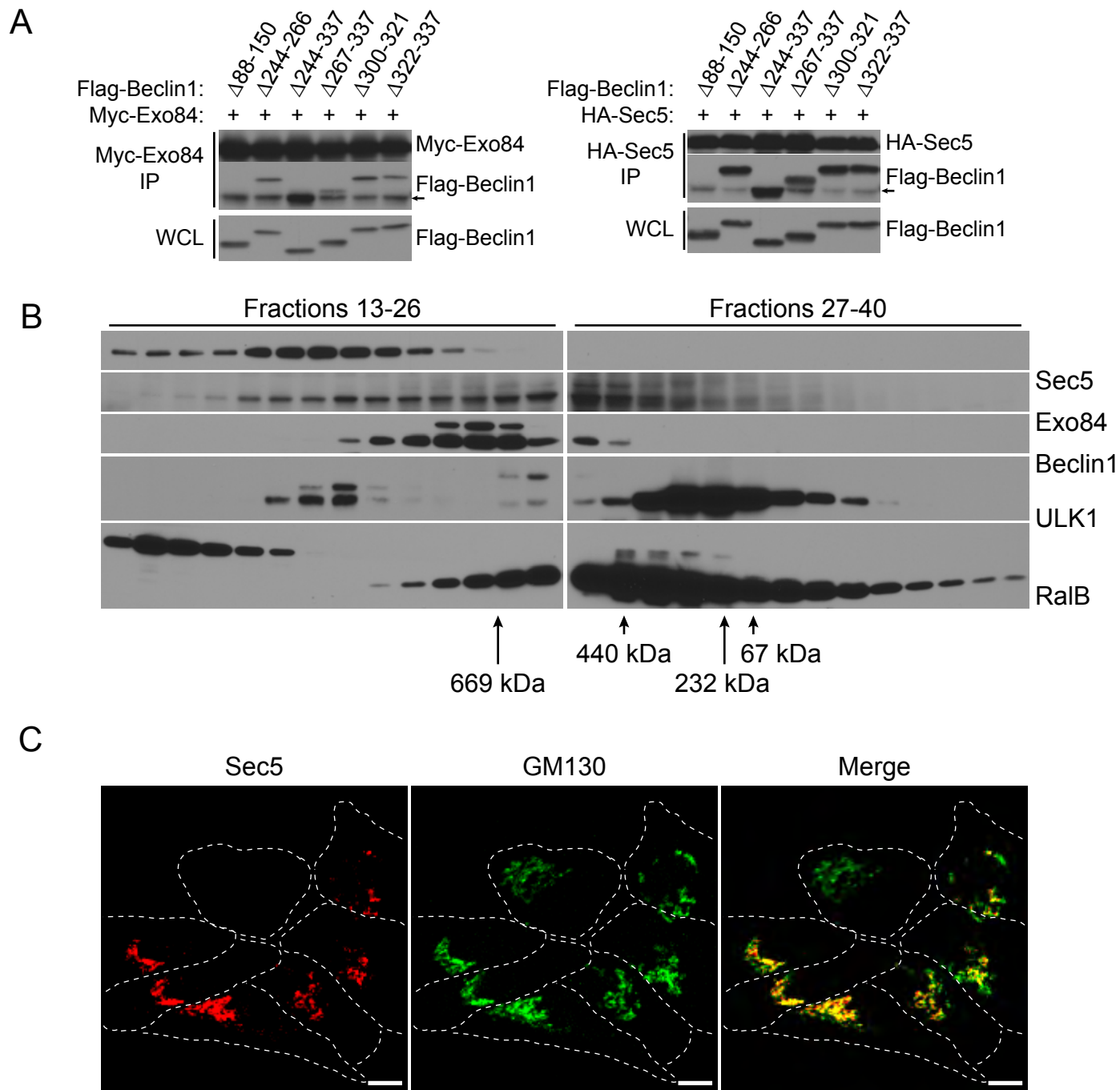
B: Depletion of RalGAP β activates RalB. Endogenous GTP-bound RalB was collected by GST-Sec5-RBD mediated affinity purification from HEK-293 cells incubated in DMEM or EBSS for 4 hours and visualized with specific anti-RalB antibody.

C: RalGAP depletion induces accumulation of GFP-LC3 punctae. HeLa cells stably expressing GFP-LC3 were depleted of the indicated proteins by siRNA transfection. Cells were cultured in Opti-MEM I (Invitrogen) plus 5% FBS for 24 hours before imaging to reduce the baseline level of autophagy. Cells were imaged by GFP fluorescence 96 hours after transfection.

D: RalGAP depletion induces accumulation of GFP-LC3 punctae. GFP-LC3 punctae in cells treated as in (C) were quantitated. The mean distribution of GFP-LC3 punctae/cell is displayed as a bar graph, data are represented as mean \pm SEM. P-values were calculated by one-way ANOVA followed by Dunnett's Multiple Comparison Test.

E: Inhibition of GFP-LC3 punctae correlates with accumulation of LC3 protein. The mean total intensity of GFP-LC3 in cells treated as in (A) was quantitated. The distribution of the mean total GFP intensity is displayed as a bar graph. P-values were calculated by one-way ANOVA followed by Dunnett's Multiple Comparison Test.

Figure 13



**Figure 13: Nutrient deprivation drives assembly of Exo84/Beclin1 complexes,
Related to Figure 8.**

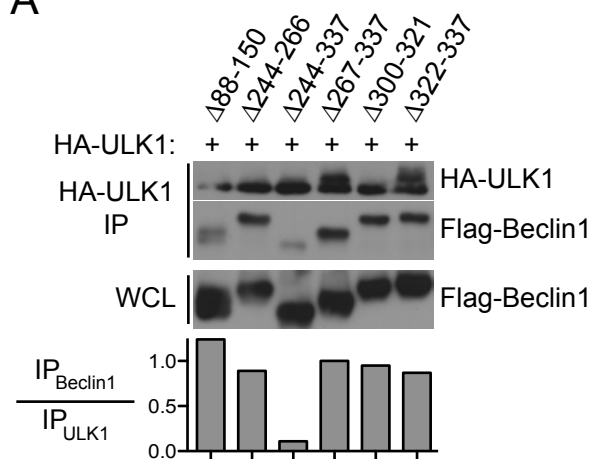
A: Exo84 and Sec5 both require amino acids 88-150 of Beclin1 to associate with Beclin1. Expression constructs for Myc-Exo84 (left panel) or HA-Sec5 (right panel) were co-transfected into HEK-293 cells together with the indicated Beclin1 deletion mutants. 48 hours post transfection the indicated proteins were immunoprecipitated with antibodies directed to the specified tag. Immunoprecipitates were analyzed for coprecipitation with the indicated Flag-Beclin1 deletion mutants. Arrow indicates minor cross reactivity with IgG heavy chain. Whole cell lysate (WCL), Immunoprecipitates (IP).

B: Sec5 and Exo84 partition into distinct high molecular weight fractions. Detergent soluble extracts from MDCK cells were separated by FPLC on a Superose 6 column. The fractions were analyzed for Sec5, Exo84, Beclin1, ULK1, and RalB. The position of molecular weight markers are indicated (Thyroglobulin 669 kDa, Apo-Ferritin 440 kDa, Catalase 232 kDa, and Bovine serum albumin 67 kDa).

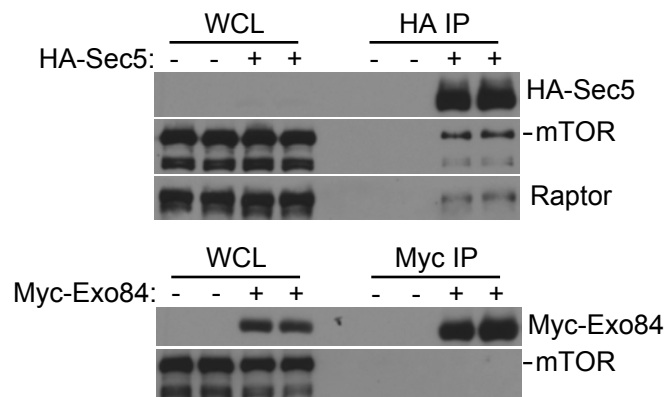
C: Sec5 co-localizes with golgi marker GM130. Endogenous immunofluorescence of Sec5 (anti-Sec5) and GM130 (anti-GM130) in MDCK cells. Dashed lines indicated cell borders as visualized in a saturated exposure. Scale bar 10 μ m.

Figure 14

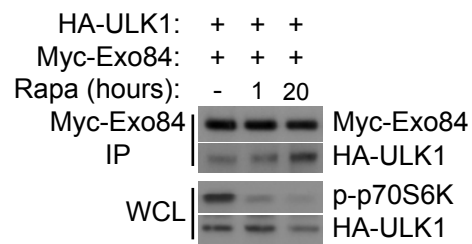
A



B



C



D

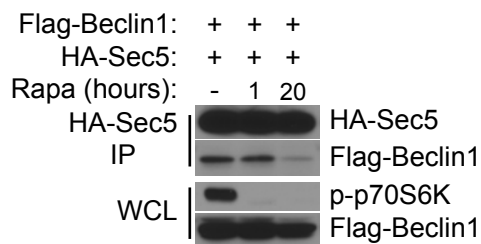


Figure 14: Active ULK1 associates with Exo84, Related to Figure 11.

A: ULK1 requires amino acids 244-337 of Beclin1 to associate with Beclin1. Expression constructs for HA-ULK1 were co-transfected into HEK-293 cells together with the indicated Beclin1 deletion mutants. 48 hours post transfection the indicated proteins were immunoprecipitated with antibodies directed to the HA tag. Immunoprecipitates were analyzed for coprecipitation with the indicated Flag-Beclin1 deletion mutants. Whole cell lysate (WCL), Immunoprecipitates (IP). $IP_{Beclin1}$ to IP_{ULK1} ratios were calculated by division of quantified Beclin1 signal by the ULK1 signal from the same sample.

B: Sec5 but not Exo84 associates with mTORC1. Expression constructs for Myc-Exo84 or HA-Sec5 were transfected into HEK-293 cells as indicated. 48 hours post transfection the indicated proteins were immunoprecipitated with antibodies directed to the specified tag. Immunoprecipitates were analyzed for coprecipitation with endogenous mTORC1 components mTOR (left and right panels) and Raptor (right panel only). Two independent experiments are shown. Whole cell lysate (WCL), Immunoprecipitates (IP).

C: ULK1/Exo84 complexes accumulate during extended Rapamycin exposure but are not responsive to short term mTOR inhibition (1 hour Rapamycin). Co-expression, co-IPs with the indicated proteins were performed as in (A) with the addition of exposure to 50nM Rapamycin or 0.1% DMSO vehicle for the indicated times before immunoprecipitation.

D: Beclin1/Sec5 complexes are dissociated during extended Rapamycin exposure but are not responsive to short term mTOR inhibition mTOR inhibition (1 hour Rapamycin). Co-expression, co-IPs with the indicated proteins were performed as in (C).

TABLE 3

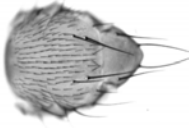

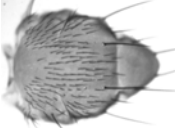
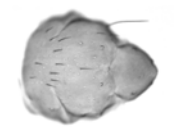
Transgene	Loss-of-microchaete phenotype (%)				Genetic interaction (pvalue)
	Wild-type	Weak	Middle	Strong	
					
dsATG1	19	0	0	81	Enhance (p=0.000)
dsATG2	13	15	45	27	No effect (p=0.479)
dsATG6	17	12	22	49	Enhance (p=0.000)
dsATG8a	16	0	19	65	Enhance (p=0.000)
dsATG14L	0	0	0	100	Enhance (p=0.000)
dsVPS34	12	8	38	40	Enhance (p=0.000)
control	14	20	44	22	-

TABLE 3. Genetic interactions between *Ral35d* and autophagy gene hypomorphs, Related to Figure 5.

Females carrying a *scaGAL4* transgene and the *Ral35d* hypomorphic mutation were crossed with males carrying dsRNA-expressing transgenes targeting the genes indicated in column 1. The loss-of-bristle phenotype of *Ral35d* males (control) and of *Ral35d* males expressing the indicated dsRNA under the control of *scaGAL4* was analyzed. The distribution of phenotypes in each genetic context is shown. Each distribution was compared to the control distribution using a Chi-Square Goodness-of-Fit test. All distributions are significantly different from control (p value<10E-4), with the exception of dsATG2 (p value=0.48). No bristle phenotype was observed in flies expressing the dsRNAs in absence of *Ral35d*. Similar genetic interactions were observed when a dominant negative allele of *Ral* (*Rals25N*) was used instead of the *Ral35d* mutant used here (data not shown).

MATERIALS AND METHODS

Plasmids. GFP-Sec3 and GFP-Sec10 (92), GFP-RalB (106), Flag-RUBICON and Flag-ATG14L (146), Myc-RLIP76 (155), Myc-Rlip(RBD) (31), Myc-Exo84 (33), Myc-rSec5 and Myc-rSec5(T11A) (136), Myc-Sec8 and HA-Sec5 (31), Flag-Beclin1 (138), GFP-ATG5 (156), GFP-2X-Fyve (157), GFP-LC3 (156), Monomeric RFP-LC3 (158), Flag-RalB, Flag-RalB(G23V), Flag-RalB(G23V, E38R), Flag-RalB(G23V, A48W), Flag-RalB(E38R), and Flag-RalB(A48W) (106), Flag-Vps34 (Liang, 2006), and HA-ULK1 and HA-ULK1(K46N) (159) were previously described.

Antibodies. Rabbit anti-GFP (sc-8334), Mouse anti-c-Myc (sc-40), Rabbit anti-HA (sc-805), Rabbit anti-ATG5 (sc-33210), Goat anti-Beclin1 (sc-10087), and Rabbit anti-Myc (sc-789) were purchased from Santa Cruz Biotechnology, inc. Rabbit anti-Flag (#F2555) and Mouse anti-Flag (#F1804) were purchased from Sigma-Aldrich, inc. Rabbit anti-VPS34 (#382100) was purchased from Invitrogen. Rabbit anti-ULK1 (#AP8104d) and Rabbit anti-UVRAG (#AP1850e) were purchased from Abgent, inc. Mouse anti-RalA (#3526) and Rabbit anti-Beclin1 (#3738) were purchased from Cell Signaling Technology, inc. Rabbit anti-ATG14L (#PD026) and anti-LC3 (#PM036) were purchased from Medical & Biological Laboratories Co. Mouse anti-RalB was provided by Larry Feig, Tufts University. Mouse and Rabbit anti-Exo70, Exo84, Sec3, Sec5, Sec6, Sec8, and Sec15 were provided by Charles Yeaman (48, 83, 160). Rabbit anti-Sec10 (#17593-1-AP) was purchased from ProteinTech Group, Inc.

Yeast Two-Hybrid. The coding sequence for full-length human SEC3 (GenBank gi:7023219) was cloned into pB27 as a C-terminal fusion to LexA and used as a bait to screen at saturation a high-complexity random-primed human placenta cDNA library as previously described (161).

Immunoprecipitation and immunoblotting. 5×10^5 HEK293 cells were seeded into 35mm dishes 18-24 hours before transfection. 500ng of each plasmid was transfected with Fugene 6 at a ratio of 3:1 (μ L Fugene 6 to μ g DNA) in to 2mL 10% FBS DMEM-H.

18-24 hours later the media was replaced with 2mL 10%FBS DMEM-H. For nutrient stimulation/starvation assays, the cells were then incubated as described with 2mL serum free DMEM-H or EBSS for the times described. The cells were lysed in lysis buffer (20 mM Tris-HCl pH 7.4, 137mM NaCl, 1% Triton-X-100, 0.5% Sodium Deoxycholate, 10mM MgCl₂, 2mM EGTA) plus protease and phosphatase inhibitors (Roche EDTA-free protease inhibitor cocktail, 1mM PMSF, 50mM NaF, 1mM NaVO₄, 80mM β -glycerophosphate). Cells were lysed for 15 minutes, then cleared at 20,000 X g for 10 minutes at 4°C. 800 μ g of lysate was diluted with lysis buffer to a concentration of 1 μ g/ μ L. Complexes were immunoprecipitated with 2 μ g of the indicated antibody for an empirically derived period ranging between 2 to 16 hours. Antibody-antigen complexes were precipitated with ProteinA/G-agarose beads for 1 hour. Complexes were washed in lysis buffer 3-4 times for 5 minutes at 4°C. Samples were subsequently separated by SDS-PAGE and transferred to Immobilon-P polyvinylidene (PVDF) membranes. Ral-GTP pulldowns were performed as described previously (9). Immunoblot analysis was performed with the indicated antibodies and visualized with SuperSignal West Pico Chemiluminescent substrate (Pierce Chemical).

Coimmunoprecipitation kinase assay. Immunoprecipitates were prepared as described above. After the final wash in lysis buffer, the beads were rinsed 3 times in 1X Reaction buffer (25 mM MOPS pH 7.5, 1mM EGTA, 0.1mM Sodium Vanadate, 15mM MgCl₂, 5 mM β -glycerol phosphate). Then 30 μ L of reaction buffer containing 1mg of myelin basic protein (MBP) and 100 μ M ATP [10 μ Ci γ -³²P-ATP] was added to the beads to initiate the reaction. The reaction proceeded for 1 hour at 30°C with intermittent shaking to mix the beads. The reaction was terminated by adding 6X laemmli SDS sample buffer and boiling.

Immunofluorescence. Cells on coverslips were fixed in 3.7% formaldehyde in PBS for 15 minutes. Coverslips were rinsed twice in PBS, quenched in 50mM NH₄Cl in PBS for 15 minutes, rinsed twice in PBS, then permeabilized in 100 μ g/mL digitonin in PBS for 10 minutes on ice (Exception anti-RalA samples were permeabilized 5 minutes in -20°C acetone). Coverslips were rinsed twice in PBS and blocked in 2% BSA in PBS for 30-60

minutes at 37°C followed by incubation with primary antibodies diluted in 2% BSA in PBS for 1-2.5 hours at 37°C. Coverslips were then washed four times for 5 minutes in PBS and incubated with secondary antibodies diluted in 2% BSA in PBS for 1-1.5 hours at 37°C. Coverslips were then washed four times for 5 minutes in PBS. Coverslips stained with two primary antibodies, were subsequently stained with a second primary-secondary antibody combination. Coverslips were mounted on glass slides with either ProLong Gold mounting medium (Invitrogen) or Vectashield fluorescent mounting medium (Vector Labs). Secondary antibodies: DyLight 488 Donkey anti-Rabbit and DyLight 594 Donkey anti-Mouse were purchased from Jackson ImmunoResearch Laboratories, inc. Alexa Fluor 350 Donkey anti-Mouse and Alexa Fluor 647 Donkey anti-Mouse were purchased from Invitrogen.

Image capture and quantitation. Epifluorescence images (Figure 5I, 5L) were captured using appropriate excitation/emission filter sets (GFP, AlexaFluor 488) (Rhodamine, AlexaFluor 594) on a 40X objective on a Zeiss Axioplan 2E. Deconvolution confocal images (Figure 5J, 5N, 6A, 6F, 7A-7F, 10G, and 13C) were captured using appropriate filter sets (DAPI Excitation: 360/40, Emission: 457/50; FITC, Excitation: 490/20, Emission 526/38; TRITC Excitation: 555/28, Emission 617/63; Cy5 Excitation: 640/20, Emission: 685/40) and the 60X objective on an Applied Precision personal DV deconvolution microscope. Deconvolution confocal images of cells were captured as Z-section stacks and the stacked images underwent 10 iterations of restorative deconvolution. In Figure 5K, cellular fluorescence intensity was quantified by ImageJ. Briefly, cells were encircled using the freehand selection tool, each cell was saved as a region of interest, and the total fluorescence of each region of interest was measured for both FITC (anti-LC3) and TRITC (anti-Myc) channels using the measure function. In Figures 5M, 5O, 6D, 10H, 10I, and 13D images were blinded, mixed, and scored for punctae by the author. In Figure 6B and 6F, punctae were quantified in ImageJ. Briefly, images were background subtracted, then thresholds were optimized to differentiate negative control (siControl) and positive control (siAtg5) samples. The analyze particles function of ImageJ was utilized to quantitate punctae for all samples under identical conditions. Finally, the number of punctae per cell was calculated by division of the total

punctae per field divided by the number of nuclei per field. In Figure 6C and 13E, mean total fluorescence was calculated in ImageJ. Briefly, cells were selected in the GFP channel using the freehand selection tool and saved as regions of interest. Then, the mean fluorescence of each region of interest was measured in the GFP channel using the measure function.

***Salmonella typhimurium* Infection.** GFP-expressing *Salmonella typhimurium* (obtained from Mary O’Riordan, University of Michigan (162)) were grown overnight in LB medium at 37°C, shaking and back-diluted 1:100. When bacteria reached exponential phase, they were washed twice with PBS and used to infect Hela and HBEC30 cells at a multiplicity of infection 10 for 1 hour. Cells were then washed 3 times with PBS and incubated in medium containing 100µg/mL gentamicin for 2 hours. Cells were then washed 3 times with PBS and incubated in medium containing 5µg/mL gentamicin for 1 hour. Cells were then fixed and processed for immuno-fluorescence.

Superose 6 FPLC. MDCK cells were grown to confluence on 15 cm dishes. Cells were washed 1X with HDF before adding EBSS for 90 minutes. Cells were washed two times before lysis in DHE buffer (20mM HEPES, 150mM NaCl, 0.5% NP40, and the protease inhibitors Pefabloc, Antipain, Leupeptin, and Pepstatin A). Collected lysates were incubated on ice for 20 min, then cleared at 20,000 X g for 10 minutes at 4°C. The supernatant was filtered through 0.22µm filter and 0.5mL of filtered sample was injected into a Superose 6 column. The column was run at a flow rate of 0.2mL/min and 0.5mL fractions were collected. The collected samples were mixed with 100µL 6X Laemmli sample buffer and boiled.

Fly genetic methods

sca-GAL4 flies were provided by F. Schweisguth and *Sec5* and *Sec6* mutants were gifts of T. Schwarz. Other mutants were provided from Bloomington and Szeged stock centers. UAS-ds transgenic strains were provided by the Vienna Drosophila RNAi Center (VDRC) (163). The *w¹¹¹⁸* strain was used as a wild-type stock. Genetic interactions were performed using methods previously described (132, 164). For each genotype, at least

100 flies were examined and distributed into 4 classes according to their microchaete numbers: flies with no missing microchaetes (“wild-type”), with 1 to 10 (“weak”), 11 to 30 (“middle”), and >30 absent microchaetes (“strong”). Distributions were compared using a Chi-Square Goodness-of-Fit test.

siRNA sequences.

siControl oligos used were siGenome Non-targeting siRNA Pool #1 (Dharmacon Catalog #D-001206-13-05). Single oligos were used to deplete RalA (Figure 6F,G), RalB (Figure 6F,G), Sec5, Sec6, and Exo84:

5'-GACAGGUUUCUGUAGAAGAdTdT-3' (RalA)

5'-GGUGAUCAUGGUUGGCAGCdTdT-3' (RalB)

5'-GGUCGGAAAGACAAGGCAGdTdT-3' (Sec5)

5'-GGGAAGAGAAAAUUGACAGdTdT-3' (Sec6)

5'-GCCACUAAACAUCGCAACUdTdT-3' (Exo84)

siGenome pools were purchased from Dharmacon were used to deplete ATG5, Beclin1, ULK1, RalA (Figure 6A-C), RalB (Figure 6A-C), Exo70, Sec3, Sec8, Sec10, and Sec15: ATG5:

5'-GGAAUAUCCUGCAGAAGAA-3'

5'-CAUCUGAGCUACCCGGAUA-3'

5'-GACAAGAAGACAUUAGUGA-3'

5'-CAAUUGGUUUGCUAUUUGA-3'

Beclin1:

5'-CUAAGGAGCUGCCGUUAUA-3'

5'-GGAUGACAGUGAACAGUUA-3'

5'-UAAGAUGGGUCUGAAAUUU-3'

5'-GCCAACAGCUUCACUCUGA-3'

ULK1:

5'-CCUAAAACGUGUCUUAUUU-3'

5'-ACUUGUAGGUGUUUAAGAA-3'

5'-GGUUAGCCCUGCCUGAAUC-3'

5'-UGUAGGUGUUUAAGAAUUG-3'

RalA:

5'-GGACUACGCUGCAAUUAGA-3'

5'-GCAGACAGCUAUCGGAAGA-3'

5'-GAAAUUCGAGCGAGAAAGA-3'

5'-GAGCUAAUGUUGACAAGGU-3'

RalB:

5'-GAAAGAUGUUGCUUACUUAU-3'

5'-GAAAUUCAGAACAAAGAAGA-3'

5'-UACCAAAGCUGACAGUUAU-3'

5'-AGACAAGAAUGGCAAGAAA-3'

Exo70:

5'-GGUUAAGGUGACUGAUUAUU-3'

5'-GACCUUCGACUCCCUGAUUAUU-3'

5'-CUAAGCACCUAUAUCUGUAUU-3'

5'-CGGAGAAGUACAUCAAGUAUU-3'

Sec3:

5'-GAAAUUAAACUGGAUCUACU-3'

5'-GUAAAGUCAUUAAGGAGUA-3'

5'-GAAUGUAGCUCUUCGACCA-3'

5'-GAUUAUUUAUCCCGACUAU-3'

Sec8:

5'-GAAUUGAGCAUAAGCAUGU-3'

5'-UAACUGAGUACUUGGAUUAU-3'

5'-GCCGAGUUGUGCAGCGUAA-3'

5'-ACUGAGUGACCUUCGACUA-3'

Sec10:

5'-GAAGUCCGAUGCAGAGCAA-3'

5'-GGAGAUACCUUAUGACACA-3'

5'-GGAAAGAAUUAGACAGCGU-3'

5'-CAUUAGGAGUGGAUCGGAA-3'

Sec15:

5'-GAAGUUUGGUGAAUGGUAU-3'
5'-GUUGAUGGCUAUAGAAGAU-3'
5'-GAUAGAGACAGUCGUGAAA-3'
5'-CCAAACUCCGUGAGGAU-3'

ACKNOWLEDGEMENTS

We thank Noboru Mishuzima for GFP-Atg5 and GFP-LC3, Zhenyu Yue for Flag-ATG14L and Flag-RUBICON, and Noriko Okazaki for HA-ULK1 and HA-ULK1(K46N). We thank members of the White and Levine labs for productive discussions. We thank Melanie Cobb for helpful discussion and assistance with kinase assays. This work was supported by grants from the National Institutes of Health (CA71443 and CA129451 to MW, and CA84254 and CA109618 to BL), ARC4845 to JC, and the Welch Foundation (I-1414 to MW). BB was supported by DOD Award Number W81XWH-06-1-0749. RR was supported by T32GM008203. YO was supported by CPRIT RP101496.

FIGURE CREDITS

I performed all of the experiments presented in Part One with the following exceptions:
Figure 6B, Anthony Orvedahl, Ph.D. assisted with quantitation of the GFP-LC3 punctae.
Figure 7F, credit to Yu-Chen Chien, Ph.D.
Figure 8H, credit to Charles Clayton Hazelett and Charles Yeaman, Ph.D.
Figure 11F, kinase assay was performed by Eric M Wauson, Ph.D.
Figure 12A, credit to Rosalyn R Ram
Figure 13B, credit to Charles Clayton Hazelett
Figure 13C, credit to Charles Clayton Hazelett and Charles Yeaman, Ph.D.
Figure 14B, credit to Yi-Hung Ou
Table 3, credit to Maria Balakireva, Ph.D. and Jacques H. Camonis, Ph.D.

Part Two: Unpublished observations in support of Ral–exocyst regulation of autophagy

RalB exhibits polarized distribution on the surface of autophagosomes

RalB protein levels are stable during extended courses of autophagy induction (see Figure 9A), which suggests that RalB is not amongst the autophagosomal proteins and membranes which are degraded. This suggests two possibilities: (1) RalB is present only on the outer membrane of the double membrane autophagosome, and/or (2) RalB is trafficked away from the autophagosome before lysosomal fusion. This observation may also suggest that RalB only coats the outer membrane of the autophagosome. To investigate these possibilities, I performed three-dimensional reconstruction of confocal image stacks to investigate the distribution of RalB on the autophagosome (Figure 15).

Figure 15

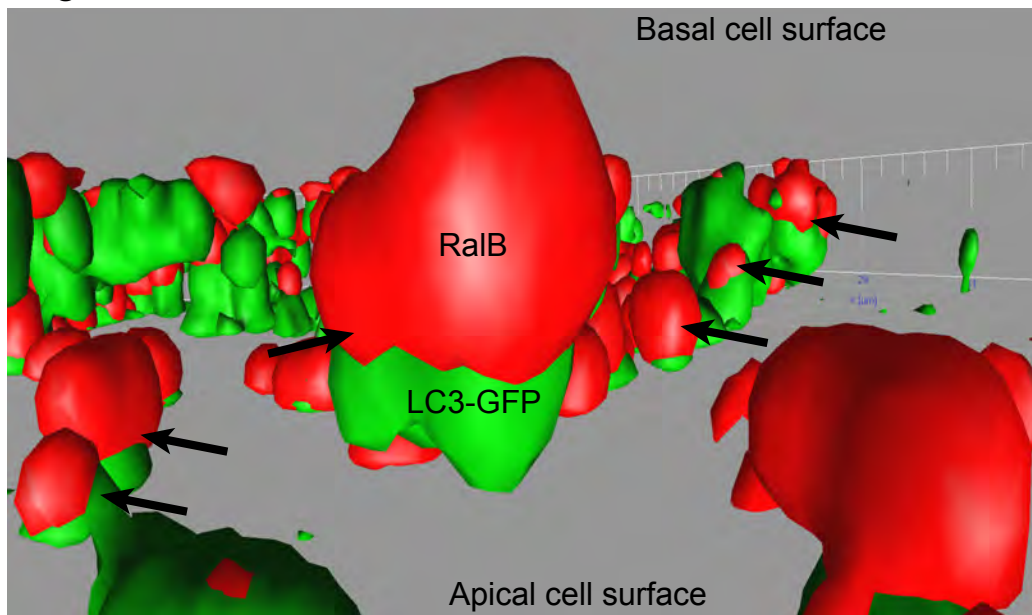


Figure 15: RalB exhibits polarized distribution on LC3-GFP punctae.

Confocal images underwent 3D modelling with IMARIS program.

Arrowheads indicate incidences of polarized RalB localization.

The polarized distribution of RalB on LC3-GFP punctae did advocate that RalB was present on the outer membrane of the autophagosome; however, it also revealed that RalB was localized to the “pole” of the autophagosome “globe” oriented to the basal cell surface. This polarity may be evidence of RalB involvement in a number of processes:

- (1) Fusion of the nascent autophagosome cup into the globular autophagosome
- (2) Recruitment and tethering of the lysosome to the autophagosome
- (3) Attachment of the autophagosome to the cytoskeletal network

In the least, it reveals a previously undescribed apical/basolateral polarity to the formed autophagosome, at least with regards to the localization of one protein, RalB, but perhaps this extends to many. There is some precedent at early stages of autophagosome biogenesis as it was reported that the isolation membrane cup has a polarized enrichment of PI-(3)-P at the tips and along the inner surface of the isolation membrane cup (165). Future study of the polarized distribution of RalB during the early stages of autophagosome biogenesis is certainly merited.

Deductive analysis of the exocyst subcomplex which regulates autophagy

As I stated in chapter two, we do not possess many of the tools that I believe would be necessary to accurately describe the composition of the Exo84-containing exocyst subcomplex which regulates autophagy. However, if I use deductive reasoning, then I may be able to approximate the composition of the subcomplex. First, recall that in chapter three, Figure 6D, only depletion of Sec3, Sec8, Exo70, and Exo84 reduced the number of autophagosomes formed in response to nutrient deprivation. Now, these observations do not rule out the presence of other exocyst subunits within the “autophagy subcomplex” as they may simply be more difficult to make limiting within the context of starvation induced autophagy. This experiment does, however, emphasize the importance of Sec3, Sec8, Exo70, and Exo84 during autophagosome biogenesis. In Table 2, I summarized the reported intra-exocyst complex interactions amongst exocyst subunits. According to these reports, it is within the realm of possibility to construct an exocyst subcomplex with just Sec3, Sec8, Exo70, and Exo84, as Sec3 interacts with Sec8. Sec8 interacts with Exo70, and Exo70 interacts with Exo84. In part one of this chapter, I described how Beclin1 and ULK1 associate with each other and Exo84 in a Ral-dependent fashion (Figures 9B, 11B). By compiling yeast two hybrid results, one can see that the RNAi-implicated exocyst subcomplex consisting of Sec3, Sec8, Exo70, and Exo84 contain all of the binding activities necessary to associate with ULK1 and Beclin1 by directly assembling with their first-degree interaction neighborhood—FIP200 and

Rubicon, ATG14L, and VPS34, respectively (Figure 16). The interaction map in Figure 16 also emphasizes the importance of Sec3 in bridging key interactions between the exocyst subcomplex and FIP200, RUBICON, and ATG14L. Exo70 and Sec8 appear to serve simply as bridging proteins to link Sec3 and Exo84; however, they also may provide docking sites for undiscovered interacting proteins that may contribute to autophagosome biogenesis as well. RalB-GTP induced Exo84 assembly with Beclin1 is likely independent of Sec3 or Exo70 because Exo84 required only the N-terminal Bcl-2 binding domain of Beclin1 (88-150), which is dispensable for interaction with ATG14L and VPS34 (138, 145, 166). I observed that Exo84 was necessary for RalB to assemble ULK1 and Beclin1 into complex (Figure 11C), which suggests that Sec3 may bring ULK1 into complex with the exocyst autophagy subcomplex, and RalB-induced assembly of Beclin1 on Exo84 facilitates ULK1-Beclin1 complex formation.

Figure 16

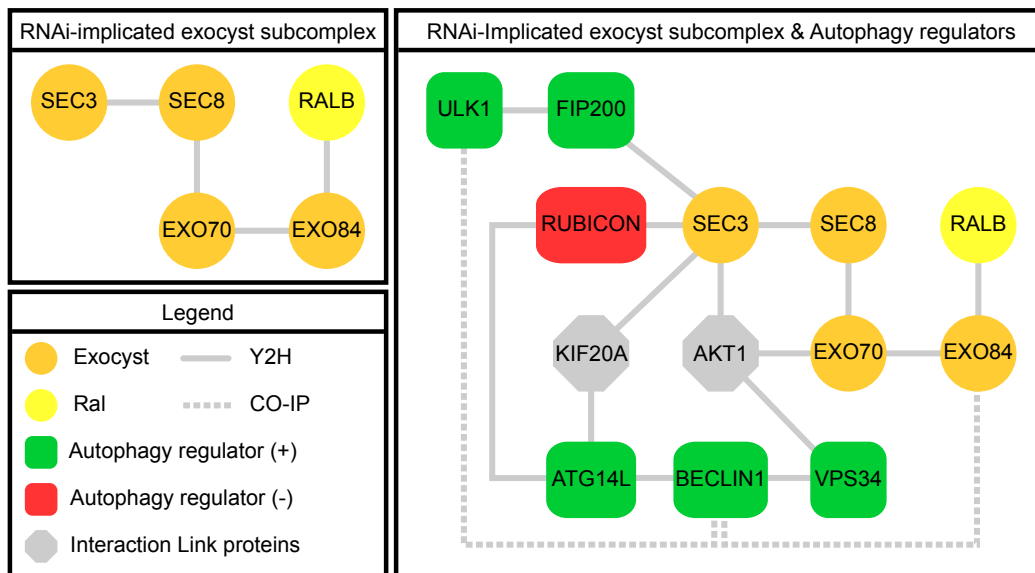


Figure 16: Exo84 subcomplex autophagy interaction network.

The subcomplex of the exocyst implicated by RNAi contain all the binding activities necessary for assembly with autophagy regulators Beclin1 and ULK1 and their associated binding partners.

CHAPTER FOUR

Part One: RalA is a positive regulator of cell growth signaling pathways

The Ral proteins are nearly identical, having only recently, evolutionarily speaking, diverged into separate genes; however, when RalA and RalB were depleted from cancer cells, their function appeared to be in stark opposition. RalA depletion reduced anchorage independent growth, and RalB depletion caused cancer cell death (9, 12). Co-depletion of both proteins reversed the defect in cancer cell survival, but not anchorage independent growth (12). As outlined in chapter two, these observations highlight that the pathways regulated by RalA and RalB can be cooperative, independent, and/or in opposition. The regulation of growth phenotypes by RalA appears to be independent and in opposition to the renewal phenotype (autophagy) regulated by RalB.

A brief introduction to amino acid regulation of mTORC1

The mammalian target of rapamycin (mTOR) is a key regulator of growth signaling. There are two distinct mTOR complexes, which are designated mTORC1 and mTORC2. mTORC2 is activated by insulin and mediates the activation of numerous downstream pathways including the activation of mTORC1 by direct phosphorylation of Akt, one of mTORC1's upstream regulators. mTORC1 is an important signal integrator which regulates growth and proliferation through modulation of protein synthesis. The signals which are integrated on mTORC1 include oxygen tension, energy availability, and nutrient availability. In other words, mTORC1 signals to the cell when conditions are appropriate for growth and proliferation. mTORC1 also inhibits the induction of autophagy by direct inhibitory phosphorylation of the key autophagy regulator ULK1; therefore, mTORC1 *promotes* growth and *inhibits* renewal.

The regulation of mTORC1 is intricate (reviewed in (167)); however, for the purpose of this thesis I will focus on how amino acids are sensed by mTORC1 because amino acids have a robust effect on regulating the formation of autophagosomes. I hypothesize that efficient utilization of nutrients provides a distinct advantage within a population of unicellular organisms, and because mammals evolved from *successful*

(proliferating) unicellular organisms, our signaling networks reflect that preference for efficiency. This efficiency is apparent within the amino acid paradigm with the cell:

- (1) When amino acids are available, mTORC1 is active, amino acid utilization by protein synthesis is increased, and autophagy (a mechanism for generating amino acids) is suppressed.
- (2) When amino acids are depleted, mTORC1 is inactive, amino acid utilization by protein synthesis is decreased, and autophagy (a mechanism for generating amino acids) is activated.

Not all amino acids are equal in their ability to activate mTORC1—the branched chain amino acid, L-leucine, is sufficient to activate mTORC1 and protein translation (168, 169). In addition, the SLC7A5/SLC3A2 bidirectional transporter regulates the simultaneous efflux of intracellular L-glutamine and influx of extracellular L-leucine (170). There is an emerging story that L-leucine can activate mTORC1 through direct binding to the heterodimer of TAS1R1 and TAS1R3 G-protein coupled receptors in pancreatic β -islet cells (171). The TAS1R1/3 L-leucine receptor triggered mTORC1 activation in a process which involves the release of intracellular Ca^{2+} stores (171).

mTORC1 localization is described to be diffuse during amino acid deprivation, but upon stimulation with amino acids (including L-leucine and L-glutamine), mTORC1 localizes to lysosomes (172). mTORC1 is tethered to the lysosome in an amino acid dependent fashion by a multiprotein complex called the Ragulator. The Ragulator constitutively localizes the G-protein heterodimers, RagA/RagC and RagB/RagD, to the lysosome (172). When amino acids are rich, the active heterodimers, RagA·GTP/RagC·GDP and RagB·GTP/RagD·GDP, are formed, and these active heterodimers are able to bind to the mTORC1 specific mTOR adaptor protein, Raptor (173). The proton-assisted amino acid transporters, PAT1 and PAT4, mediate efflux of amino acids from acidified compartments, and strangely, these transporters are necessary for mTORC1 activation by exogenously introduced amino acids (174). In addition, the lysosomes themselves undergo nutrient dependent positioning—under rich conditions lysosomes are present at the periphery, but under deprived conditions, lysosomes cluster at a perinuclear region (175). In the absence of an extracellular supply of amino acids, autophagy contributes an important source of amino acids to the cell, and the regulation

of mTORC1 on lysosomes reflects the tight coupling between amino acid utilization and generation (by autophagolysosomes).

The small G-protein Rheb is a critical regulator of mTOR. Under nutrient poor conditions, mTOR is bound upstream of its kinase domain by FKBP38 (176). When nutrients are rich, Rheb is activated, and Rheb·GTP binds tightly to FKBP38 relieving its inhibition on mTORC1. The regulation of Rheb·GTP levels is accomplished by the Rheb specific GAP, TSC1/2 (tuberous sclerosis tumor suppressor complex 1/2) (177). The TSC1/2 complex is a regulatory node in mTORC1 regulation, and it is regulated by numerous positive and negative phosphorylation events (reviewed in (167)). Amongst these events, is the inhibition of TSC1/2 (activation of mTORC1) by Akt phosphorylation of TSC2 at Ser-939 and Thr-1462 (178, 179). Akt is described to transduce the presence of insulin to mTORC1 because Akt is robustly phosphorylated at Ser-473 by mTORC2 in response to insulin administration (180). However, mTORC1 can still be activated by amino acids (to a lesser amplitude) in the absence of insulin. Akt is reported to be necessary for this activation, and mTORC2 was necessary for the activation of Akt (181). Thus, it appears that both insulin and amino acids stimulate mTORC1 through an mTORC2 → Akt signaling pathway, but I choose to classify insulin as an mTORC1 “state amplifier” because it is not able to activate mTORC1 in the absence of amino acids. This classification is only relevant in the context of studying the signaling pathways, because in the context of the human body, insulin is released in response to feeding, therefore, a high insulin, low amino acid condition may not represent a physiologically relevant scenario.

The autophagy regulator, VPS34, has also been implicated in nutrient sensing. VPS34 overexpression was sufficient to induce phosphorylation of S6K1 at Thr-389, a site commonly used to measure mTORC1 activity, and this effect is insulin independent (182, 183). Pan-cellular VPS34 activity is decreased upon amino acid or glucose starvation, but is rapamycin-insensitive, so VPS34 is not acting downstream of mTORC1 (182, 183). Amino acids are described to increase intracellular calcium concentration, $[Ca^{2+}]_i$, and calcium chelators block amino acid induced S6K1 phosphorylation at Thr-389 (184). The reported mechanism is that increased $[Ca^{2+}]_i$ stabilizes the binding of calcium-bound Calmodulin to a conserved Calmodulin binding domain within VPS34,

thereby activating VPS34 (184). Intriguingly, in the absence of amino acids, increased $[Ca^{2+}]$ alone was sufficient to induce phosphorylation of mTORC1 targets without activation of Akt or MAPK. In addition, this activation was rapamycin insensitive, but required VPS34 and Rheb (184). These data are highly controversial; however, I hope to provide some clarity by the end of this chapter.

RalA regulates mTORC1 activation in response to amino acids

Depletion of RalA was reported to markedly reduce (~20–30% of control) the phosphorylation of Ser-389 on S6K1 in response to amino acids or glucose re-feeding but not insulin re-stimulation (152). In contrast, depletion of RalB modestly reduced (~70–80% of control) phosphorylation of Ser-389 on S6K1 in response to amino acids or glucose re-feeding but not insulin re-stimulation (152). RalA functions downstream of Rheb in mTORC1 activation:

- (1) RalA depletion inhibited dominant-active Rheb(S16H)-mediated S6K1 phosphorylation [113].
- (2) Dominant-active RalA(Q72L) overexpression was sufficient to restore amino acid induced S6K1 phosphorylation in cells overexpressing dominant-negative Rheb(S20N) [113].

Consistent with observations in cytokinesis, RalGDS depletion mimicked the effects of RalA depletion, reduced (~10–20% of control) phosphorylation of Ser-389 on S6K1 in response to amino acids or glucose re-feeding but not insulin re-stimulation (152). As expected, inhibition of Ral–effector binding by overexpression of the Ral Binding Domain (RBD) of Sec5 also suppressed amino acid induced S6K1 phosphorylation (152). Although the exact mechanism by which RalA contributes to mTORC1 activation was not reported, it may be related to Vps34 activation. In cells growing under nutrient rich conditions, a probe for PI-(3)-P, GFP-2X-Fyve, was distributed diffusely throughout the cytosol; however, when Ral–effector binding was inhibited by overexpression of Rlip(RBD), the probe did not distribute widely and instead became concentrated in a perinuclear compartment (Figure 17). These data suggest that either RalA or RalB is important for the trafficking or activation of VPS34 away from this perinuclear compartment. Future studies are merited to investigate whether depletion of RalA, RalB,

or both is sufficient to affect the distribution of GFP-2X-Fyve under nutrient rich conditions. It will also be important to measure Vps34-mTOR association when Ral-effector signaling is disrupted by Rlip(RBD) overexpression.

Figure 17

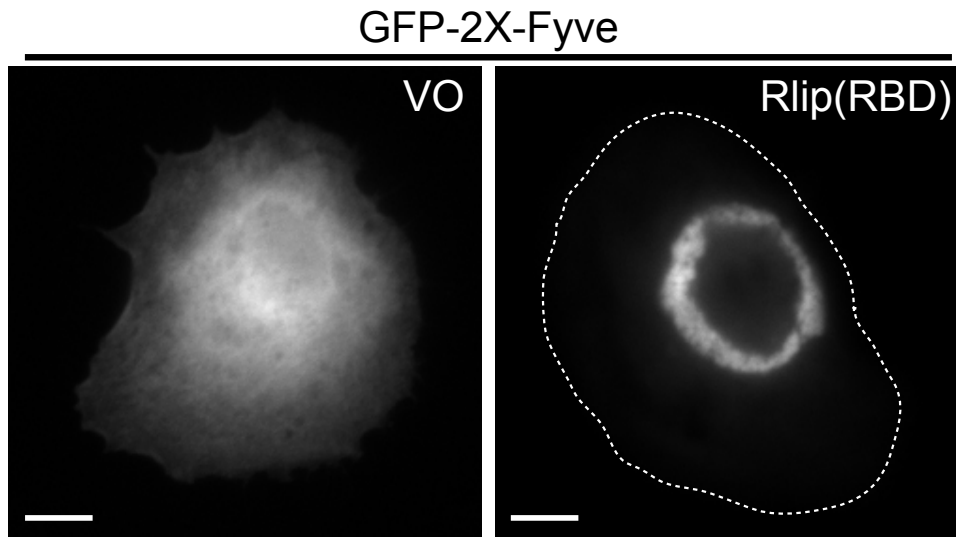


Figure 17: Rlip(RBD) disrupts GFP-2X-Fyve distribution.

PI-(3)-P probe GFP-2X-Fyve was co-expressed with vector control (vo) or Rlip(RBD) in HBEC30 cells. Scale bar 10 μ m.

Part Two: The exocyst is a proximal integrator of both growth and renewal signaling pathways

Sec5 is a central assembly point for regulators of cell growth and cell renewal

In contrast to Exo84, Sec5 was dispensable for autophagosome formation (Figure 6B-D). However, under nutrient rich conditions, Sec5 assembled with Beclin1, VPS34, and ULK1 (Figure 6B, 10B, 11E), and Sec5 but not Exo84 associated with mTORC1 (Figure 14B). It follows that Sec5 may facilitate the assembly of VPS34 and mTORC1 during nutrient rich conditions. These observations also illustrate that Sec5 is centrally placed to mediate crosstalk between both growth and renewal pathways. Consistent with this assertion, RalB required association with both Sec5 and Exo84 to fully assemble VPS34 with Exo84 (Figure 18A). However, RalB required association with only Sec5 to disassemble VPS34 from Sec5 (Figure 18B). These data suggest that disassembly of

VPS34 from Sec5 may be necessary for loading VPS34 into complex with Exo84. Because VPS34 has been implicated in both mTORC1 activation (182, 183) and autophagosome formation, it is tempting to speculate that the identity of the exocyst subcomplex that VPS34 associates with determines the outcome of VPS34 activity (Sec5: mTORC1 activation, Exo84: autophagy biogenesis).

Figure 18

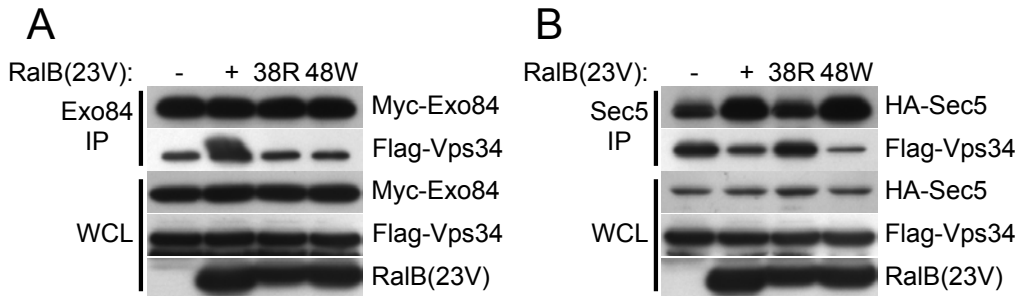


Figure 18: RalB-induced assembly of Exo84 and VPS34 requires dual subunit interactions. (A,B) The indicated proteins were overexpressed in HEK293 cells, then immunoprecipitated with an antibody directed to the specified tag. Immunoprecipitates were analyzed for coprecipitation with Flag-VPS34. Whole-cell lysate: WCL, immunoprecipitation: IP.

As described in chapter two, Sec5 is a key regulator of TBK1 during viral infection. Recently, it was reported that TBK1 forms a co-activation complex with Akt during viral infection, glucose stimulation, and EGF stimulation (185). Both TBK1 and Akt associated with the exocyst complex; however, Akt was always present in complex with the exocyst, while TBK1 was recruited in response to glucose stimulation (185). These data suggest that Akt may represent an interaction node for the exocyst, and the activity of exocyst-associated Akt, may be regulated by the recruitment of upstream kinases such as TBK1 or mTORC2. Depletion of both TBK1 and Sec3 reduced baseline Ser-473 phosphorylation of Akt (185). Thus, Sec3 appears to be a functional hub for both cell growth and cell renewal signaling. TBK1 and Akt form a complex *in vitro*, and TBK1 can phosphorylate Akt on both Thr-308 and Ser-473, which suggests that TBK1 may represent a PI-(3)-K independent mechanism for Akt activation (185). Glucose stimulation of Akt and mTORC1 activity was ablated in TBK1^{-/-} MEFs (185). Insulin stimulation of Akt and mTORC1 activity was blunted in cells knocked out for TBK1 and

its closely related homologue, IKK ϵ (186). Thus, TBK1 appears to be an important mediator of nutrient stimulation of cell growth through Akt and mTORC1. Consistently, TBK1 depletion inhibits amino acid induced activation of Akt and mTORC1 (Figure 19).

Figure 19

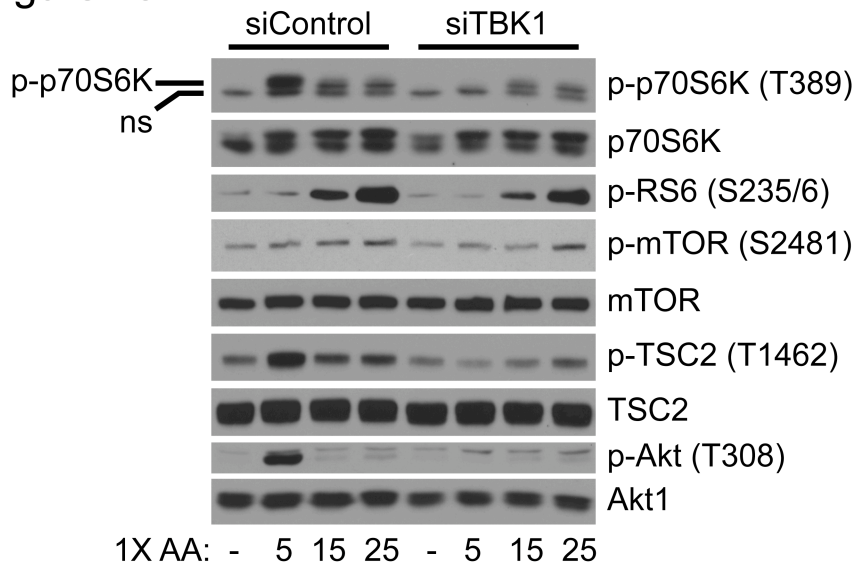


Figure 19: TBK1 is required for mTORC1 activation.

HEK-293 cells were transfected with the indicated oligos for 72 hours, starved of amino acids for 2 hours, loaded with 1mM L-glutamine and 10 μ g/mL insulin for 1 hour, then stimulated for the indicated times with 1X essential amino acids. (ns) non-specific band.

Future studies should focus on how RalA, RalB, and the exocyst or a subcomplex of the exocyst contributes to amino acid induced activation of Akt and mTORC1. Specifically:

- (1) Deplete RalA, RalB, and each exocyst subunit and measure amino acid induced mTORC1 activation.
- (2) Deplete RalA, RalB, and each exocyst subunit and measure amino acid induced mTORC1 localization to peripheral versus perinuclear lysosomes.
- (3) Measure the activity of the exocyst associated kinase pools of TBK1, Akt, mTORC1, and mTORC2 during glucose and amino acid stimulation.

As mentioned earlier, the heterodimeric TAS1R1/3 G-protein coupled taste receptors mediate L-leucine detection in pancreatic β -islet cells (171). In gustatory cells and pancreatic β -islet cells, the TAS1R1/3 receptor is displayed on the cells surface, which

seems appropriate for the function of these cells as ‘professional’ amino acid sensors (171, 187, 188). To investigate whether the TAS1R1/3 receptor regulates mTORC1 activation in non-‘professional’ amino acid sensing cells, I depleted the receptor from HEK-293 cells. Upon depletion of TAS1R1/3, amino acid mediated Akt phosphorylation of TSC2 and mTORC1 activation was delayed (Figure 20). The observation that amino acid sensing was delayed but not inhibited suggests there may be multiple mechanisms or multiple phases to mTORC1 activation by amino acids.

Figure 20

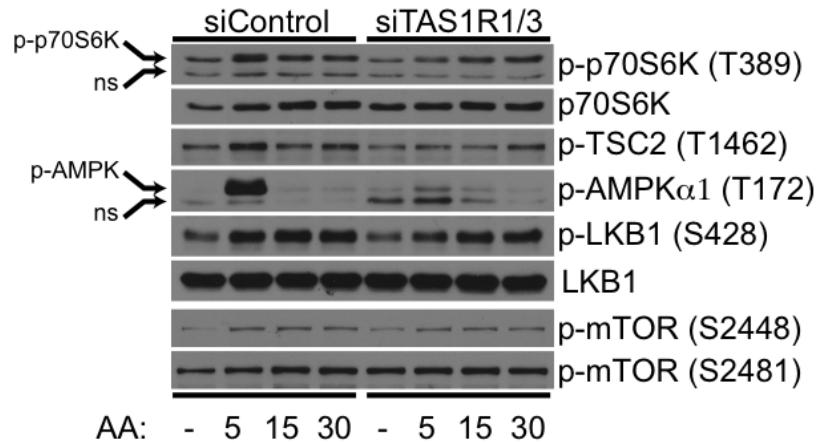


Figure 20: The TAS1R1/3 L-leucine receptor is required for mTORC1 activation. HEK-293 cells were transfected with the indicated oligos for 72 hours, starved of amino acids for 2 hours, loaded with 1mM L-glutamine and 10μg/mL insulin for 1 hour, then stimulated for the indicated times with 1X essential amino acids.

Surprisingly, activation of AMPK and its upstream regulator LKB1 was also blunted by depletion of TAS1R1/3 suggesting crosstalk between amino acid and energy sensing pathways (Figure 20). These results are preliminary but suggest that the TAS1R1/3 may contribute to amino acid sensing in a wide range of cell types. Future studies are merited.

The involvement of TAS1R1/3 provides a tempting scenario where increased $[Ca^{2+}]_i$ initiated by L-leucine binding to the TAS1R1/3 receptor triggers activation of a CaM–Vps34–mTORC1 complex. A subcomplex containing at least Sec5 and Sec3 may act to organize the assembly of the CaM–Vps34–mTORC1 complex. The presence of TBK1 and Akt within the complex may act to relieve inhibition of Rheb by phosphorylation of the Rheb GAP, TSC1/2. In addition, RalA may act as a trigger for the assembly and mobilization of this mTORC1 exocyst subcomplex as increased $[Ca^{2+}]_i$ has

previously been reported to trigger RalA association with a CaM-Myo1C actin motor complex (100). This may account for why inhibition of Ral-effector coupling with Rlip(RBD) disrupted the distribution of PI-(3)-P during nutrient rich conditions (Figure 17). This pathway may only mediate ‘fast-sensing’ of amino acids, and may be dispensable for the sensing of amino acids generated by lysosomes, which may account for why Vps34 is dispensable for TORC1 function in *D. Melanogaster* (189). If so, inhibition of lysosomal maturation would exaggerate the importance of the ‘fast-sensing’ amino acid sensor, and this experiment is certainly merited in the future.

Figure 21

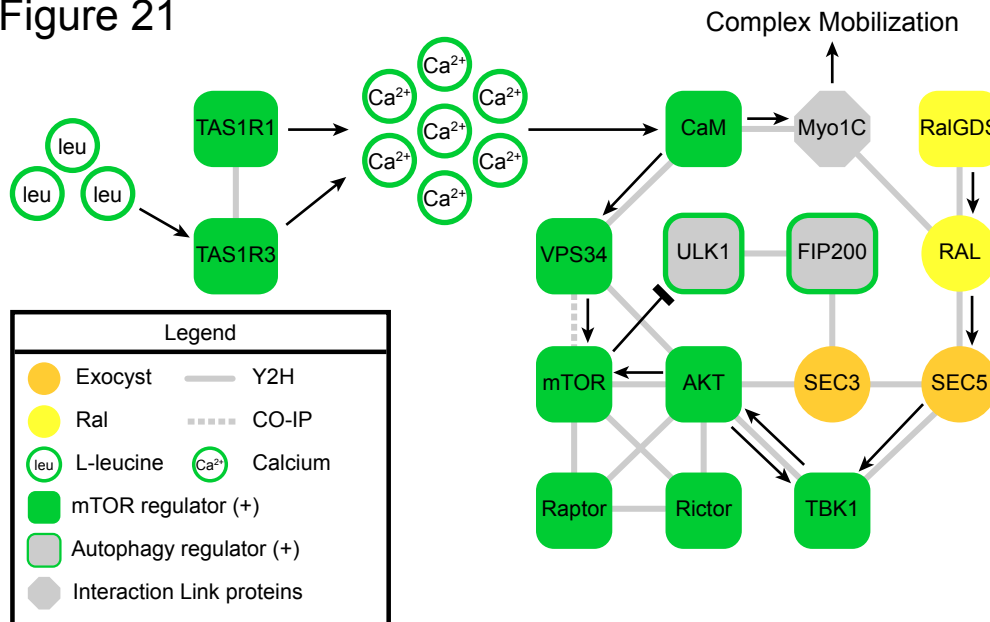


Figure 21: mTORC1 exocyst subcomplex regulation/interaction network. Sec5 and Sec3 are central interaction hubs for regulatory components of mTORC1. Arrows mark how signals may be transduced to mTOR during leucine rich conditions.

These observations, which are summarized in Figure 21, suggest ‘fast-sensing’ of amino acids may take place through the following steps:

- (1) L-leucine binds to TAS1R1/3 triggering increased $[Ca^{2+}]_i$
- (2) L-leucine somehow stimulates RalGDS to activate RalA, which in turn, triggers the assembly and activation of TBK1 into the complex.

- (3) TBK1 activates Akt, which then triggers Rheb activation through phosphorylation and inhibition of TSC1/2.
- (4) Rheb·GTP binds to FKBP38, relieving its inhibition on mTOR.
- (5) Increased $[Ca^{2+}]_i$ facilitates the assembly of active CaM–Vps34–mTORC1 and CaM–Myo1C–RalA complexes.
- (6) The fully assembled complex is activated and mobilized throughout the cell periphery along actin cables, and the kinase activity of the Sec3-associated autophagy regulator ULK1 is inhibited by direct phosphorylation by mTORC1, which allows high fidelity engagement of cell growth (amino acid utilization) while suppressing cell renewal (autophagy).

Much work remains to be done to elaborate whether such a system is utilized within the cell, but given the information I have now, it is a tempting hypothesis.

MATERIALS AND METHODS

Figure 17. GFP 2X-Fyve was transiently over-expressed in HBEC30 cells plated to acid washed coverslips. Three hours before fixation, cells were stimulated with fresh growth medium (defined Keratinocyte Medium with supplements, Invitrogen). Cells were fixed in 3.7% Formaldehyde in PBS mounted in Vectashield.

Figure 18. Co-expression co-immunoprecipitations were performed as described in Chapter 3.

Figure 19 & 20. Cells were transfected with siRNAs targeting the indicated proteins for 72 hours, then starved in EBSS for two hours. Then, cells were pre-loaded with 1mM L-Glutamine and 10 μ g/mL insulin for 1 hour before stimulation with 1X Essential amino acids for the times indicated. siGenome siRNA Pools targeting TAS1R1 and TAS1R3 were purchased from Dharmacon and combined equally to create a single pool of siRNAs targeting both proteins. A single siRNA sequence targeting TBK1 was used and has been previously described (9).

CONCLUDING REMARKS

During my graduate career, I set out to learn about the spatial and temporal regulation of signaling pathways by small G-proteins. In this goal, I believe I was successful; however, I was surprised to learn something fundamental to cell biology that would improve my own health and well being—the balance between growth and renewal pathways within cells and within the body is critical to maintaining high fidelity function. Prior to this study, I had been enjoying three meals a day with almost no interruption for most of my adult life, and yet, these studies revealed the critical nature of fasting periods to engage cell renewal pathways. I have since adapted periodic fasting as a tool to stimulate renewal of the cells which make up my own body, and I have been delighted with the results. I hope the reader of this thesis may also consider the benefits of fasting-stimulated cell renewal for their own health and well being.

BIBLIOGRAPHY

1. Chardin P, Tavittian A. The ral gene: a new ras related gene isolated by the use of a synthetic probe. *EMBO J.* 1986;5(9):2203-8. PMID: 1167101.
2. Colicelli J. Human RAS superfamily proteins and related GTPases. *Sci STKE.* 2004;2004(250):RE13. PMID: 2828947.
3. Camonis JH, White MA. Ral GTPases: corrupting the exocyst in cancer cells. *Trends Cell Biol.* 2005;15(6):327-32.
4. Feig LA. Ral-GTPases: approaching their 15 minutes of fame. *Trends Cell Biol.* 2003;13(8):419-25.
5. Feig LA, Urano T, Cantor S. Evidence for a Ras/Ral signaling cascade. *Trends Biochem Sci.* 1996;21(11):438-41.
6. Hamad NM, Elconin JH, Karnoub AE, Bai W, Rich JN, Abraham RT, et al. Distinct requirements for Ras oncogenesis in human versus mouse cells. *Genes Dev.* 2002;16(16):2045-57. PMID: 186434.
7. Rangarajan A, Hong SJ, Gifford A, Weinberg RA. Species- and cell type-specific requirements for cellular transformation. *Cancer Cell.* 2004;6(2):171-83.
8. Ward Y, Wang W, Woodhouse E, Linnoila I, Liotta L, Kelly K. Signal pathways which promote invasion and metastasis: critical and distinct contributions of extracellular signal-regulated kinase and Ral-specific guanine exchange factor pathways. *Mol Cell Biol.* 2001;21(17):5958-69. PMID: 87314.
9. Chien Y, Kim S, Bumeister R, Loo YM, Kwon SW, Johnson CL, et al. RalB GTPase-mediated activation of the IkappaB family kinase TBK1 couples innate immune signaling to tumor cell survival. *Cell.* 2006;127(1):157-70.
10. Lim KH, Baines AT, Fiordalisi JJ, Shipitsin M, Feig LA, Cox AD, et al. Activation of RalA is critical for Ras-induced tumorigenesis of human cells. *Cancer Cell.* 2005;7(6):533-45.
11. Lim KH, O'Hayer K, Adam SJ, Kendall SD, Campbell PM, Der CJ, et al. Divergent roles for RalA and RalB in malignant growth of human pancreatic carcinoma cells. *Curr Biol.* 2006;16(24):2385-94.
12. Chien Y, White MA. RAL GTPases are linchpin modulators of human tumour-cell proliferation and survival. *EMBO Rep.* 2003;4(8):800-6. PMID: 1326339.
13. Falsetti SC, Wang DA, Peng H, Carrico D, Cox AD, Der CJ, et al. Geranylgeranyltransferase I inhibitors target RalB to inhibit anchorage-dependent growth and induce apoptosis and RalA to inhibit anchorage-independent growth. *Mol Cell Biol.* 2007;27(22):8003-14. PMID: 2169159.

14. Sablina AA, Chen W, Arroyo JD, Corral L, Hector M, Bulmer SE, et al. The tumor suppressor PP2A Abeta regulates the RalA GTPase. *Cell*. 2007;129(5):969-82. PMID: 1945132.
15. Baysal BE, Willett-Brozick JE, Taschner PE, Dauwerse JG, Devilee P, Devlin B. A high-resolution integrated map spanning the SDHD gene at 11q23: a 1.1-Mb BAC contig, a partial transcript map and 15 new repeat polymorphisms in a tumour-suppressor region. *Eur J Hum Genet*. 2001;9(2):121-9.
16. Calin GA, di Iasio MG, Caprini E, Vorechovsky I, Natali PG, Sozzi G, et al. Low frequency of alterations of the alpha (PPP2R1A) and beta (PPP2R1B) isoforms of the subunit A of the serine-threonine phosphatase 2A in human neoplasms. *Oncogene*. 2000;19(9):1191-5.
17. Takagi Y, Futamura M, Yamaguchi K, Aoki S, Takahashi T, Saji S. Alterations of the PPP2R1B gene located at 11q23 in human colorectal cancers. *Gut*. 2000;47(2):268-71. PMID: 1727986.
18. Tamaki M, Goi T, Hirono Y, Katayama K, Yamaguchi A. PPP2R1B gene alterations inhibit interaction of PP2A-Abeta and PP2A-C proteins in colorectal cancers. *Oncol Rep*. 2004;11(3):655-9.
19. Wang SS, Esplin ED, Li JL, Huang L, Gazdar A, Minna J, et al. Alterations of the PPP2R1B gene in human lung and colon cancer. *Science*. 1998;282(5387):284-7.
20. Wu JC, Chen TY, Yu CT, Tsai SJ, Hsu JM, Tang MJ, et al. Identification of V23RalA-Ser194 as a critical mediator for Aurora-A-induced cellular motility and transformation by small pool expression screening. *J Biol Chem*. 2005;280(10):9013-22.
21. Bivona TG, Quatela SE, Bodemann BO, Ahearn IM, Soskis MJ, Mor A, et al. PKC regulates a farnesyl-electrostatic switch on K-Ras that promotes its association with Bcl-XL on mitochondria and induces apoptosis. *Mol Cell*. 2006;21(4):481-93.
22. Hanahan D, Weinberg RA. The hallmarks of cancer. *Cell*. 2000;100(1):57-70.
23. Bissell MJ, Radisky D. Putting tumours in context. *Nat Rev Cancer*. 2001;1(1):46-54. PMID: 2975572.
24. Yin J, Pollock C, Tracy K, Chock M, Martin P, Oberst M, et al. Activation of the RalGEF/Ral pathway promotes prostate cancer metastasis to bone. *Mol Cell Biol*. 2007;27(21):7538-50. PMID: 2169046.
25. Oxford G, Smith SC, Hampton G, Theodorescu D. Expression profiling of Ral-depleted bladder cancer cells identifies RREB-1 as a novel transcriptional Ral effector. *Oncogene*. 2007;26(50):7143-52.

26. Smith SC, Oxford G, Wu Z, Nitz MD, Conaway M, Frierson HF, et al. The metastasis-associated gene CD24 is regulated by Ral GTPase and is a mediator of cell proliferation and survival in human cancer. *Cancer Res.* 2006;66(4):1917-22.
27. Gonzalez-Garcia A, Pritchard CA, Paterson HF, Mavria G, Stamp G, Marshall CJ. RalGDS is required for tumor formation in a model of skin carcinogenesis. *Cancer Cell.* 2005;7(3):219-26.
28. Cantor SB, Urano T, Feig LA. Identification and characterization of Ral-binding protein 1, a potential downstream target of Ral GTPases. *Mol Cell Biol.* 1995;15(8):4578-84. PMID: 230698.
29. Jullien-Flores V, Dorseuil O, Romero F, Letourneur F, Saragosti S, Berger R, et al. Bridging Ral GTPase to Rho pathways. RLIP76, a Ral effector with CDC42/Rac GTPase-activating protein activity. *J Biol Chem.* 1995;270(38):22473-7.
30. Frankel P, Aronheim A, Kavanagh E, Balda MS, Matter K, Bunney TD, et al. RalA interacts with ZONAB in a cell density-dependent manner and regulates its transcriptional activity. *EMBO J.* 2005;24(1):54-62. PMID: 544910.
31. Moskalenko S, Henry DO, Rosse C, Mirey G, Camonis JH, White MA. The exocyst is a Ral effector complex. *Nat Cell Biol.* 2002;4(1):66-72.
32. Sugihara K, Asano S, Tanaka K, Iwamatsu A, Okawa K, Ohta Y. The exocyst complex binds the small GTPase RalA to mediate filopodia formation. *Nat Cell Biol.* 2002;4(1):73-8.
33. Moskalenko S, Tong C, Rosse C, Mirey G, Formstecher E, Daviet L, et al. Ral GTPases regulate exocyst assembly through dual subunit interactions. *J Biol Chem.* 2003;278(51):51743-8.
34. Jullien-Flores V, Mahe Y, Mirey G, Leprince C, Meunier-Bisceuil B, Sorkin A, et al. RLIP76, an effector of the GTPase Ral, interacts with the AP2 complex: involvement of the Ral pathway in receptor endocytosis. *J Cell Sci.* 2000;113 (Pt 16):2837-44.
35. Nakashima S, Morinaka K, Koyama S, Ikeda M, Kishida M, Okawa K, et al. Small G protein Ral and its downstream molecules regulate endocytosis of EGF and insulin receptors. *EMBO J.* 1999;18(13):3629-42. PMID: 1171441.
36. Singhal SS, Awasthi YC, Awasthi S. Regression of melanoma in a murine model by RLIP76 depletion. *Cancer Res.* 2006;66(4):2354-60.
37. Singhal SS, Singhal J, Yadav S, Dwivedi S, Boor PJ, Awasthi YC, et al. Regression of lung and colon cancer xenografts by depleting or inhibiting RLIP76 (Ral-binding protein 1). *Cancer Res.* 2007;67(9):4382-9.

38. Panner A, Nakamura JL, Parsa AT, Rodriguez-Viciano P, Berger MS, Stokoe D, et al. mTOR-independent translational control of the extrinsic cell death pathway by RalA. *Mol Cell Biol.* 2006;26(20):7345-57. PMID: 1636864.
39. de Ruiter ND, Wolthuis RM, van Dam H, Burgering BM, Bos JL. Ras-dependent regulation of c-Jun phosphorylation is mediated by the Ral guanine nucleotide exchange factor-Ral pathway. *Mol Cell Biol.* 2000;20(22):8480-8. PMID: 102154.
40. Henry DO, Moskalenko SA, Kaur KJ, Fu M, Pestell RG, Camonis JH, et al. Ral GTPases contribute to regulation of cyclin D1 through activation of NF-kappaB. *Mol Cell Biol.* 2000;20(21):8084-92. PMID: 86418.
41. Chang L, Kamata H, Solinas G, Luo JL, Maeda S, Venuprasad K, et al. The E3 ubiquitin ligase itch couples JNK activation to TNFalpha-induced cell death by inducing c-FLIP(L) turnover. *Cell.* 2006;124(3):601-13.
42. Micheau O, Lens S, Gaide O, Alevizopoulos K, Tschopp J. NF-kappaB signals induce the expression of c-FLIP. *Mol Cell Biol.* 2001;21(16):5299-305. PMID: 87253.
43. Balda MS, Matter K. The tight junction protein ZO-1 and an interacting transcription factor regulate ErbB-2 expression. *EMBO J.* 2000;19(9):2024-33. PMID: 305688.
44. Kavanagh E, Buchert M, Tsapara A, Choquet A, Balda MS, Hollande F, et al. Functional interaction between the ZO-1-interacting transcription factor ZONAB/DbpA and the RNA processing factor symplekin. *J Cell Sci.* 2006;119(Pt 24):5098-105.
45. Balda MS, Garrett MD, Matter K. The ZO-1-associated Y-box factor ZONAB regulates epithelial cell proliferation and cell density. *J Cell Biol.* 2003;160(3):423-32. PMID: 2172662.
46. Sourisseau T, Georgiadis A, Tsapara A, Ali RR, Pestell R, Matter K, et al. Regulation of PCNA and cyclin D1 expression and epithelial morphogenesis by the ZO-1-regulated transcription factor ZONAB/DbpA. *Mol Cell Biol.* 2006;26(6):2387-98. PMID: 1430269.
47. Guo W, Sacher M, Barrowman J, Ferro-Novick S, Novick P. Protein complexes in transport vesicle targeting. *Trends Cell Biol.* 2000;10(6):251-5.
48. Hsu SC, TerBush D, Abraham M, Guo W. The exocyst complex in polarized exocytosis. *Int Rev Cytol.* 2004;233:243-65.
49. Inoue M, Chang L, Hwang J, Chiang SH, Saltiel AR. The exocyst complex is required for targeting of Glut4 to the plasma membrane by insulin. *Nature.* 2003;422(6932):629-33.
50. Rosse C, Hatzoglou A, Parrini MC, White MA, Chavrier P, Camonis J. RalB mobilizes the exocyst to drive cell migration. *Mol Cell Biol.* 2006;26(2):727-34. PMID: 1346891.

51. Chen XW, Inoue M, Hsu SC, Saltiel AR. RalA-exocyst-dependent recycling endosome trafficking is required for the completion of cytokinesis. *J Biol Chem.* 2006;281(50):38609-16.
52. Beutler B. Inferences, questions and possibilities in Toll-like receptor signalling. *Nature.* 2004;430(6996):257-63.
53. Buss H, Dorrie A, Schmitz ML, Hoffmann E, Resch K, Kracht M. Constitutive and interleukin-1-inducible phosphorylation of p65 NF- κ B at serine 536 is mediated by multiple protein kinases including I κ B kinase (IKK)- α , IKK β , IKK ϵ , TRAF family member-associated (TANK)-binding kinase 1 (TBK1), and an unknown kinase and couples p65 to TATA-binding protein-associated factor II31-mediated interleukin-8 transcription. *J Biol Chem.* 2004;279(53):55633-43.
54. Fitzgerald KA, McWhirter SM, Faia KL, Rowe DC, Latz E, Golenbock DT, et al. IKK ϵ and TBK1 are essential components of the IRF3 signaling pathway. *Nat Immunol.* 2003;4(5):491-6.
55. Hiscott J. Another detour on the Toll road to the interferon antiviral response. *Nat Struct Mol Biol.* 2004;11(11):1028-30.
56. Kato H, Takeuchi O, Sato S, Yoneyama M, Yamamoto M, Matsui K, et al. Differential roles of MDA5 and RIG-I helicases in the recognition of RNA viruses. *Nature.* 2006;441(7089):101-5.
57. Kawai T, Takahashi K, Sato S, Coban C, Kumar H, Kato H, et al. IPS-1, an adaptor triggering RIG-I- and Mda5-mediated type I interferon induction. *Nat Immunol.* 2005;6(10):981-8.
58. Lee HK, Dunzendorfer S, Soldau K, Tobias PS. Double-stranded RNA-mediated TLR3 activation is enhanced by CD14. *Immunity.* 2006;24(2):153-63.
59. McWhirter SM, Fitzgerald KA, Rosains J, Rowe DC, Golenbock DT, Maniatis T. IFN-regulatory factor 3-dependent gene expression is defective in Tbk1-deficient mouse embryonic fibroblasts. *Proc Natl Acad Sci U S A.* 2004;101(1):233-8. PMID: 314168.
60. McWhirter SM, Tenoever BR, Maniatis T. Connecting mitochondria and innate immunity. *Cell.* 2005;122(5):645-7.
61. Sharma S, tenOever BR, Grandvaux N, Zhou GP, Lin R, Hiscott J. Triggering the interferon antiviral response through an IKK-related pathway. *Science.* 2003;300(5622):1148-51.
62. Hacker H, Karin M. Regulation and function of IKK and IKK-related kinases. *Sci STKE.* 2006;2006(357):re13.
63. Boehm JS, Zhao JJ, Yao J, Kim SY, Firestein R, Dunn IF, et al. Integrative genomic approaches identify IKBKE as a breast cancer oncogene. *Cell.* 2007;129(6):1065-79.

64. Korherr C, Gille H, Schafer R, Koenig-Hoffmann K, Dixelius J, Egland KA, et al. Identification of proangiogenic genes and pathways by high-throughput functional genomics: TBK1 and the IRF3 pathway. *Proc Natl Acad Sci U S A*. 2006;103(11):4240-5. PMID: 1449677.
65. Mantovani A, Balkwill F. RalB signaling: a bridge between inflammation and cancer. *Cell*. 2006;127(1):42-4.
66. Buess M, Nuyten DS, Hastie T, Nielsen T, Pesich R, Brown PO. Characterization of heterotypic interaction effects in vitro to deconvolute global gene expression profiles in cancer. *Genome Biol*. 2007;8(9):R191. PMID: 2375029.
67. Adli M, Baldwin AS. IKK-i/IKKepsilon controls constitutive, cancer cell-associated NF-kappaB activity via regulation of Ser-536 p65/RelA phosphorylation. *J Biol Chem*. 2006;281(37):26976-84.
68. Kuranaga E, Kanuka H, Tonoki A, Takemoto K, Tomioka T, Kobayashi M, et al. Drosophila IKK-related kinase regulates nonapoptotic function of caspases via degradation of IAPs. *Cell*. 2006;126(3):583-96.
69. Downward J. Signal transduction. Prelude to an anniversary for the RAS oncogene. *Science*. 2006;314(5798):433-4.
70. Smith SC, Oxford G, Baras AS, Owens C, Havaleshko D, Brautigan DL, et al. Expression of ral GTPases, their effectors, and activators in human bladder cancer. *Clin Cancer Res*. 2007;13(13):3803-13.
71. Frech M, Schlichting I, Wittinghofer A, Chardin P. Guanine nucleotide binding properties of the mammalian RalA protein produced in *Escherichia coli*. *J Biol Chem*. 1990;265(11):6353-9.
72. Shirakawa R, Fukai S, Kawato M, Higashi T, Kondo H, Ikeda T, et al. Tuberous sclerosis tumor suppressor complex-like complexes act as GTPase-activating proteins for Ral GTPases. *J Biol Chem*. 2009;284(32):21580-8. PMID: 2755882.
73. Leonardi P, Kassin E, Hernandez-Munoz I, Diaz R, Inghirami G, Pellicer A. Human rgr: transforming activity and alteration in T-cell malignancies. *Oncogene*. 2002;21(33):5108-16.
74. Jimenez M, Perez de Castro I, Benet M, Garcia JF, Inghirami G, Pellicer A. The Rgr oncogene induces tumorigenesis in transgenic mice. *Cancer Res*. 2004;64(17):6041-9.
75. Tian X, Rusanescu G, Hou W, Schaffhausen B, Feig LA. PDK1 mediates growth factor-induced Ral-GEF activation by a kinase-independent mechanism. *EMBO J*. 2002;21(6):1327-38. PMID: 125928.

76. Yoshizaki H, Mochizuki N, Gotoh Y, Matsuda M. Akt-PDK1 complex mediates epidermal growth factor-induced membrane protrusion through Ral activation. *Mol Biol Cell*. 2007;18(1):119-28. PMID: 1751317.
77. Ceriani M, Scandiuizzi C, Amigoni L, Tisi R, Berruti G, Martegani E. Functional analysis of RalGPS2, a murine guanine nucleotide exchange factor for RalA GTPase. *Exp Cell Res*. 2007;313(11):2293-307.
78. Tartaglia M, Pennacchio LA, Zhao C, Yadav KK, Fodale V, Sarkozy A, et al. Gain-of-function SOS1 mutations cause a distinctive form of Noonan syndrome. *Nat Genet*. 2007;39(1):75-9.
79. Sjoblom T, Jones S, Wood LD, Parsons DW, Lin J, Barber TD, et al. The consensus coding sequences of human breast and colorectal cancers. *Science*. 2006;314(5797):268-74.
80. Bamford S, Dawson E, Forbes S, Clements J, Pettett R, Dogan A, et al. The COSMIC (Catalogue of Somatic Mutations in Cancer) database and website. *Br J Cancer*. 2004;91(2):355-8. PMID: 2409828.
81. Greenman C, Stephens P, Smith R, Dalgliesh GL, Hunter C, Bignell G, et al. Patterns of somatic mutation in human cancer genomes. *Nature*. 2007;446(7132):153-8. PMID: 2712719.
82. TerBush DR, Maurice T, Roth D, Novick P. The Exocyst is a multiprotein complex required for exocytosis in *Saccharomyces cerevisiae*. *EMBO J*. 1996;15(23):6483-94. PMID: 452473.
83. Kee Y, Yoo JS, Hazuka CD, Peterson KE, Hsu SC, Scheller RH. Subunit structure of the mammalian exocyst complex. *Proc Natl Acad Sci U S A*. 1997;94(26):14438-43. PMID: 25013.
84. Boyd C, Hughes T, Pypaert M, Novick P. Vesicles carry most exocyst subunits to exocytic sites marked by the remaining two subunits, Sec3p and Exo70p. *J Cell Biol*. 2004;167(5):889-901. PMID: 2172445.
85. Finger FP, Hughes TE, Novick P. Sec3p is a spatial landmark for polarized secretion in budding yeast. *Cell*. 1998;92(4):559-71.
86. Mehta SQ, Hiesinger PR, Beronja S, Zhai RG, Schulze KL, Verstreken P, et al. Mutations in *Drosophila* sec15 reveal a function in neuronal targeting for a subset of exocyst components. *Neuron*. 2005;46(2):219-32.
87. Wu S, Mehta SQ, Pichaud F, Bellen HJ, Quirocho FA. Sec15 interacts with Rab11 via a novel domain and affects Rab11 localization in vivo. *Nat Struct Mol Biol*. 2005;12(10):879-85.

88. Dong G, Hutagalung AH, Fu C, Novick P, Reinisch KM. The structures of exocyst subunit Exo70p and the Exo84p C-terminal domains reveal a common motif. *Nat Struct Mol Biol.* 2005;12(12):1094-100.
89. Hamburger ZA, Hamburger AE, West AP, Jr., Weis WI. Crystal structure of the *S.cerevisiae* exocyst component Exo70p. *J Mol Biol.* 2006;356(1):9-21.
90. Sivaram MV, Furgason ML, Brewer DN, Munson M. The structure of the exocyst subunit Sec6p defines a conserved architecture with diverse roles. *Nat Struct Mol Biol.* 2006;13(6):555-6.
91. Munson M, Novick P. The exocyst defrocked, a framework of rods revealed. *Nat Struct Mol Biol.* 2006;13(7):577-81.
92. Matern HT, Yeaman C, Nelson WJ, Scheller RH. The Sec6/8 complex in mammalian cells: characterization of mammalian Sec3, subunit interactions, and expression of subunits in polarized cells. *Proc Natl Acad Sci U S A.* 2001;98(17):9648-53. PMCID: 55506.
93. Vega IE, Hsu SC. The exocyst complex associates with microtubules to mediate vesicle targeting and neurite outgrowth. *J Neurosci.* 2001;21(11):3839-48.
94. Lalli G, Hall A. Ral GTPases regulate neurite branching through GAP-43 and the exocyst complex. *J Cell Biol.* 2005;171(5):857-69. PMCID: 2171284.
95. Lalli G. RalA and the exocyst complex influence neuronal polarity through PAR-3 and aPKC. *J Cell Sci.* 2009;122(Pt 10):1499-506.
96. Inoue M, Chiang SH, Chang L, Chen XW, Saltiel AR. Compartmentalization of the exocyst complex in lipid rafts controls Glut4 vesicle tethering. *Mol Biol Cell.* 2006;17(5):2303-11. PMCID: 1446102.
97. Whiteman EL, Cho H, Birnbaum MJ. Role of Akt/protein kinase B in metabolism. *Trends Endocrinol Metab.* 2002;13(10):444-51.
98. Chen XW, Leto D, Xiong T, Yu G, Cheng A, Decker S, et al. A Ral GAP complex links PI 3-kinase/Akt signaling to RalA activation in insulin action. *Mol Biol Cell.* 2011;22(1):141-52. PMCID: 3016972.
99. Chen XW, Leto D, Xiao J, Goss J, Wang Q, Shavit JA, et al. Exocyst function is regulated by effector phosphorylation. *Nat Cell Biol.* 2011;13(5):580-8.
100. Chen XW, Leto D, Chiang SH, Wang Q, Saltiel AR. Activation of RalA is required for insulin-stimulated Glut4 trafficking to the plasma membrane via the exocyst and the motor protein Myo1c. *Dev Cell.* 2007;13(3):391-404.
101. Albertson R, Riggs B, Sullivan W. Membrane traffic: a driving force in cytokinesis. *Trends Cell Biol.* 2005;15(2):92-101.

102. Echard A, Hickson GR, Foley E, O'Farrell PH. Terminal cytokinesis events uncovered after an RNAi screen. *Curr Biol*. 2004;14(18):1685-93. PMID: 2899696.
103. Gromley A, Yeaman C, Rosa J, Redick S, Chen CT, Mirabelle S, et al. Centriolin anchoring of exocyst and SNARE complexes at the midbody is required for secretory-vesicle-mediated abscission. *Cell*. 2005;123(1):75-87.
104. Schweitzer JK, Burke EE, Goodson HV, D'Souza-Schorey C. Endocytosis resumes during late mitosis and is required for cytokinesis. *J Biol Chem*. 2005;280(50):41628-35.
105. Schweitzer JK, D'Souza-Schorey C. Finishing the job: cytoskeletal and membrane events bring cytokinesis to an end. *Exp Cell Res*. 2004;295(1):1-8.
106. Cascone I, Selimoglu R, Ozdemir C, Del Nery E, Yeaman C, White M, et al. Distinct roles of RalA and RalB in the progression of cytokinesis are supported by distinct RalGEFs. *EMBO J*. 2008;27(18):2375-87. PMID: 2543054.
107. Kissova I, Deffieu M, Manon S, Camougrand N. Uth1p is involved in the autophagic degradation of mitochondria. *J Biol Chem*. 2004;279(37):39068-74.
108. Noda T, Matsuura A, Wada Y, Ohsumi Y. Novel system for monitoring autophagy in the yeast *Saccharomyces cerevisiae*. *Biochem Biophys Res Commun*. 1995;210(1):126-32.
109. Yang Z, Huang J, Geng J, Nair U, Klionsky DJ. Atg22 recycles amino acids to link the degradative and recycling functions of autophagy. *Mol Biol Cell*. 2006;17(12):5094-104. PMID: 1679675.
110. Hosokawa N, Hara T, Kaizuka T, Kishi C, Takamura A, Miura Y, et al. Nutrient-dependent mTORC1 association with the ULK1-Atg13-FIP200 complex required for autophagy. *Mol Biol Cell*. 2009;20(7):1981-91. PMID: 2663915.
111. Hosokawa N, Sasaki T, Iemura S, Natsume T, Hara T, Mizushima N. Atg101, a novel mammalian autophagy protein interacting with Atg13. *Autophagy*. 2009;5(7):973-9.
112. Jung CH, Jun CB, Ro SH, Kim YM, Otto NM, Cao J, et al. ULK-Atg13-FIP200 complexes mediate mTOR signaling to the autophagy machinery. *Mol Biol Cell*. 2009;20(7):1992-2003. PMID: 2663920.
113. Mercer CA, Kaliappan A, Dennis PB. A novel, human Atg13 binding protein, Atg101, interacts with ULK1 and is essential for macroautophagy. *Autophagy*. 2009;5(5):649-62.
114. Suzuki K, Kirisako T, Kamada Y, Mizushima N, Noda T, Ohsumi Y. The pre-autophagosomal structure organized by concerted functions of APG genes is essential for autophagosome formation. *EMBO J*. 2001;20(21):5971-81. PMID: 125692.
115. Mizushima N, Noda T, Yoshimori T, Tanaka Y, Ishii T, George MD, et al. A protein conjugation system essential for autophagy. *Nature*. 1998;395(6700):395-8.

116. Mizushima N, Sugita H, Yoshimori T, Ohsumi Y. A new protein conjugation system in human. The counterpart of the yeast Apg12p conjugation system essential for autophagy. *J Biol Chem.* 1998;273(51):33889-92.
117. Amar N, Lustig G, Ichimura Y, Ohsumi Y, Elazar Z. Two newly identified sites in the ubiquitin-like protein Atg8 are essential for autophagy. *EMBO Rep.* 2006;7(6):635-42. PMCID: 1479593.
118. Tanida I, Sou YS, Ezaki J, Minematsu-Ikeguchi N, Ueno T, Kominami E. HsAtg4B/HsApg4B/autophagin-1 cleaves the carboxyl termini of three human Atg8 homologues and delipidates microtubule-associated protein light chain 3- and GABAA receptor-associated protein-phospholipid conjugates. *J Biol Chem.* 2004;279(35):36268-76.
119. Tanida I, Tanida-Miyake E, Komatsu M, Ueno T, Kominami E. Human Apg3p/Aut1p homologue is an authentic E2 enzyme for multiple substrates, GATE-16, GABARAP, and MAP-LC3, and facilitates the conjugation of hApg12p to hApg5p. *J Biol Chem.* 2002;277(16):13739-44.
120. Fujita N, Itoh T, Omori H, Fukuda M, Noda T, Yoshimori T. The Atg16L complex specifies the site of LC3 lipidation for membrane biogenesis in autophagy. *Mol Biol Cell.* 2008;19(5):2092-100. PMCID: 2366860.
121. Hanada T, Noda NN, Satomi Y, Ichimura Y, Fujioka Y, Takao T, et al. The Atg12-Atg5 conjugate has a novel E3-like activity for protein lipidation in autophagy. *J Biol Chem.* 2007;282(52):37298-302.
122. Kabeya Y, Mizushima N, Ueno T, Yamamoto A, Kirisako T, Noda T, et al. LC3, a mammalian homologue of yeast Apg8p, is localized in autophagosome membranes after processing. *EMBO J.* 2000;19(21):5720-8. PMCID: 305793.
123. George MD, Baba M, Scott SV, Mizushima N, Garrison BS, Ohsumi Y, et al. Apg5p functions in the sequestration step in the cytoplasm-to-vacuole targeting and macroautophagy pathways. *Mol Biol Cell.* 2000;11(3):969-82. PMCID: 14824.
124. Kabeya Y, Mizushima N, Yamamoto A, Oshitani-Okamoto S, Ohsumi Y, Yoshimori T. LC3, GABARAP and GATE16 localize to autophagosomal membrane depending on form-II formation. *J Cell Sci.* 2004;117(Pt 13):2805-12.
125. Mizushima N, Yamamoto A, Hatano M, Kobayashi Y, Kabeya Y, Suzuki K, et al. Dissection of autophagosome formation using Apg5-deficient mouse embryonic stem cells. *J Cell Biol.* 2001;152(4):657-68. PMCID: 2195787.
126. Bodemann BO, White MA. Ral GTPases and cancer: linchpin support of the tumorigenic platform. *Nat Rev Cancer.* 2008;8(2):133-40.
127. Bhuvanakantham R, Li J, Tan TT, Ng ML. Human Sec3 protein is a novel transcriptional and translational repressor of flavivirus. *Cell Microbiol.* 2010;12(4):453-72.

128. Ishikawa H, Barber GN. STING is an endoplasmic reticulum adaptor that facilitates innate immune signalling. *Nature*. 2008;455(7213):674-8. PMID: 2804933.
129. Ishikawa H, Ma Z, Barber GN. STING regulates intracellular DNA-mediated, type I interferon-dependent innate immunity. *Nature*. 2009;461(7265):788-92.
130. Formstecher E, Aresta S, Collura V, Hamburger A, Meil A, Trehin A, et al. Protein interaction mapping: a *Drosophila* case study. *Genome Res*. 2005;15(3):376-84. PMID: 551564.
131. Grindstaff KK, Yeaman C, Anandasabapathy N, Hsu SC, Rodriguez-Boulan E, Scheller RH, et al. Sec6/8 complex is recruited to cell-cell contacts and specifies transport vesicle delivery to the basal-lateral membrane in epithelial cells. *Cell*. 1998;93(5):731-40.
132. Balakireva M, Rosse C, Langevin J, Chien YC, Ghossein M, Gonzy-Treboul G, et al. The Ral/exocyst effector complex counters c-Jun N-terminal kinase-dependent apoptosis in *Drosophila melanogaster*. *Mol Cell Biol*. 2006;26(23):8953-63. PMID: 1636832.
133. Frische EW, Pellis-van Berkel W, van Haaften G, Cuppen E, Plasterk RH, Tijsterman M, et al. RAP-1 and the RAL-1/exocyst pathway coordinate hypodermal cell organization in *Caenorhabditis elegans*. *EMBO J*. 2007;26(24):5083-92. PMID: 2140109.
134. Hase K, Kimura S, Takatsu H, Ohmae M, Kawano S, Kitamura H, et al. M-Sec promotes membrane nanotube formation by interacting with Ral and the exocyst complex. *Nat Cell Biol*. 2009;11(12):1427-32.
135. Jin R, Junutula JR, Matern HT, Ervin KE, Scheller RH, Brunger AT. Exo84 and Sec5 are competitive regulatory Sec6/8 effectors to the RalA GTPase. *EMBO J*. 2005;24(12):2064-74. PMID: 1150893.
136. Spiczka KS, Yeaman C. Ral-regulated interaction between Sec5 and paxillin targets Exocyst to focal complexes during cell migration. *J Cell Sci*. 2008;121(Pt 17):2880-91.
137. Fass E, Shvets E, Degani I, Hirschberg K, Elazar Z. Microtubules support production of starvation-induced autophagosomes but not their targeting and fusion with lysosomes. *J Biol Chem*. 2006;281(47):36303-16.
138. Pattingre S, Tassa A, Qu X, Garuti R, Liang XH, Mizushima N, et al. Bcl-2 antiapoptotic proteins inhibit Beclin 1-dependent autophagy. *Cell*. 2005;122(6):927-39.
139. Gillooly DJ, Morrow IC, Lindsay M, Gould R, Bryant NJ, Gaullier JM, et al. Localization of phosphatidylinositol 3-phosphate in yeast and mammalian cells. *EMBO J*. 2000;19(17):4577-88. PMID: 302054.
140. Chan EY, Kir S, Tooze SA. siRNA screening of the kinome identifies ULK1 as a multidomain modulator of autophagy. *J Biol Chem*. 2007;282(35):25464-74.

141. Vergne I, Roberts E, Elmaoued RA, Tosch V, Delgado MA, Proikas-Cezanne T, et al. Control of autophagy initiation by phosphoinositide 3-phosphatase Jumpy. *EMBO J*. 2009;28(15):2244-58. PMCID: 2726690.
142. Zeng X, Overmeyer JH, Maltese WA. Functional specificity of the mammalian Beclin-Vps34 PI 3-kinase complex in macroautophagy versus endocytosis and lysosomal enzyme trafficking. *J Cell Sci*. 2006;119(Pt 2):259-70.
143. Itakura E, Kishi C, Inoue K, Mizushima N. Beclin 1 forms two distinct phosphatidylinositol 3-kinase complexes with mammalian Atg14 and UVRAG. *Mol Biol Cell*. 2008;19(12):5360-72. PMCID: 2592660.
144. Matsunaga K, Saitoh T, Tabata K, Omori H, Satoh T, Kurotori N, et al. Two Beclin 1-binding proteins, Atg14L and Rubicon, reciprocally regulate autophagy at different stages. *Nat Cell Biol*. 2009;11(4):385-96.
145. Sun Q, Fan W, Chen K, Ding X, Chen S, Zhong Q. Identification of Barkor as a mammalian autophagy-specific factor for Beclin 1 and class III phosphatidylinositol 3-kinase. *Proc Natl Acad Sci U S A*. 2008;105(49):19211-6. PMCID: 2592986.
146. Zhong Y, Wang QJ, Li X, Yan Y, Backer JM, Chait BT, et al. Distinct regulation of autophagic activity by Atg14L and Rubicon associated with Beclin 1-phosphatidylinositol-3-kinase complex. *Nat Cell Biol*. 2009;11(4):468-76. PMCID: 2664389.
147. Lee SB, Kim S, Lee J, Park J, Lee G, Kim Y, et al. ATG1, an autophagy regulator, inhibits cell growth by negatively regulating S6 kinase. *EMBO Rep*. 2007;8(4):360-5. PMCID: 1852764.
148. Lipschutz JH, Mostov KE. Exocytosis: the many masters of the exocyst. *Curr Biol*. 2002;12(6):R212-4.
149. He B, Guo W. The exocyst complex in polarized exocytosis. *Curr Opin Cell Biol*. 2009;21(4):537-42. PMCID: 2725219.
150. Delgado MA, Elmaoued RA, Davis AS, Kyei G, Deretic V. Toll-like receptors control autophagy. *EMBO J*. 2008;27(7):1110-21. PMCID: 2323261.
151. Shi CS, Kehrl JH. TRAF6 and A20 regulate lysine 63-linked ubiquitination of Beclin-1 to control TLR4-induced autophagy. *Sci Signal*. 2010;3(123):ra42.
152. Maehama T, Tanaka M, Nishina H, Murakami M, Kanaho Y, Hanada K. RalA functions as an indispensable signal mediator for the nutrient-sensing system. *J Biol Chem*. 2008;283(50):35053-9.
153. Toschi A, Lee E, Xu L, Garcia A, Gadir N, Foster DA. Regulation of mTORC1 and mTORC2 complex assembly by phosphatidic acid: competition with rapamycin. *Mol Cell Biol*. 2009;29(6):1411-20. PMCID: 2648237.

154. Voss M, Weernink PA, Haupenthal S, Moller U, Cool RH, Bauer B, et al. Phospholipase D stimulation by receptor tyrosine kinases mediated by protein kinase C and a Ras/Ral signaling cascade. *J Biol Chem*. 1999;274(49):34691-8.
155. Rosse C, L'Hoste S, Offner N, Picard A, Camonis J. RLIP, an effector of the Ral GTPases, is a platform for Cdk1 to phosphorylate epsin during the switch off of endocytosis in mitosis. *J Biol Chem*. 2003;278(33):30597-604.
156. Mizushima N, Yamamoto A, Matsui M, Yoshimori T, Ohsumi Y. In vivo analysis of autophagy in response to nutrient starvation using transgenic mice expressing a fluorescent autophagosome marker. *Mol Biol Cell*. 2004;15(3):1101-11. PMID: 363084.
157. Vieira OV, Botelho RJ, Rameh L, Brachmann SM, Matsuo T, Davidson HW, et al. Distinct roles of class I and class III phosphatidylinositol 3-kinases in phagosome formation and maturation. *J Cell Biol*. 2001;155(1):19-25. PMID: 2150784.
158. Bampton ET, Goemans CG, Niranjan D, Mizushima N, Tolkovsky AM. The dynamics of autophagy visualized in live cells: from autophagosome formation to fusion with endo/lysosomes. *Autophagy*. 2005;1(1):23-36.
159. Okazaki N, Yan J, Yuasa S, Ueno T, Kominami E, Masuho Y, et al. Interaction of the Unc-51-like kinase and microtubule-associated protein light chain 3 related proteins in the brain: possible role of vesicular transport in axonal elongation. *Brain Res Mol Brain Res*. 2000;85(1-2):1-12.
160. Yeaman C. Ultracentrifugation-based approaches to study regulation of Sec6/8 (exocyst) complex function during development of epithelial cell polarity. *Methods*. 2003;30(3):198-206.
161. Fromont-Racine M, Rain JC, Legrain P. Toward a functional analysis of the yeast genome through exhaustive two-hybrid screens. *Nat Genet*. 1997;16(3):277-82.
162. Radtke AL, Delbridge LM, Balachandran S, Barber GN, O'Riordan MX. TBK1 protects vacuolar integrity during intracellular bacterial infection. *PLoS Pathog*. 2007;3(3):e29. PMID: 1808071.
163. Dietzl G, Chen D, Schnorrer F, Su KC, Barinova Y, Fellner M, et al. A genome-wide transgenic RNAi library for conditional gene inactivation in *Drosophila*. *Nature*. 2007;448(7150):151-6.
164. Rorth P. Gal4 in the *Drosophila* female germline. *Mech Dev*. 1998;78(1-2):113-8.
165. Obara K, Noda T, Niimi K, Ohsumi Y. Transport of phosphatidylinositol 3-phosphate into the vacuole via autophagic membranes in *Saccharomyces cerevisiae*. *Genes Cells*. 2008;13(6):537-47.

166. Furuya N, Yu J, Byfield M, Pattingre S, Levine B. The evolutionarily conserved domain of Beclin 1 is required for Vps34 binding, autophagy and tumor suppressor function. *Autophagy*. 2005;1(1):46-52.
167. Dunlop EA, Tee AR. Mammalian target of rapamycin complex 1: signalling inputs, substrates and feedback mechanisms. *Cell Signal*. 2009;21(6):827-35.
168. Fox HL, Pham PT, Kimball SR, Jefferson LS, Lynch CJ. Amino acid effects on translational repressor 4E-BP1 are mediated primarily by L-leucine in isolated adipocytes. *Am J Physiol*. 1998;275(5 Pt 1):C1232-8.
169. Xu G, Kwon G, Cruz WS, Marshall CA, McDaniel ML. Metabolic regulation by leucine of translation initiation through the mTOR-signaling pathway by pancreatic beta-cells. *Diabetes*. 2001;50(2):353-60.
170. Nicklin P, Bergman P, Zhang B, Triantafellow E, Wang H, Nyfeler B, et al. Bidirectional transport of amino acids regulates mTOR and autophagy. *Cell*. 2009;136(3):521-34.
171. Eric M. Wauson EZ, A-Young Lee, Marcy Guerra, Anwasha B. Ghosh, Angie L. Bookout, Chris P. Chambers, Arif Jivan, Kathy McGlynn, Ralph J. Deberardinis, and Melanie H. Cobb. The G protein-coupled taste receptor T1R1/T1R3 regulates mTORC1 and autophagy. Manuscript in Review. 2011.
172. Sancak Y, Bar-Peled L, Zoncu R, Markhard AL, Nada S, Sabatini DM. Ragulator-Rag complex targets mTORC1 to the lysosomal surface and is necessary for its activation by amino acids. *Cell*. 2010;141(2):290-303. PMID: 3024592.
173. Sancak Y, Peterson TR, Shaul YD, Lindquist RA, Thoreen CC, Bar-Peled L, et al. The Rag GTPases bind raptor and mediate amino acid signaling to mTORC1. *Science*. 2008;320(5882):1496-501. PMID: 2475333.
174. Heublein S, Kazi S, Ogmundsdottir MH, Attwood EV, Kala S, Boyd CA, et al. Proton-assisted amino-acid transporters are conserved regulators of proliferation and amino-acid-dependent mTORC1 activation. *Oncogene*. 2010;29(28):4068-79. PMID: 3018277.
175. Korolchuk VI, Saiki S, Lichtenberg M, Siddiqi FH, Roberts EA, Imarisio S, et al. Lysosomal positioning coordinates cellular nutrient responses. *Nat Cell Biol*. 2011;13(4):453-60. PMID: 3071334.
176. Bai X, Ma D, Liu A, Shen X, Wang QJ, Liu Y, et al. Rheb activates mTOR by antagonizing its endogenous inhibitor, FKBP38. *Science*. 2007;318(5852):977-80.
177. Garami A, Zwartkruis FJ, Nobukuni T, Joaquin M, Roccio M, Stocker H, et al. Insulin activation of Rheb, a mediator of mTOR/S6K/4E-BP signaling, is inhibited by TSC1 and 2. *Mol Cell*. 2003;11(6):1457-66.

178. Cai SL, Tee AR, Short JD, Bergeron JM, Kim J, Shen J, et al. Activity of TSC2 is inhibited by AKT-mediated phosphorylation and membrane partitioning. *J Cell Biol.* 2006;173(2):279-89. PMCID: 2063818.
179. Inoki K, Li Y, Zhu T, Wu J, Guan KL. TSC2 is phosphorylated and inhibited by Akt and suppresses mTOR signalling. *Nat Cell Biol.* 2002;4(9):648-57.
180. Frias MA, Thoreen CC, Jaffe JD, Schroder W, Sculley T, Carr SA, et al. mSin1 is necessary for Akt/PKB phosphorylation, and its isoforms define three distinct mTORC2s. *Curr Biol.* 2006;16(18):1865-70.
181. Tato I, Bartrons R, Ventura F, Rosa JL. Amino acids activate mammalian target of rapamycin complex 2 (mTORC2) via PI3K/Akt signaling. *J Biol Chem.* 2011;286(8):6128-42. PMCID: 3057817.
182. Byfield MP, Murray JT, Backer JM. hVps34 is a nutrient-regulated lipid kinase required for activation of p70 S6 kinase. *J Biol Chem.* 2005;280(38):33076-82.
183. Nobukuni T, Joaquin M, Roccio M, Dann SG, Kim SY, Gulati P, et al. Amino acids mediate mTOR/raptor signaling through activation of class 3 phosphatidylinositol 3OH-kinase. *Proc Natl Acad Sci U S A.* 2005;102(40):14238-43. PMCID: 1242323.
184. Gulati P, Gaspers LD, Dann SG, Joaquin M, Nobukuni T, Natt F, et al. Amino acids activate mTOR complex 1 via Ca²⁺/CaM signaling to hVps34. *Cell Metab.* 2008;7(5):456-65. PMCID: 2587347.
185. Ou YH, Torres M, Ram R, Formstecher E, Roland C, Cheng T, et al. TBK1 directly engages Akt/PKB survival signaling to support oncogenic transformation. *Mol Cell.* 2011;41(4):458-70. PMCID: 3073833.
186. Xie X, Zhang D, Zhao B, Lu MK, You M, Condorelli G, et al. IkappaB kinase epsilon and TANK-binding kinase 1 activate AKT by direct phosphorylation. *Proc Natl Acad Sci U S A.* 2011;108(16):6474-9. PMCID: 3081021.
187. Hennigs JK, Burhenne N, Stahler F, Winnig M, Walter B, Meyerhof W, et al. Sweet taste receptor interacting protein CIB1 is a general inhibitor of InsP3-dependent Ca²⁺ release in vivo. *J Neurochem.* 2008;106(5):2249-62.
188. Oya M, Suzuki H, Watanabe Y, Sato M, Tsuboi T. Amino acid taste receptor regulates insulin secretion in pancreatic beta-cell line MIN6 cells. *Genes Cells.* 2011;16(5):608-16.
189. Juhasz G, Hill JH, Yan Y, Sass M, Baehrecke EH, Backer JM, et al. The class III PI(3)K Vps34 promotes autophagy and endocytosis but not TOR signaling in *Drosophila*. *J Cell Biol.* 2008;181(4):655-66. PMCID: 2386105.